Quasigeodesic Flows on Hyperbolic 3-Manifolds Which Fiber Over the Circle

Diane Hoffoss

May 1998

UNIVERSITY OF CALIFORNIA

Santa Barbara

Quasigeodesic Flows on Hyperbolic 3-Manifolds Which Fiber Over the Circle

A Dissertation submitted in partial satisfaction
of the requirements for the degree of

Doctor of Philosophy
in
Mathematics
by

Linda Diane Hoffoss

Committee in charge:

Professor Daryl Cooper, Chairperson

Professor D. Darren Long

Professor Martin Scharlemann

June, 1998

The dissertation of Linda Diane Hoffoss is approved

Committee Chairperson

June, 1998

ACKNOWLEDGMENTS

I owe thanks to a great many people. I am, of course, the very most grateful to my advisor, Daryl Cooper, for motivating and encouraging me, for listening to me, and for making everything we discussed interesting. You brought out my potential, never gave up on me, and helped me become a mathematician. You have been a more fantastic math father than I even knew how to ask for.

I would like to thank Sergio Fenley and Lee Mosher for all their encouragement. Thank you, Lee, for sharing your wealth of interesting ideas and for suggesting my next research project. And thank you, Sergio, for listening to and commenting on my proposed approaches to this problem all along, for pointing out where you felt the difficulties would lie in my theorem and suggesting things that might work, for keeping in touch with me and telling me you thought my theorem was important. The interest you and Lee showed made me very proud.

The topology group UCSB has been incredibly inspiring. Professors Martin Scharlemann, Darren Long, and Kenneth Millett have provided a tremendous and varied learning environment and have made my study at UCSB fun. Brian Mangum and Patrick Shanahan, my closest colleagues in graduate school, are the best people I could ever hope to work and learn with. It is easier to talk about math with you two than anyone else. Thanks Pat, for your good nature, your math smarts, and your tireless enthusiasm. Thanks, Brian, for the many hours you spent working on math with me,

for always being counted on to tell the obvious joke, and for being my very closest friend for so many years. Thanks also to Joseph Maher for proofreading messy calculations, for helping me with computer problems, for having faith that I would finish. Thank you Anneke Bart for taking care of uncountable small details and covering classes while I was out of town. You were all wonderful to be with in graduate school. I am glad that we are all permanent colleagues and we will see each other at conferences for the rest of our careers.

I am grateful to Dan Farkas and Bill Floyd for encouraging me to go to the Geometry Supercomputer Project, and I am especially grateful to Jeff Weeks for giving me such an interesting programming problem in topology that I decided to do my Ph.D. in that area. I appreciated Al Marden's enthusiasm and Charlie Gunn's daily question and answer sessions at the Geometry Project. And thanks to Mike Freedman for suggesting UCSB as a place for me to study topology, even though that meant leaving UCSD's topology program.

I would like to thank my Santa Barbara neighbors Sara Fargo and Katie Deming for cooking me dinners and watching my cat, for encouraging me and giving me self-confidence. And thank you so much, Norene, for your patience, understanding, and insight.

Finally, I am grateful to the entire Math Department at Colorado College, especially to Jane McDougall and Gowri Meda, for supporting me and cheering me on as I finished my thesis during my toughest teaching block.

VITA

May 13, 1967 — Born — Oakland, California

1989 — B.S., Virginia Polytechnic Institute and State University

1989 — Visiting Researcher, Geometry Supercomputer Project, Minneapolis, Minnesota

1989-90 — Member of Technical Staff, Bellcore, Morristown, New Jersey

1993 — M.A., University of California, Santa Barbara

1993-1997 —Teaching Associate/Assistant, Department of Mathematics, University of California, Santa Barbara

1997-1998 —Visiting Assistant Professor, Department of Mathematics and Computer Science, The Colorado College, Colorado Springs, Colorado

FIELDS OF STUDY

Major Field: Low Dimensional Topology

ABSTRACT

Quasigeodesic Flows on Hyperbolic 3-Manifolds
Which Fiber Over the Circle

by

Linda Diane Hoffoss

A hyperbolic 3-manifold M which fibers over the circle admits a 1-dimensional foliation called the suspension flow. We show that such a flow can be isotoped to be quasigeodesic in the hyperbolic metric on M, where quasigeodesic means that flow lines are uniformly efficient in measuring distance in free homotopy classes.

Contents

List of Figures

Chapter 1

Introduction

The classification of 3-manifolds is a major long term goal for many topologists. One way to begin to understand the structure of 3-manifolds is using flows. A **flow** on a manifold is a foliation of the manifold by coherently oriented one-manifolds. Flows are not rare; in fact, every closed 3-manifold has a flow given by the integral curves of a continuous, nowhere zero vector field (since the Euler characteristic of such a manifold is 0). By understanding what flows a manifold will admit one can deduce information about the topology of the manifold.

This thesis considers a specific flow called the suspension flow on hyperbolic 3-manifolds M which fiber over the circle. Thurston [Th] has shown that such a 3-manifold can be represented as a product of a hyperbolic surface (the fiber, F) with the unit interval $[0, 1]$, with $F \times \{1\}$ glued to $F \times \{0\}$ using a pseudo-Anosov monodromy map. The manifold M is then

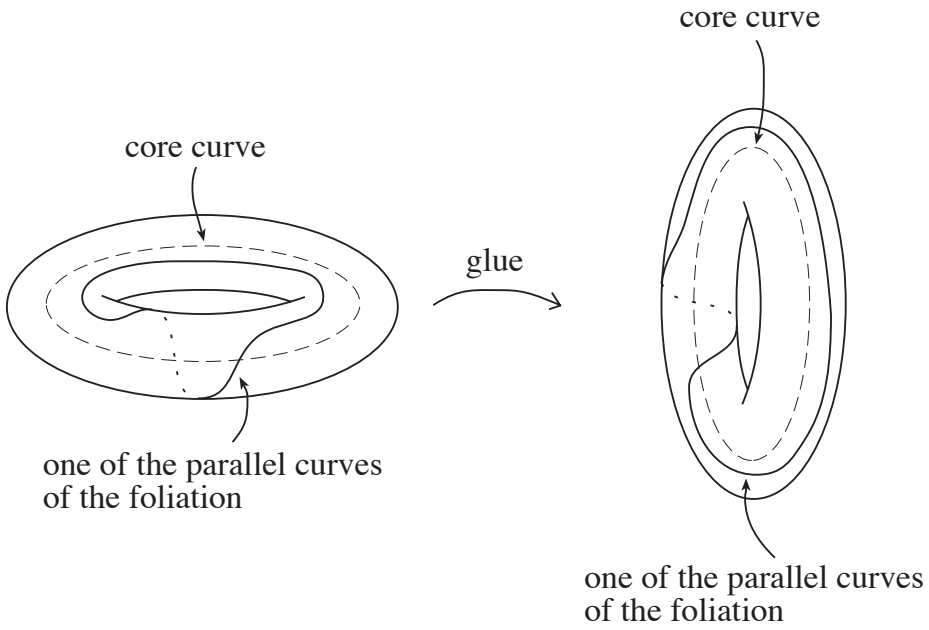

Figure 1.1: The Hopf fibration on $\mathbb{S}^3$.

called the **suspension** of F. Thus M is covered by $F \times \mathbb{R}^1$; the flow on M obtained by projecting the 1-manifolds $\{x\} \times \mathbb{R}^1$ (where $x \in F$) down from $F \times \mathbb{R}^1$ to M is called the **suspension flow**.

Not all flows on a manifold give useful information about the topology of the manifold. For example, the Hopf fibration of $\mathbb{S}^3$ (see Figure 1.1) is a flow on the three-sphere by circles. However, these closed loops do not indicate information about the topology of $\mathbb{S}^3$, as $\mathbb{S}^3$ is simply connected. In this thesis we study flows whose closed curves are nonzero in the fundamental group of the manifold.

Even when the flow lines do not form any closed curves one may still

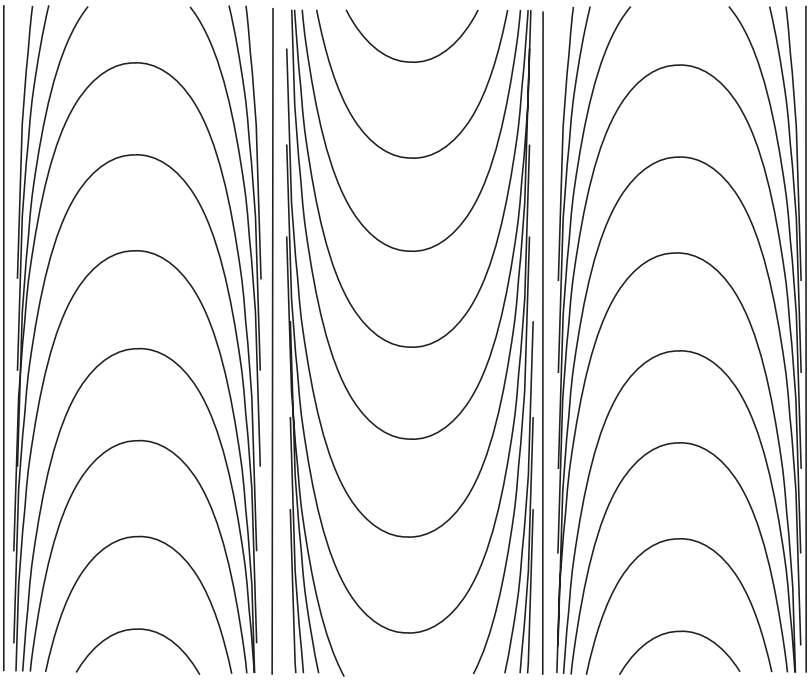

Figure 1.2: The Reeb foliation on $\mathbb{R}^2$.

hope to gather some information about the manifold, by expecting that whenever the endpoints of a long segment of flow line lie near each other, this "near loop" indicates fundamental group information about the manifold. The Reeb foliation on $\mathbb{R}^2$ (see Figure 1.2) is an example of a flow which has unboundedly long flow line segments whose endpoints lie within a bounded distance of each other, and yet $\pi_1(\mathbb{R}^2) = 1$. We will rule out this behavior.

This approach of concentrating mainly on the flows which hold fundamental group information in the above ways is similar to what is done in surface theory. The types of surfaces one typically studies are incompressible surfaces, which carry some fundamental group of the original mani-

fold. Two dimensional laminations, which are generalizations of surfaces in an analogous way that foliations are generalizations of closed loops, are treated similarly: the laminations which are most interesting are essential laminations, those whose fundamental group indicate information about the fundamental group of the original manifold.

One way to guarantee that the information you get from a flow is relevant to the topology of the manifold is to consider quasigeodesic flows. A **quasigeodesic flow** is a flow that when lifted to the universal cover of the manifold, has no closed loops or "near loops". These flow lines on the original manifold, then, will indicate some topology whenever they either form closed loops or travel long distances and then return to a point near where they started (forming a "near loop").

One reason quasigeodesic foliations are interesting is that they are product covered. A flow on a manifold is **product covered** if the flow is covered by a product foliation of the universal cover of M. In this case, the quotient of the universal cover $\widetilde{M}$ of M obtained by identifying each flow line to a point (called the **orbit space**) is homeomorphic to $\mathbb{R}^2$ or $\mathbb{S}^2$. Cooper and Long [CL] show that if a foliation without closed leaves on a manifold M is product covered, then $\pi_1(M)$ acts freely on this plane, thus the subgroup of $\pi_1(M)$ mapping a flow line to itself is either trivial or cyclic.

It is the goal of this dissertation to establish that the suspension flow on any hyperbolic 3-manifold which fibers over the circle is quasigeodesic.

1.1 Background

In the 1970's, Cannon and Thurston [CT] showed that the suspension flow on a closed hyperbolic 3-manifold which fibers over the circle is quasigeodesic. This thesis addresses the case where the manifold in question is not closed, but instead has finitely many cusps. In the cusped situation the Cannon-Thurston technique breaks down, for the generalization of the metric they use on closed manifolds is not quasi-isometric to the hyperbolic metric on the cusped manifold, as it places the cusps at only a finite distance in the manifold.

Instead, a modification of the metric described in [CT] in neighborhoods of the cusps which pushes the cusps out to infinity produces a metric which is quasi-isometric to the hyperbolic metric on the manifold. We will show that the suspension flow lines are quasigeodesic in this modified metric, and thus they are quasigeodesic (with perhaps a different quasigeodesic constant) in the hyperbolic metric on M.

1.2 Setting

As Cannon and Thurston have proven the suspension flow lines are quasigeodesic in the closed case, in this thesis we will consider cusped manifolds. Unless otherwise specified, M will denote a cusped hyperbolic 3-manifold which fibers over the circle throughout this thesis.

1.2.1 Precise Definitions

In this section we will make precise some of the concepts loosely defined above.

Definition 1.2.1 *A **path** in M is a continuous map from (an interval in) $\mathbb{R}^1$ to M.*

In this thesis, a path is defined as a map into M rather than the image of such a map, so that closed loops in M may still lift to the universal cover as infinite lines, and thus don't necessarily violate the quasigeodesic condition defined below.

Definition 1.2.2 *A **flow** on a 3-manifold M is a continuous map $\Phi : \mathbb{R}^1 \times M \to M$ so that*

1. *For each p in M, the map $\Phi|_{\mathbb{R}^1 \times \{p\}}$ is an immersion, and*
2. *For each t, s in $\mathbb{R}^1$, p in M, if we denote $\Phi_s = \Phi|_{\{s\} \times M}$, then $\Phi_t \circ \Phi_s = \Phi_{t+s}$.*

Definition 1.2.3 *A **flow line** though the point p in M is the map $\Phi|_{\mathbb{R}^1 \times \{p\}} : \mathbb{R}^1 \times \{p\} \to M$. We will commonly think of a flow line as merely a map from $\mathbb{R}^1$ to M.*

Thus a flow line is a path in M. Since we have chosen our paths and flow lines as maps from $\mathbb{R}^1$ into M, a closed loop will lift to an infinite line in the universal cover if and only if it has infinite order in π_1.

Example 1.2.4 (Flows on Manifolds)

1. *Consider the manifold $M = \mathbb{S}^2 \times \mathbb{S}^1$, and define a map $\Phi : \mathbb{R}^1 \times M \to M$ by $\Phi(t, p) = (p, e^{2\pi i t})$. Then Φ is a flow on M, with flow lines given by wrapping the real line around the $\mathbb{S}^1$ direction infinitely many times.*

2. *Let M be a manifold and v be a continuous nowhere zero vector field on M. Then the integral curves of v create a flow on M.*

The arguments in this thesis require calculating the distance along segments of path in various metrics. The metric involved will be made clear by the context; however, a bit of notation will be used to distinguish which path is being used to calculate distance.

Notation 1.2.5 *If a and b are points on a path c in a given metric on M, let $\boldsymbol{d_c(a, b)}$ denote the length of the segment of path c between a and b in the given metric.*

Recall that if γ is a geodesic segment in $\mathbb{H}^3$ between points a and b, then the length of γ between a and b, $d_\gamma(a,b)$, gives the distance between a and b.

Definition 1.2.6 *A path c in M is **quasigeodesic** in a particular metric m if there exists $K > 1, L > 0$ such that for all a, b lying on the lift $\tilde{c}$ of c to the universal cover of M with $d_{\tilde{c}}(a,b) > L$,*

$$d_{\tilde{c}}(a,b) \leq K \cdot d_{\widetilde{M}}(a,b),$$

where $d_{\widetilde{M}}(a,b)$ is the distance in $\widetilde{M}$ between a and b using the metric m.

Figure 1.3 shows examples of paths in a hyperbolic manifold M lifted to the universal cover $\widetilde{M}$ of M which are quasigeodesic and others which are not quasigeodesic. In this thesis we will encounter several different quasigeodesic constants, as well as many different metrics. To indicate which constant or metric is being considered, a quasigeodesic with multiplicative quasigeodesic constant K will sometimes be referred to as a K-quasigeodesic; a quasigeodesic of a particular metric m may be called an m-quasigeodesic.

Definition 1.2.7 *A flow on M is **uniformly quasigeodesic** if there exists a uniform $K > 1, L > 0$ such that every flow line is a K-quasigeodesic.*

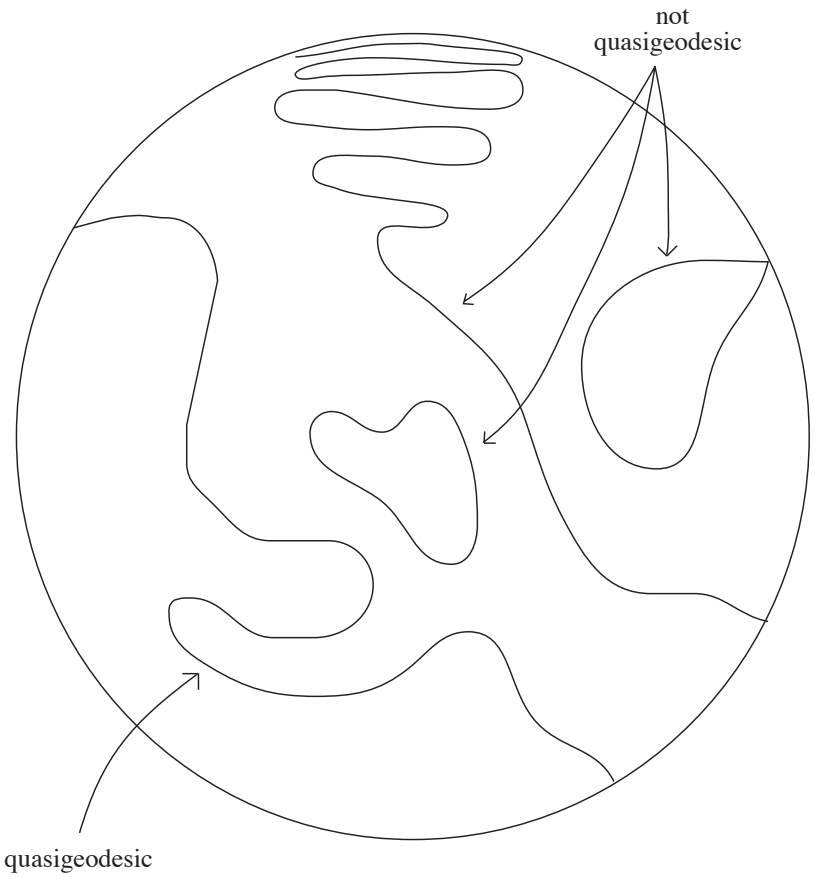

Figure 1.3: Quasigeodesic and non-quasigeodesic paths lifted to $\widetilde{M} = \mathbb{H}^3$.

Thus a flow is uniformly quasigeodesic if all sufficiently long segments of flow lines are efficient at measuring distances, up to a uniform constant multiple K.

Example 1.2.8 (Quasigeodesic flows)

1. *Consider the space $\mathbb{T}^2 \times \mathbb{S}^1$, foliated using $\{point\} \times \mathbb{S}^1$. If we lift to the universal cover, given by $\mathbb{R}^2 \times \mathbb{R}^1$, then flow lines lift to lines $\{point\} \times \mathbb{R}^1$. This flow is visibly geodesic in the Euclidean metric on R^3, and therefore quasigeodesic as well.*

2. *In fact, the suspension foliation on any torus bundle over the circle is quasigeodesic.*

3. *The suspension flow on any closed hyperbolic 3-manifold fibering over the circle is quasigeodesic [CT].*

Example 1.2.9 (Non-quasigeodesic flow)

1. *Any lens space can be described by glueing two solid tori together along their boundaries. Cover the boundary of the first torus with infinitely many parallel copies of some (p, q) curve, where $\frac{p}{q}$ is an irrational number. Then each (p, q) curve does not close up, but instead wraps around and around the boundary of the torus. Let the foliation on*

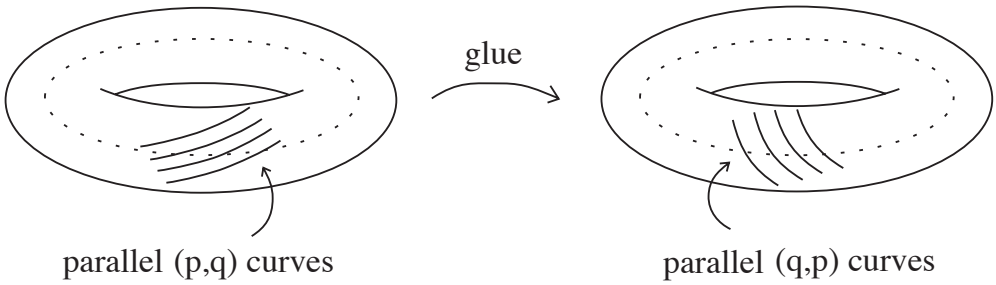

Figure 1.4: A foliation of a lens space.

the boundary of the first torus induce the foliation on the boundary of the second torus so that the foliations match up when the tori are glued together. Carry both boundary foliations through concentric tori until you reach the core curve (see Figure 1.4). This describes a flow on the lens space, given by lines instead of circles (as in the previous example). However, this flow is not quasigeodesic, for all the flow lines except for the two core curves wrap infinitely many times around a torus, while geodesics in the universal cover of the lens space ($\mathbb{S}^3$) are great circles, which do not wrap around tori.

Example 1.2.10 (Manifolds which do not admit a quasigeodesic flow)

1. *If M admits a quasigeodesic flow then its universal cover is $F \times \mathbb{R}^1$, where F is a simply connected surface. Thus any manifold with finite fundamental group can not admit a quasigeodesic flow.*

2. *Let M be the connect sum of 2 hyperbolic 3-manifolds. Then M has universal cover a connect sum of infinitely many copies of $\mathbb{R}^3$, thus $\pi_2 M$ is infinitely generated. Therefore, the universal cover of M is not homeomorphic to $F \times \mathbb{R}^1$ for some simply connected surface F. Therefore M does not admit a quasigeodesic flow.*

1.2.2 Pseudo-Anosov Homeomorphisms and the Singular Solv Metric

The manifolds considered in this thesis are cusped hyperbolic 3-manifolds which fiber over the circle. The reason for this choice of manifold is that by a theorem of Thurston, these manifolds have a particularly nice description, which gives rise to an easily described flow.

Theorem 1.2.11 (Thurston) *A manifold M is a hyperbolic 3-manifold which fibers over the circle if and only if M can be represented as the product of a hyperbolic surface F (the fiber) with the unit interval, with $F \times \{1\}$ glued to $F \times \{0\}$ using a pseudo-Anosov monodromy map Ψ:*

$$M = F \times [0,1])/((x,1) \sim (\Psi x, 0)).$$

Note that the manifolds we will be interested in are cusped 3-manifolds; thus the fiber surface F will be punctured. If F^+ is the closure of F, then

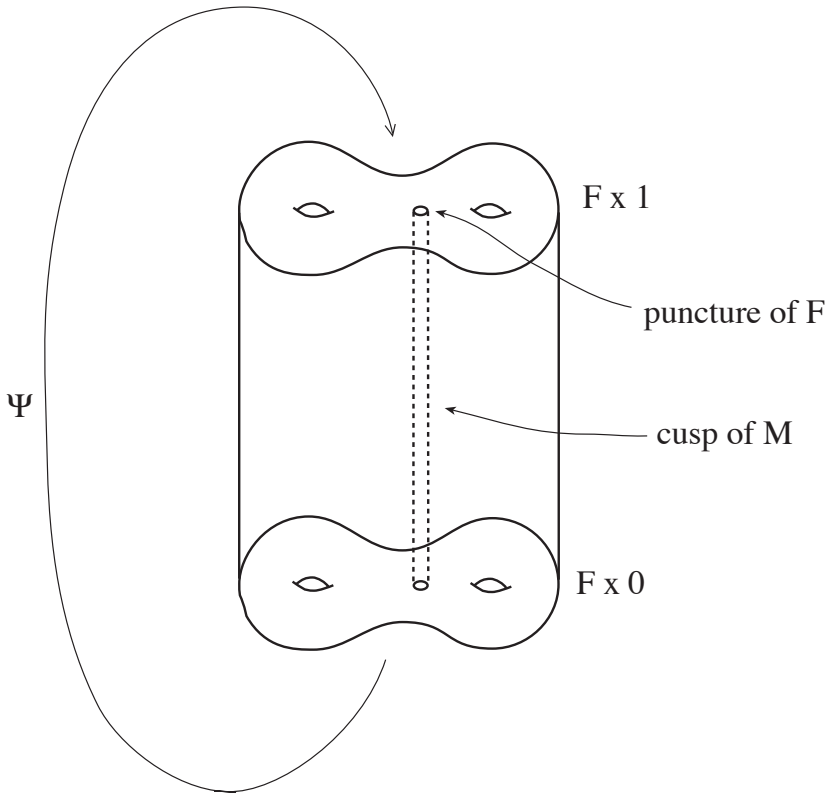

Figure 1.5: M represented as $F \times I$, with top glued to bottom using pseudo-Anosov monodromy Ψ.

$F = F^+ \setminus \{p_1, p_2, \ldots, p_j\}$, where each p_i is a point in F^+. (Note that F^+ need not be hyperbolic itself, for the punctured torus is a hyperbolic surface whereas the torus is not).

The monodromy map $\Psi : F \to F$ can be extended to a map $\Psi^+ : F^+ \to F^+$ which permutes the points $\{p_1, \ldots, p_j\}$. Since there are only finitely many points in $F^+ \setminus F$, the flow lines in the suspension of F^+ through each of these points must eventually form closed loops. In other words, if

$$M^+ = F^+ \times [0,1])/((x,1) \sim (\Psi^+ x, 0)),$$

then $M^+ \setminus M$ consists of finitely many closed loops. We will sometimes refer to one of these closed loops as a missing flow line:

Definition 1.2.12 *A **missing flow line** of M is one of the closed loops in the set $M^+ \setminus M$.*

Loosely speaking, a pseudo-Anosov homeomorphism from a hyperbolic surface to itself is an area preserving homeomorphism which stretches in one eigendirection while shrinking in a transverse eigendirection, except possibly at finitely many singularities. These eigendirections will describe a pair of 1-dimensional singular foliations on the hyperbolic surface.

Definition 1.2.13 *A **1-dimensional foliation** $\mathcal{F}$ of a 3-manifold M is a partition of M into disjoint, connected, 1-submanifolds which is locally a product; i.e.,*

1. *$M = \bigcup \ell_x$, where $\ell_x \in \mathcal{F}$ is a 1-manifold, and*

2. *Every $x \in M$ has a neighborhood whose foliation is homeomorphic to the product foliation on $D^2 \times I$ (the foliation given by $\{$point in $D^2\} \times I$).*

*The ℓ_x's are called **leaves**.*

Examples 1.2.14

1. *The image of a flow is coherently oriented, 1-dimensional foliation on M.*

2. *The image of a flow line is an oriented leaf.*

It will be easier to understand pseudo-Anosov homeomorphisms if we first consider Anosov homeomorphisms.

Definition 1.2.15 *A homeomorphism Ψ from the torus to itself is **Anosov** if the following two statements hold:*

1. *There exists a pair of transversely measured 1-dimensional foliations on the torus which are preserved by Ψ.*

2. *Written in the local coordinates given by these transversely measured foliations, the map* Ψ *has the form*

$$\begin{pmatrix} \mu & 0 \\ 0 & \mu^{-1} \end{pmatrix},$$

where μ *is a real number not equal to* ± 1.

By swapping coordinates we may choose μ to be the eigenvalue which is greater than one. The pair of transverse measured 1-dimensional foliations follow along the directions given by the two eigenvectors of the map, v_+ and v_- corresponding to eigenvalues μ and μ^{-1}. These two foliations are referred to as the **stable** and **unstable** foliations of the map Ψ (the stable foliation is in the direction corresponding to v_-).

Since the determinant of the above matrix is 1, the Anosov map Ψ is area preserving. If we choose R to be a quadrilateral in $\mathbb{T}^2$ with edges parallel to the two eigenvectors v_+ and v_-, then ΨR will be a quadrilateral which has been stretched by a factor of μ in the v_+ direction and shrunk by a factor of μ in the v_- direction (see Figure 1.6).

There is a natural metric called the **Solv** metric that one may put on a manifold M obtained by using the Anosov map Ψ to suspend the surface $\mathbb{T}^2$. The map Ψ stretches one eigendirection on $\mathbb{T}^2 \times \{1\}$ and shrinks the other eigendirection on $\mathbb{T}^2 \times \{1\}$ by a factor of μ, and then glues $\mathbb{T}^2 \times \{1\}$ to $\mathbb{T}^2 \times \{0\}$. The Solv metric is defined on the universal cover of M so that the covering translation corresponding to the Anosov map Ψ is an isometry.

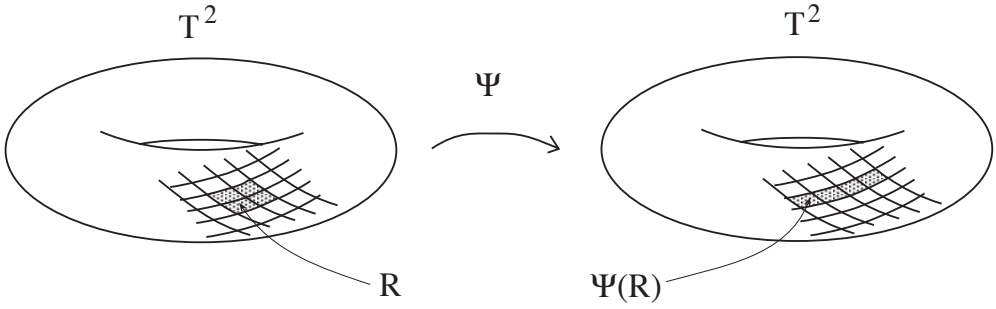

Figure 1.6: The map Ψ stretches along one eigendirection and shrinks along the other.

This metric effectively scales the euclidean metric on M at each level torus $\mathbb{T}^2 \times \{t\}$.

The universal cover $\widetilde{M}$ of M is homeomorphic to $\mathbb{R}^2 \times \mathbb{R}^1$. Think of $\widetilde{M}$ with the $\mathbb{R}^2$ direction horizontal and the $\mathbb{R}^1$ direction vertical, and choose coordinates x, y, z on $\widetilde{M}$ such that the positive x- and y-axes correspond to the eigenvectors v_- and v_+. Then the Solv metric shrinks along the x axis and stretches along the y axis as $t \to \infty$.

A pseudo-Anosov homeomorphism on a hyperbolic surface F behaves locally just like an Anosov homeomorphism on a torus. Like an Anosov map on a torus, a pseudo-Anosov map preserves a pair of transversely measured 1-dimensional foliations on the hyperbolic surface F. Near most points of the surface F, the pseudo-Anosov homeomorphism stretches each region of the hyperbolic surface by some factor λ along the unstable foliation and shrinks it by a factor of λ along the stable foliation, just as in the Anosov case. However, the Euler characteristic of a hyperbolic surface is negative,

therefore both of these foliations will usually have finitely many singularities (the only exception is the case of a punctured torus, where there need not be any singularities). Therefore the resulting pair of transverse 1-dimensional foliations may contain finitely many singular points.

Definition 1.2.16 *A **pseudo-Anosov** homeomorphism Ψ from a hyperbolic surface F to itself is a map which preserves 2 transversely measured, 1-dimensional, singular foliations on F, permutes the singularities of these foliations, and is given in local coordinates by the matrix*

$$\begin{pmatrix} \lambda & 0 \\ 0 & \lambda^{-1} \end{pmatrix}$$

away from the singularities.

There are no closed leaves in these transversely measured foliations. Otherwise, there would be a shortest one, but it will be shrunk by one of Ψ, Ψ^{-1} – a contradiction. Thus the only singularities these foliations may have are n-pronged singularities, as shown in Figure 1.7.

A natural metric on $\mathbb{R}^3$ similar to the Solv metric, called the **singular Solv** metric, gives a metric on a hyperbolic 3-manifold which fibers over the circle, as follows. Such a 3-manifold can be represented by some hyperbolic surface F cross I, with top glued to bottom using pseudo-Anosov monodromy Ψ. The map Ψ gives rise to a pair of transverse, (usually) singular,

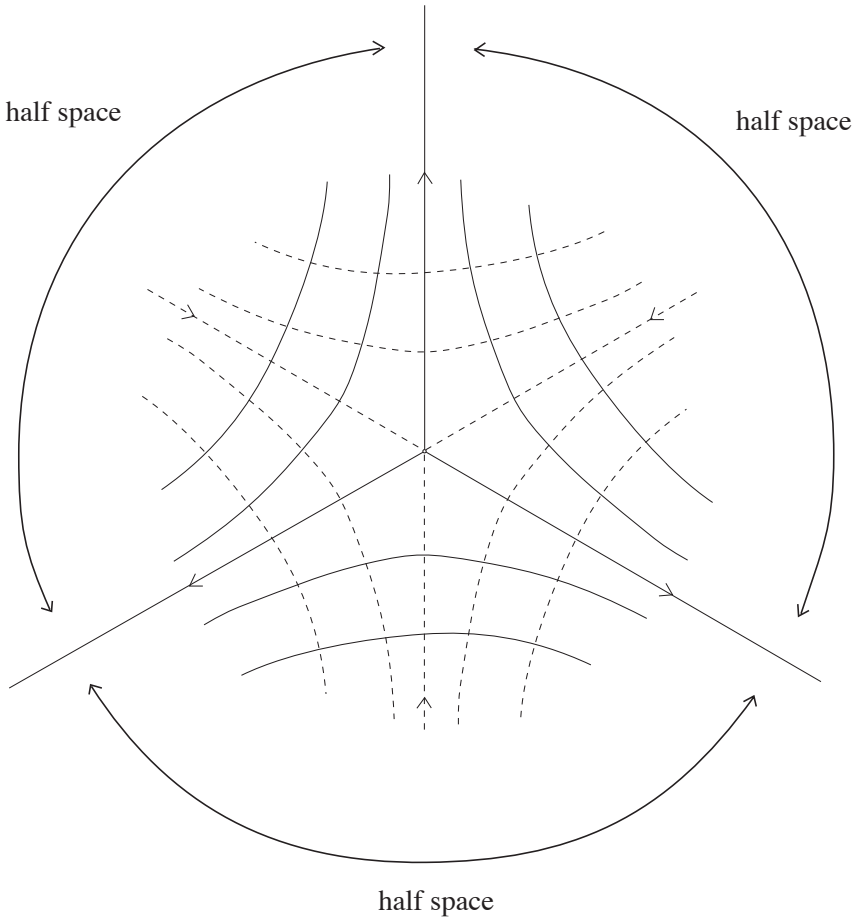

Figure 1.7: A 3-pronged singularity.

1-dimensional foliations on F. Suspending this pair of 1-dimensional foliations through the manifold M produces a pair of singular, 2-dimensional foliations on M. The singular Solv metric is then given by the description below.

Definition 1.2.17 *The* ***singular Solv metric*** *on M is given as follows: The pseudo-Anosov monodromy Φ provides M with a pair of 2-dimensional, transverse, singular foliations. In neighborhoods disjoing from these finitely many singularities, the singular Solv metric agrees with the Solv metric. In a neighborhood of each singularity, the singular Solv metric is given by decomposing the neighborhood into a finite number of half spaces (see Figure 1.7), putting the Solv metric on each of the half spaces, and glueing them back together using isometries.*

When there are an even number, $2n$, of prongs, this may be viewed as taking an n-fold branched cover of Solv, branched over a vertical geodesic.

Thus, in the manifold M that we are considering, the fiber F is filled with a pair of potentially singular one-dimensional foliations, where each foliation consists of the integral curves of the vector field given by one of the eigenvectors of the pseudo-Anosov map Ψ. Foliating each level surface $F\times\{t\}$ by these integral curves gives M the corresponding pair of singular 2-dimensional foliations, which are transverse to the fiber F. The intersections of this pair of 2-dimensional foliations form the flow lines of the suspension

flow on M.

1.2.3 A Hyperbolic Cusp

The fiber F can be thought of as $F^+ \setminus \{p_1, \ldots p_j\}$; the manifold M has finitely many cusps. In order for the modified metric on M to be complete, the cusps given by these torus boundary components must be "pushed off to infinity": a hyperbolic cusp is a product $\mathbb{T}^2 \times [0, \infty)$ with a metric which scales the level tori $\mathbb{T}^2 \times \{t\}$ down exponentially as $t \to \infty$, as indicated in Figure 1.8a. A convenient way to think of a hyperbolic cusp is to envision it as the vertical column in $\mathbb{H}^3$ described by $\{\text{parallelogram in the plane } z = 1\} \times [1, \infty)$ with opposite sides of each $\{\text{parallelogram}\} \times \{t\}$ glued together to make $\mathbb{T}^2 \times \{t\}$, as in Figure 1.8b. More formally,

Definition 1.2.18 *A **hyperbolic cusp** is a quotient H_t/Γ, where $H_t = \{(x, y, z) | z \geq t\}$ and Γ is a discrete group of parabolics isomorphic to $\mathbb{Z} \times \mathbb{Z}$ generated by*

$$\begin{pmatrix} 1 & \alpha \\ 0 & 1 \end{pmatrix} \quad \textit{and} \quad \begin{pmatrix} 1 & \beta \\ 0 & 1 \end{pmatrix},$$

where α and β are complex numbers. The metric on the cusp is given by the upper half space metric on H_t.

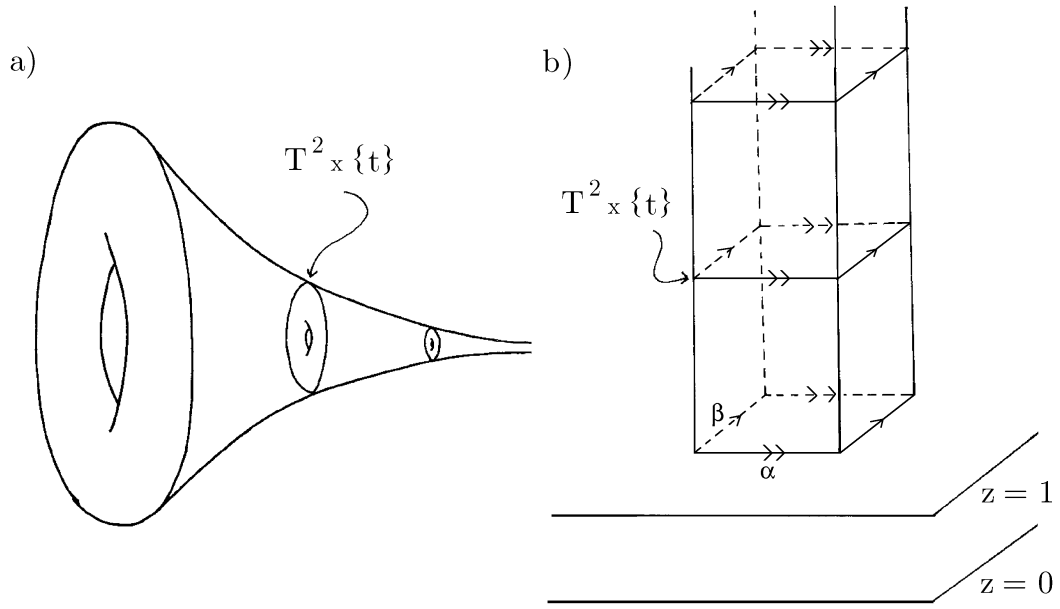

Figure 1.8: A schematic picture of a hyperbolic cusp.

The **shape** of such a cusp as defined above is given by the two vectors α and β, as seen in Figure 1.8b.

Thus the universal cover of a hyperbolic cusp is isometric to the horoball consisting of all points above and including the plane $z = 1$ in the upper half space model of $\mathbb{H}^3$. This set will be referred to as the **standard cusp** in $\mathbb{H}^3$. If $\pi : \mathbb{H}^3 \to M$ is the universal cover of M, then $\pi^{-1}(\text{cusp})$ is a union of **horoballs** in $\mathbb{H}^3$; so called because in the Poincare ball model of hyperbolic space, the preimage of a cusp appears as a collection of round balls which are tangent to the sphere at infinity. The boundary of a horoball is called a **horosphere**.

Once and for all, fix an open horotorus neighborhood of each cusp in M so that in $\widetilde{M}$, each horoball is at least distance 1000 from all the others. This chooses a fixed collection of horoballs in $\widetilde{M}$, one for each preimage under $\pi_1 M$ of each cusp of M. When we refer to the horoballs in $\widetilde{M}$, we will most often be thinking of this specific collection of fixed horoballs. This fixed collection will be referred to often in this thesis; to emphasize this choice we will set it aside in a note:

Note 1.2.19 *We have fixed, for each cusp in M, an open horotorus neighborhood with the property that each horoball in $\widetilde{M}$ is at least a distance 1000 from all the other horoballs.*

At times during the proof it will be necessary to consider the compact space N obtained by removing these open neighborhoods of the cusps from M. This space N is called the **neutered space** of the manifold M (terminology due to R. Schwarz); its universal cover is obtained from the universal cover of M by removing its horoballs. Figure 1.9 is a picture of the neutered space of a 2-dimensional manifold.

The singular stable and unstable 2-dimensional foliations which arise from the action of Ψ on F extend to singular stable and unstable 2-dimensional foliations on the closure F^+. Thus, the points $p_1, \ldots p_j$ which comprise $F^+ \setminus F$ may be regular or singular points on F. Therefore M may have two different types of cusps, those which correspond to tori boundary components arising from a non-singular point or from a singular point. Call these two types of cusps **regular cusps** and **singular cusps**, respectively.

1.2.4 A Useful Intermediate Cover of M

Much of the discussion in this thesis will involve a specific **intermediate cover** $\widehat{M}$ of M. Recall that M^+ and F^+ denote the closures of M and F respectively. Removing the preimages $q^{-1}(p_1), \ldots, q^{-1}(p_j)$ from the universal cover $q : \widetilde{F^+} \to F^+$ gives an intermediate cover of F which we will call $\widehat{F}$; namely, $\widehat{F} = \widetilde{F^+} \setminus \{q^{-1}(p_1), \ldots, q^{-1}(p_j)\}$. Thus F^+ is the cover corresponding to the kernel of $\pi_1 F \to \Pi_1 F^+$. Loosely speaking, $\widehat{F}$ is obtained by unwrapping the part of the fundamental group of F which corresponds

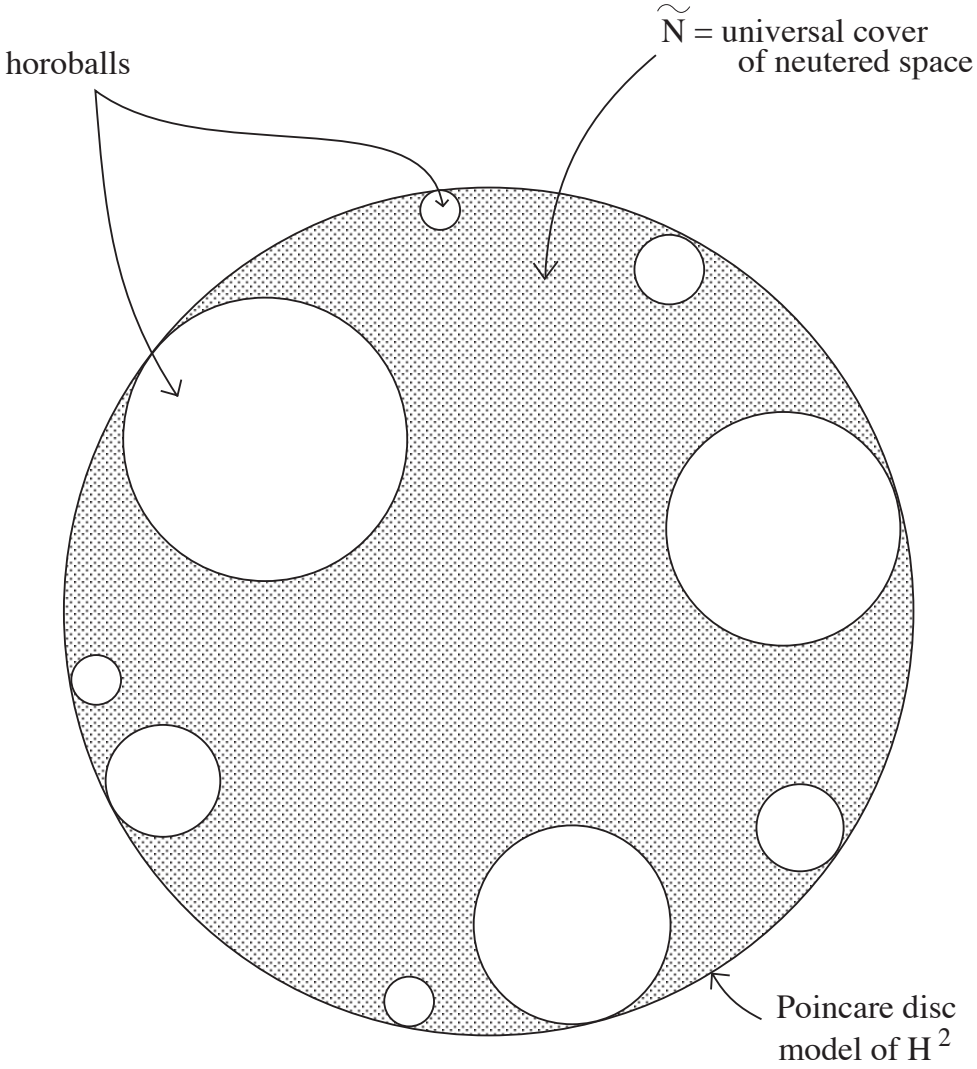

Figure 1.9: The universal cover of the neutered space of a manifold.

to the fundamental group of F^+, and which leaves the fundamental group around the punctures in F untouched. Let $\widehat{M}$ be the intermediate cover of M given by $\widehat{F} \times \mathbb{R}^1$.

The manifold $\widehat{M}$ can be seen as a subset of $\widetilde{M^+}$, the universal cover of the closure of M. Let $\widehat{M}$ inherit the subspace metric of the singular Solv metric on $\widetilde{M^+}$. Then $\widehat{M}$ is homeomorphic to $\mathbb{R}^3$ with infinitely many "vertical" cylinders removed, where a cylinder is defined as

$$\{(x, y, z) | d_{Solv}((x, y, z), \text{cusp line}) \leq \epsilon\}$$

for some fixed $\epsilon > 0$. Each of these cylinders covers one of the torus boundary components of M.

These vertical cylinders will correspond either to regular cusps or singular cusps. Under the singular Solv metric on $\mathbb{R}^3$, each cylinder is circular in cross-section. However, in the Euclidean metric on $\mathbb{R}^3$, these cylinders are not circular. On the contrary; the boundary of a regular cusp in $\widehat{M}$ in the Euclidean metric is a cylinder which becomes elongated in one cross-sectional direction and shortened in a transverse direction as $z \in \mathbb{R}^1$ tends to infinity. An accurate yet perhaps difficult to visualize picture of a regular cusp under the Euclidean metric is given in Figure 1.10. The elongating and shortening effect can be more easily seen if we "square off" a cusp so that it has 4 sides, two of which are parallel to one eigenvector of the pseudo-Anosov monodromy, the other two parallel to the other eigenvector (see Figure 1.11).

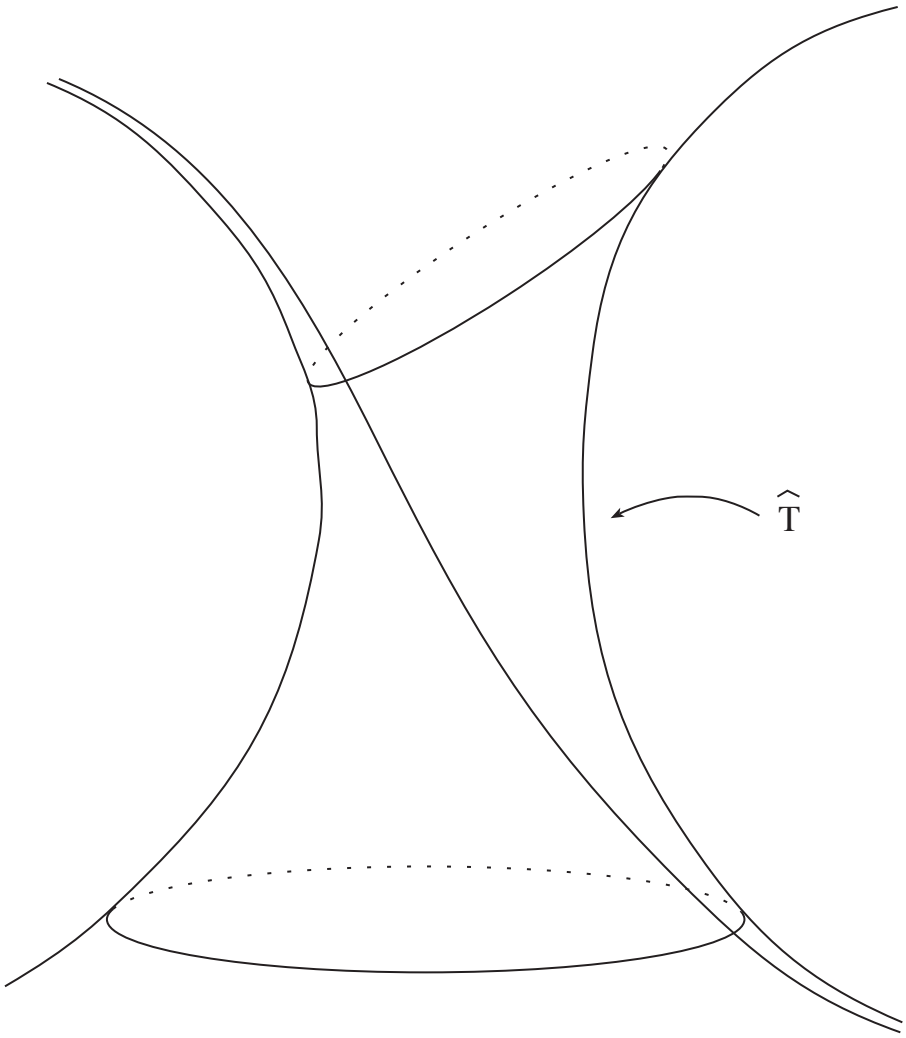

Figure 1.10: A portion of a regular cusp of $\widehat{M}$.

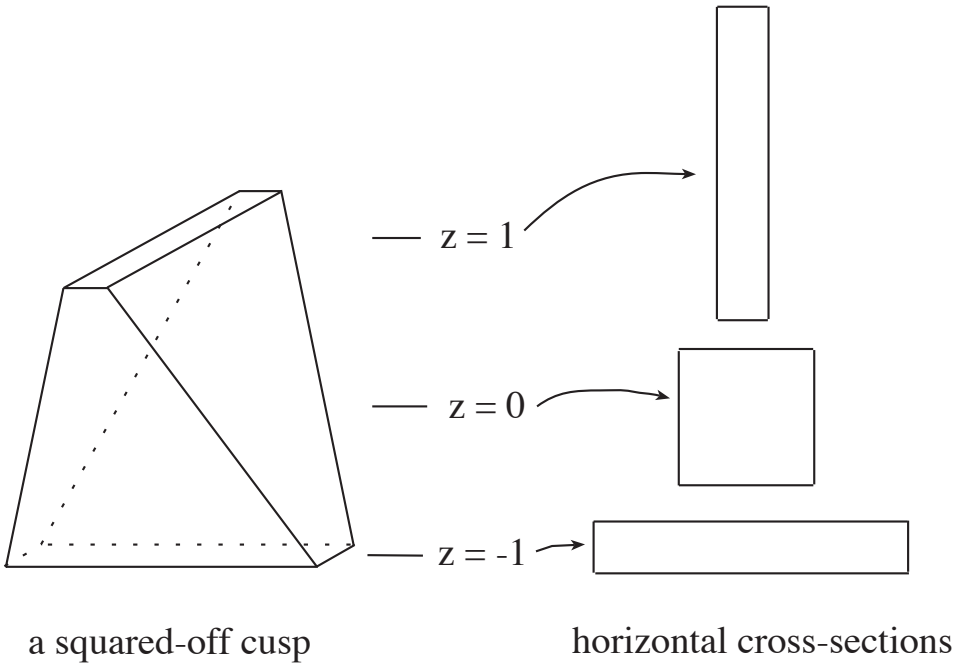

Figure 1.11: A portion of a "squared-off" regular cusp of $\widehat{M}$.

A singuar cusp is slightly more complicated: in the Euclidean metric it is a cylinder which becomes more eccentrically star shaped, lengthened along the unstable singular foliation and shortened along the stable singular foliation, as z tends to infinity, as in Figure 1.12.

We will modify the metric on the intermediate cover of each cusp (which will have the effect of modifying the metric in M) so that it agrees with the singular Solv metric on the boundary of the cusp, but gets scaled on successive concentric cylinders so that the cusp is isometric to a hyperbolic cusp. Let $\widehat{T}$ represent a preimage in $\widehat{M}$ of a cusp in M. The modification of the metric in $\widehat{T}$ will be performed by mapping the universal cover of $\widehat{T}$ to the standard cusp in the upper half space model of hyperbolic space, then giving $\widehat{T}$ the pull-back metric. Modifying the metric in the neighborhoods of all the cusps in this fashion gives rise to the **modified singular Solv metric**. This modified metric will be shown to be quasi-isometric to the hyperbolic metric on M. This thesis will show that the flow lines are quasigeodesic in this modified metric, and hence quasigeodesic in the hyperbolic metric on M.

1.3 Main Result

The main result of this thesis is the following theorem:

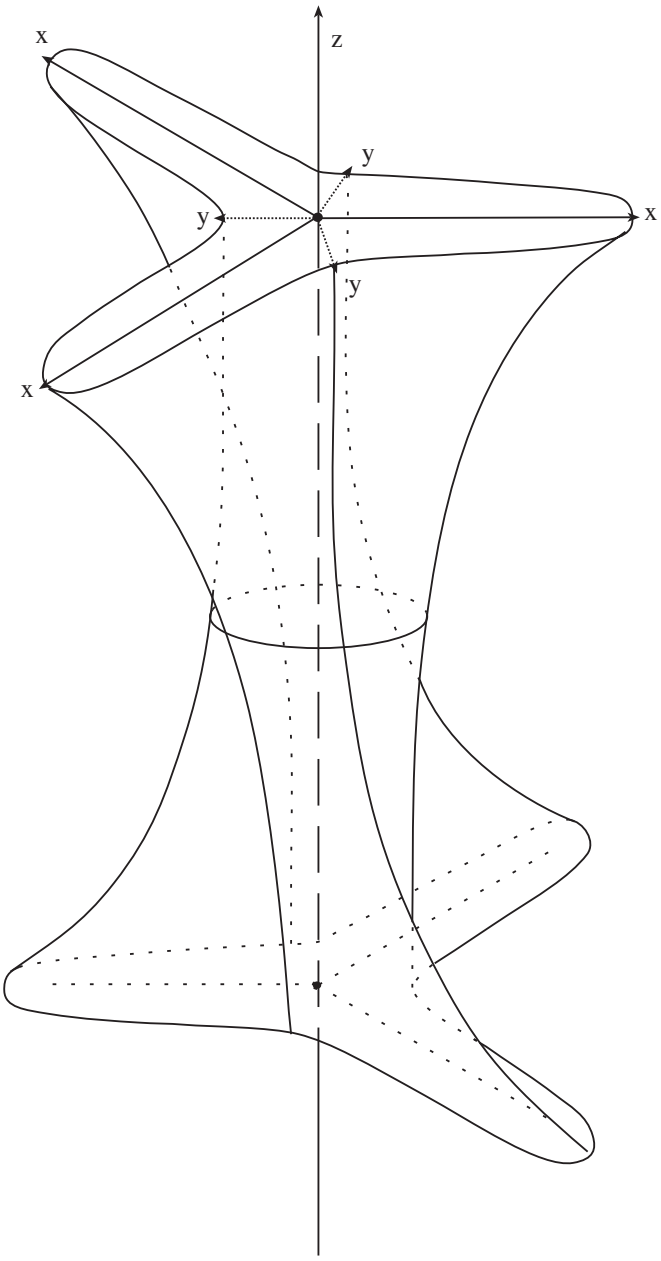

Figure 1.12: A portion of a singular cusp of $\widehat{M}$.

Theorem 1.3.1 (Main Theorem) *The suspension flow on a cusped hyperbolic 3-manifold M which fibers over the circle is uniformly quasigeodesic.*

Any path is quasigeodesic if and only if it makes reasonably paced progress along inside a neighborhood of a true geodesic. To make this concept precise,

Definition 1.3.2 *A path $c \subseteq \mathbb{H}^3$ **tracks** a geodesic segment $\gamma \subseteq \mathbb{H}^3$ if*

1. *There exists $R > 0$ so that c lies within a neighborhood of radius R of γ.*

2. *There exists $Q > 0$ such that if the length of a subpath of c with endpoints a and b is at least Q, then the distance between $\pi(a)$ and $\pi(b)$ along γ is at least 1, where π denotes orthogonal projection onto γ.*

We will often refer to the property stated in part 2 of the definition by saying the subpath of c makes **reasonable progress** along γ.

Clearly any finite segment of path tracks any geodesic by letting R be the maximum distance between a point on the segment and its projection onto the geodesic, and letting Q be larger than the length of the segment. Thus it is only interesting to remark that a path tracks a geodesic if the path has infinite length, or if one is looking for uniform values for R and Q for infinitely many flow lines.

Proposition 3.1.1 says that a path is a quasigeodesic if and only if it tracks a true geodesic. Thus we will show that the flow lines of the suspension flow on M are uniformly quasigeodesic by showing that there are (uniform) constants R and Q so that each flow line tracks a geodesic, with tracking constant R and Q. Separate arguments address the situations inside and outside of the cusps.

Consider the path of the flow line in the large. If we push the flow lines out of the cusps into the neutered space of the manifold, we can for the moment ignore the effect of the cusps on the flow lines. We will show that a "pushed" flow line loosely tracks the geodesic which connects its endpoints, in that it follows along inside a neighborhood of the geodesic *together with the horoballs it intersects* (recall that we have chosen a fixed collection of horoballs, one for each preimage under $\pi_1 M$ of each cusp of M – Note 1.2.19). This will give us an idea of the path of a flow line outside the cusps.

Definition 1.3.3 *A* ***string of beads*** *along a geodesic γ in $\mathbb{H}^3$ consists of γ together with all the horoballs which γ intersects.*

Therefore, for the periods of time that the unpushed flow line spends outside the cusps, it tracks a geodesic. But what about the portions of flow lines which lie inside the cusps? There could conceivably be a sequence of flow lines which go further and further into the cusp, each one being more

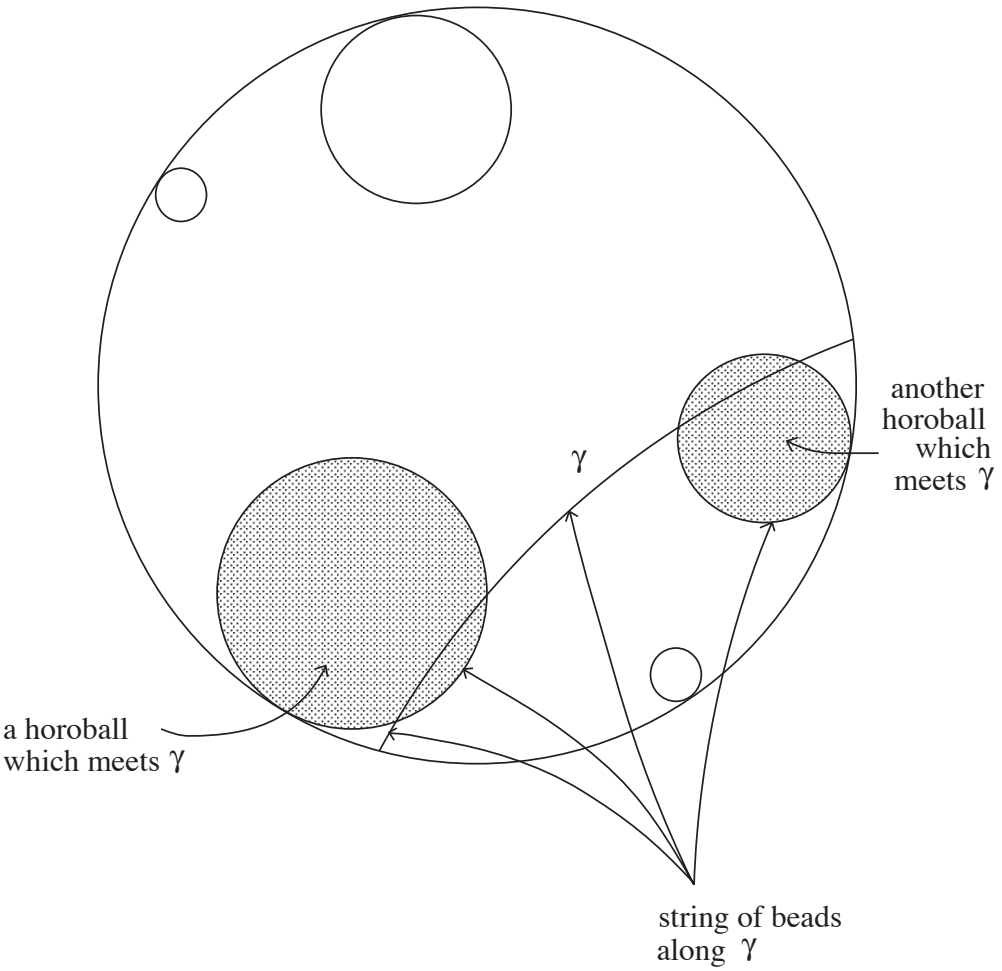

Figure 1.13: The string of beads along a geodesic.

crooked and thus needing a larger quasigeodesic constant than the previous. However, a direct calculation will show that this does not happen; the flow lines are uniformly quasigeodesic in the cusp. Thus any portion of flow line which lies in a cusp passes near the geodesic connecting its endpoints when inside the cusp, as well. Therefore, we will be able to show that flow lines stay near hyperbolic geodesics at all times; hence they are quasigeodesic.

1.4 Outline

We will show that the flow lines of the suspension flow of M are quasigeodesic by showing they track geodesics with uniform tracking constants. Much of the proof relies on the fact that the portions of the flow lines which lie inside the cusps are uniformly quasigeodesic. Thus Chapter 2 is devoted to establishing this proposition. Chapter 3 shows that the flow lines lie inside uniform radius neighborhoods of geodesics, and Chapter 4 guarantees that the flow lines progress along these neighborhoods at a reasonable pace, as described in the second part of the definition of tracking.

The flow lines are shown to be quasigeodesic in the cusp using a direct calculation. First, we will define a map which takes the universal cover of a neighborhood of a missing flow line onto the universal cover of a standard cusp, which is the horoball given by $z \geq 1$ in the upper half space model of hyperbolic space. Under this map, some of the flow lines will become

trapped in the cusp, never to return to the neutered space of the manifold, while other flow lines will enter the cusp at some point and then eventually leave the cusp. The flow lines which become trapped in the cusp are seen as Euclidean straight lines going off to infinity in the upper half space model of $\mathbb{H}^3$; these trapped flow lines are shown to be quasigeodesic by a fairly simple calculation. The flow lines which enter and then eventually leave the cusp are called the returning flow lines, and are somewhat more complicated to handle. Using an argument based on the rate at which the returning flow lines dive into the cusp and a rather extensive calculation, we are able to show that if a returning flow line is sufficiently long, the length of such a flow line is bounded above by a universal constant multiple of the hyperbolic distance between the endpoints.

The bulk of the rest of the proof lies in Chapter 3, where we show that flow lines satisfy part 1 of the definition of tracking; that is, that there is a constant $R_\Phi > 0$ such that every flow line lies within a neighborhood of radius R_Φ around a geodesic. This result is first shown for arbitrary finite segments of flow lines, and then extended to entire flow lines. This section of the proof requires creating several constants; to minimize confusion, a glossary of symbols is included at the end of this document.

The segments of flow lines which lie inside a cusp are quasigeodesic with quasigeodesic constant $K_c = K_{\text{cusp}}$. Since the neutered space N of M is compact, flow line segments which lie in N are uniformly quasigeodesic as well. However, it does not follow that an entire flow line is

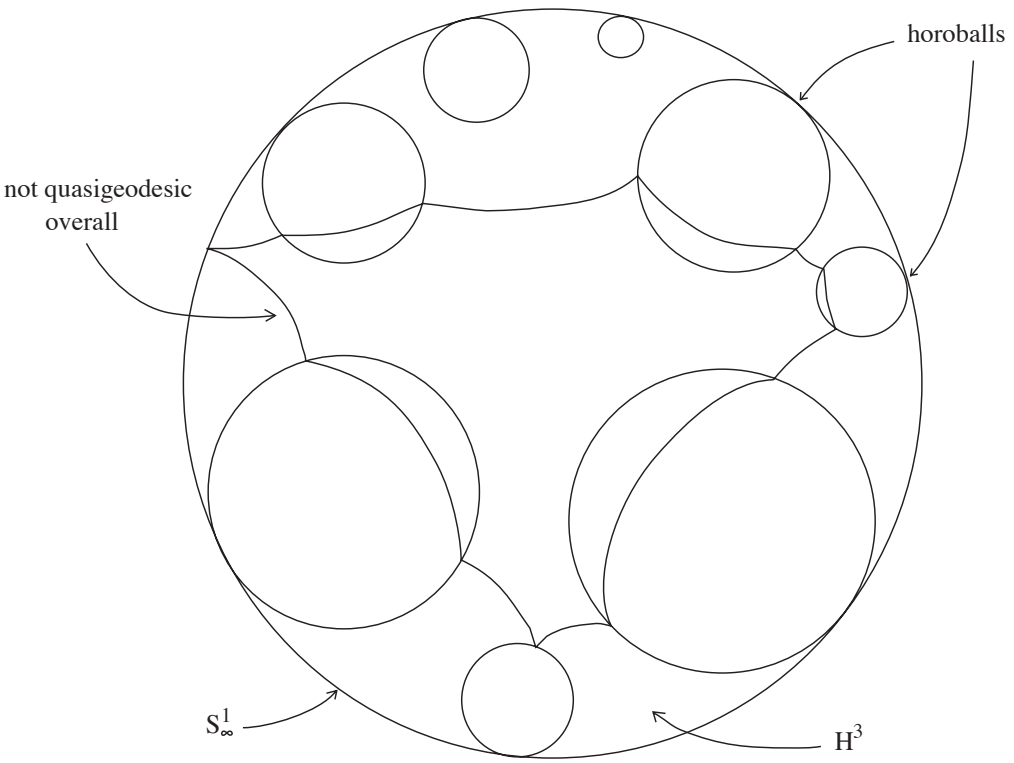

Figure 1.14: A path made of quasigeodesic segments need not be quasigeodesic overall.

quasigeodesic: these segments may be arranged so that the overall path is not quasigeodesic, as in Figure 1.14.

Therefore we should consider the path of the flow line in the large. If we push each flow line out of the cusps and into the neutered space, we have a path which lies entirely in N (see Figure 1.15).

Definition 1.4.1 *Given a path c in M, its associated* ***pushed path*** $\overline{c}$ *is*

obtained from c by pushing each point in c out to its unique nearest neighbor in N.

Each point in a path c does indeed have a unique nearest neighbor in N, for any point of c which is in N remains fixed, and any point of c inside a cusp projects orthogonally to a unique point on the boundary of the cusp. Note that this nearest point retraction $r : M \to N$ is homotopic to the identity, and that $\overline{c} = r \circ c$.

We will see that each segment of such a "pushed" flow line is a K_{p}-quasigeodesic *in the neutered space*, where $K_{\mathrm{p}} = K_{\mathrm{pushed}}$ does not depend on choice of flow line. Next we show any quasigeodesic in the neutered space stays close to a string of beads, where distance here is measured in the hyperbolic metric. This will give us a constant $R_{\mathrm{p}} = R_{\mathrm{pushed}} > 0$, depending only on K_{p}, so that a pushed flow line segment lies within hyperbolic distance R_{p} of the string of beads along the hyperbolic geodesic connecting its endpoints (see Figure 1.16). Thus each pushed flow line segment roughly follows along the path of the hyperbolic geodesic connecting its endpoints, at least as closely as it can given that it may not enter any cusp that the geodesic enters.

Flow line segments are identical to their corresponding pushed flow line segments except for the portions which lie inside the cusps. In Chapter 2 we showed that flow line segments are quasigeodesic in the cusp. Thus, there is a constant $R_{\mathrm{c}} = R_{\mathrm{cusp}}$ so that every portion of flow line segment which lies entirely inside the cusp lies within an R_{c}-neighborhood of the

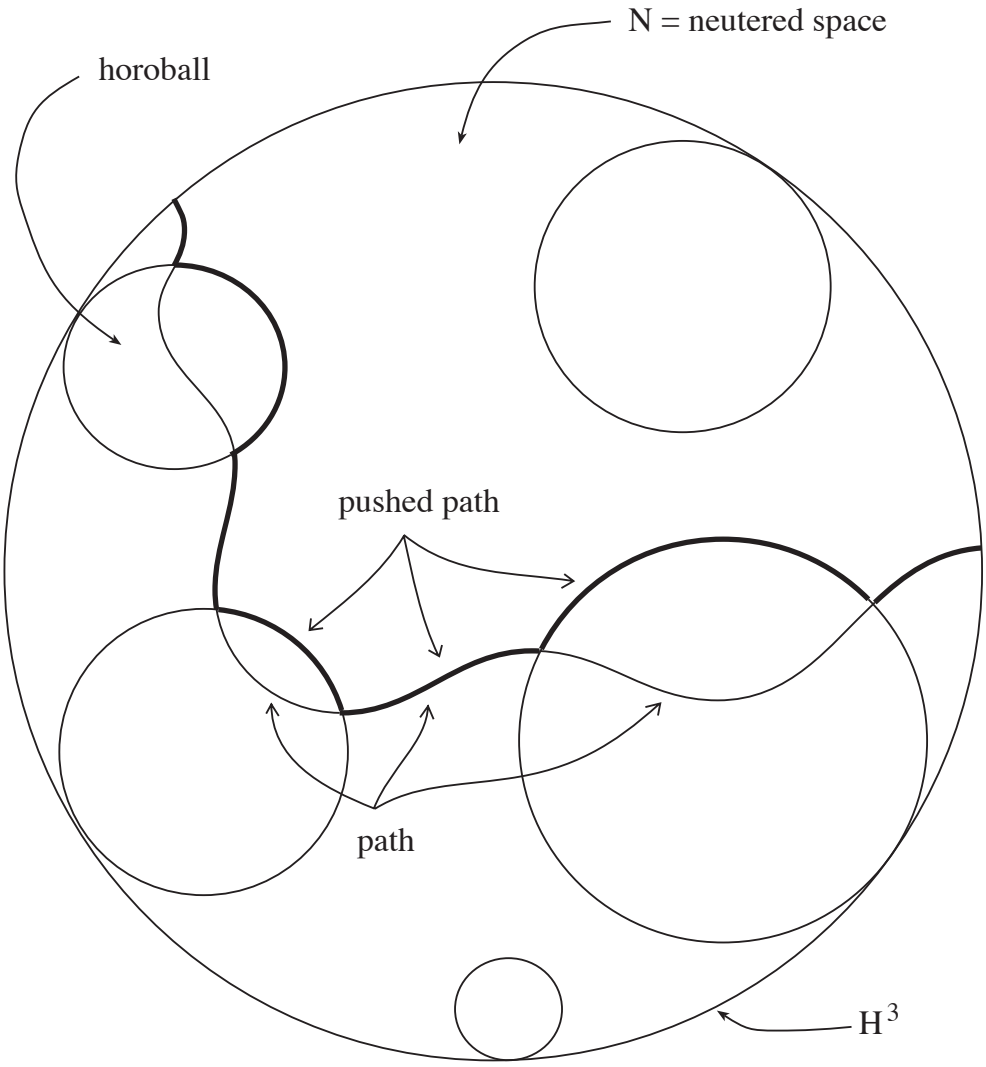

Figure 1.15: A pushed path.

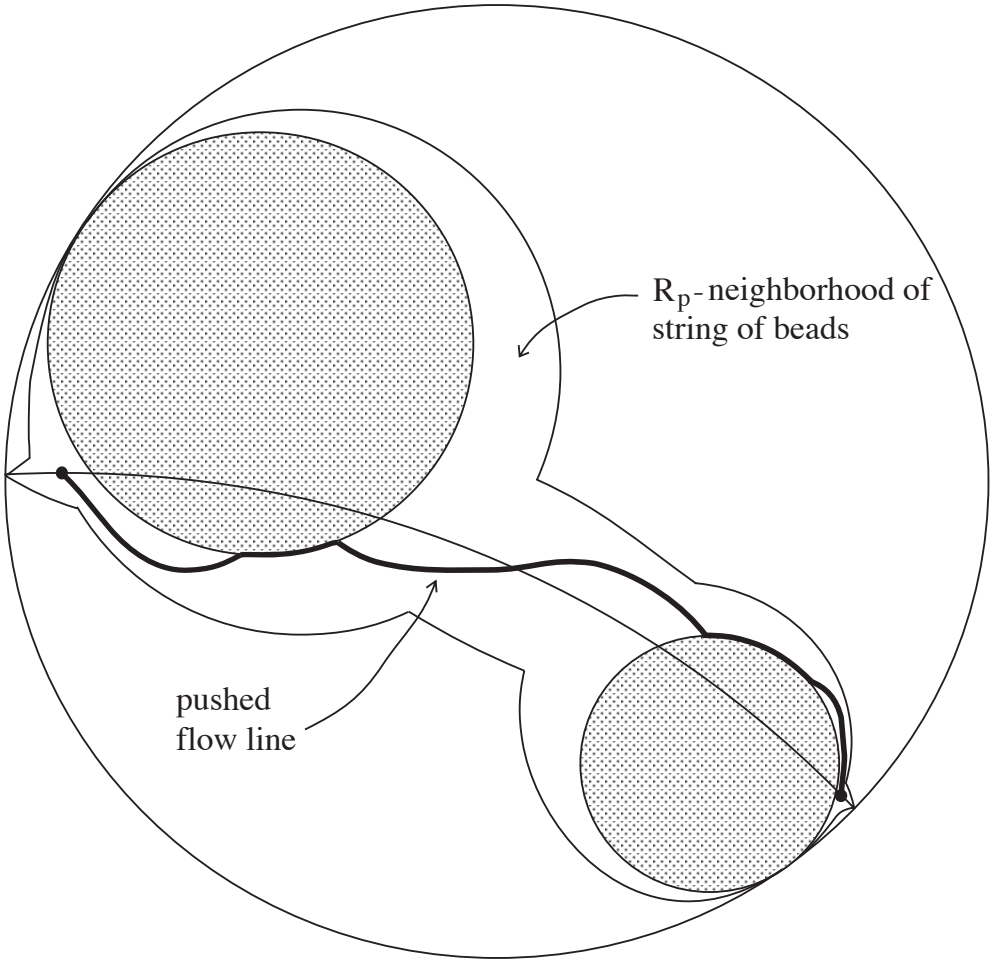

Figure 1.16: Pushed flow lines lie within R_{p}-neighborhoods of strings of beads.

geodesic connecting its endpoints. Thus a flow line segment lies within an $R_{\mathrm{s}} = R_{\text{string of beads}}$ neighborhood of the string of beads along the geodesic connecting its endpoints, where $R_{\mathrm{s}} = R_{\mathrm{p}} + R_{\mathrm{c}}$ (see Figure 1.17).

Finally, we find a constant R_Φ such that each flow line segment lies within an R_Φ-neighborhood of the geodesic connecting its endpoints, rather than just the string of beads along this geodesic. This is the most involved part of the proof. Each flow line segment has portions which lie outside all the cusps, and others which pass through a cusp. These cusps need not all be beads of the string of beads connecting the endpoints of the flow line segment. A separate argument is needed to address the portions of flow line which lie entirely outside all cusps, and portions of flow line which travel through at least one cusp. Both arguments are outlined below.

First, we will consider portions of a flow line segment which lie outside of all cusps. Portions which also lie outside R_{s}-neighborhoods of a cusp must lie within R_{s} of the string, so these ones automatically satisfy the condition we're looking for. Portions which lie within an R_{s}-neighborhood of a cusp are slightly more problematic; in fact, this is where most of the work in the proof takes place. The Limited Time Lemma finds a maximum length M_{s} (depending only on R_{s}) of a flow line segment which lies within a neighborhood of radius R_{s} of a cusp without actually entering that cusp. We can get from any point on such a flow line segment to the string by first following along the flow line until we reach the boundary of the R_{s}-neighborhood of the bead (a distance at most M_{s}), then taking a path of

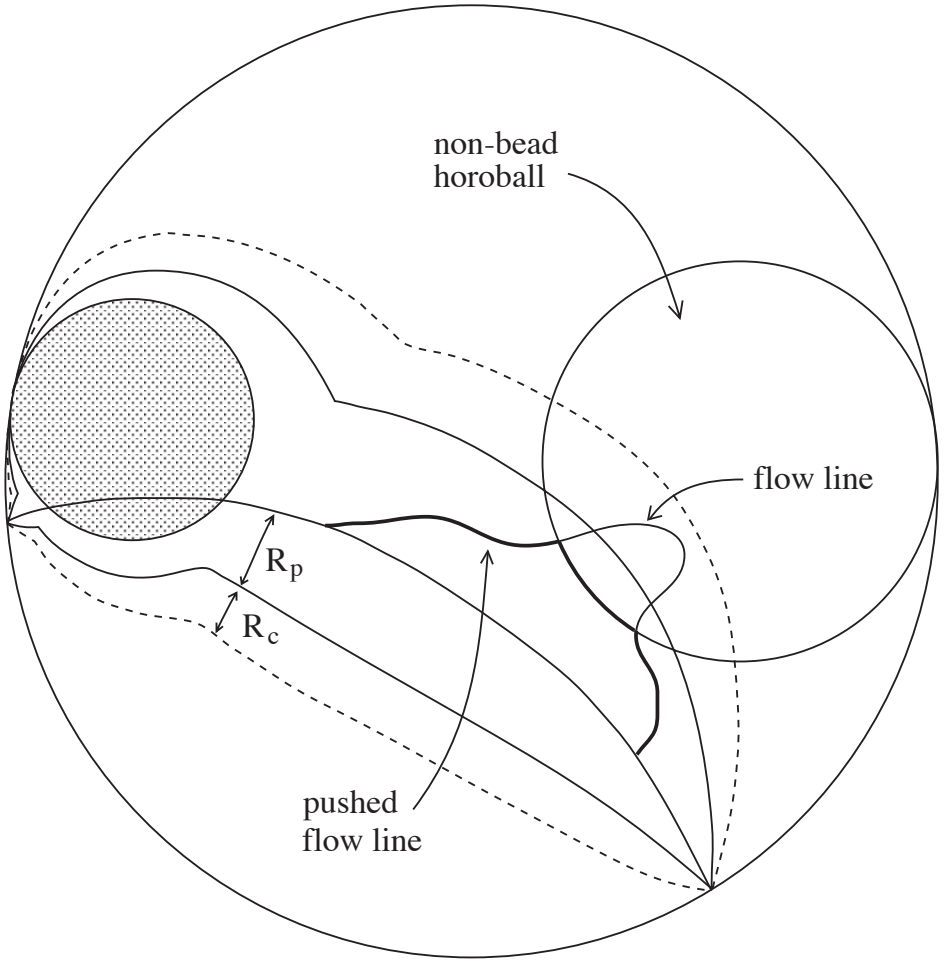

Figure 1.17: Flow line segments lie within $R_{\mathrm{p}} + R_{\mathrm{c}} = R_{\mathrm{s}}$-neighborhoods of strings of beads.

length at most R_{s} to the string (see Figure 1.18). Thus segments of flow line outside the cusps must be within radius $R_{\mathrm{s}} + M_{\mathrm{s}}$ of the associated geodesic.

Next we will consider portions of a flow line segment which travel through at least one cusp. Let γ be the geodesic connecting the endpoints of a segment of flow line which travels through at least one cusp. Any segment of flow line inside a cusp is quasigeodesic, therefore by Proposition 3.1.1 (paths are quasigeodesic if and only if they track a geodesic), it remains within a R_{c} neighborhood of a geodesic segment γ' contained in the cusp, with endpoints within $R_{\mathrm{s}} + M_{\mathrm{s}}$ of the original geodesic γ (see Figure 1.19). Since neighborhoods of geodesics are convex, the geodesics γ and γ' lie within $R_{\mathrm{s}} + M_{\mathrm{s}}$ of each other. Therefore, the portions of flow line which lie inside the cusp lie within $R_{\mathrm{fs}} = R_{\text{flow segments}} = R_{\mathrm{s}} + M_{\mathrm{s}} + R_{\mathrm{c}}$ of the original geodesic γ. Since segments of flow line outside the beads must lie near the string, it follows that the entire flow line segment, both portions inside and outside the cusps, lies within R_{fs} of the geodesic connecting its endpoints.

Passing to longer and longer subsegments of a flow line, we will see that the endpoints of a flow line are distinct on the sphere at infinity, and that each entire flow line lies inside a $R_{\Phi} = R_{\mathrm{fs}} + 1$ neighborhood of the geodesic connecting its endpoints at the sphere at infinity. This geodesic, then, is the canonical geodesic associated to a flow line. Hence flow lines satisfy part 1 of the definition of tracking.

Finally, in Chapter 4 we see through a direct calculation that flow lines make reasonable progress through the neighborhoods of their canonical as-

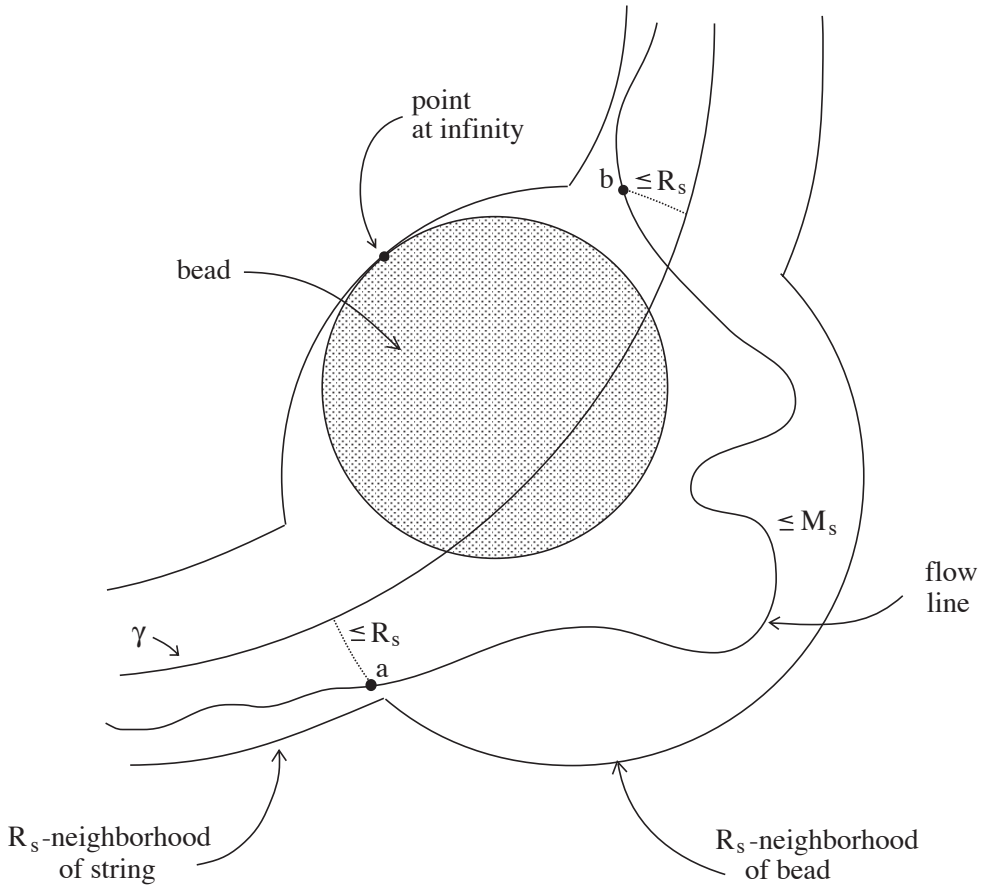

Figure 1.18: A flow line segment in an $R_{\rm s}$ neighborhood of a bead which does not enter the bead lies within $R_{\rm s} + M_{\rm s}$ of the string.

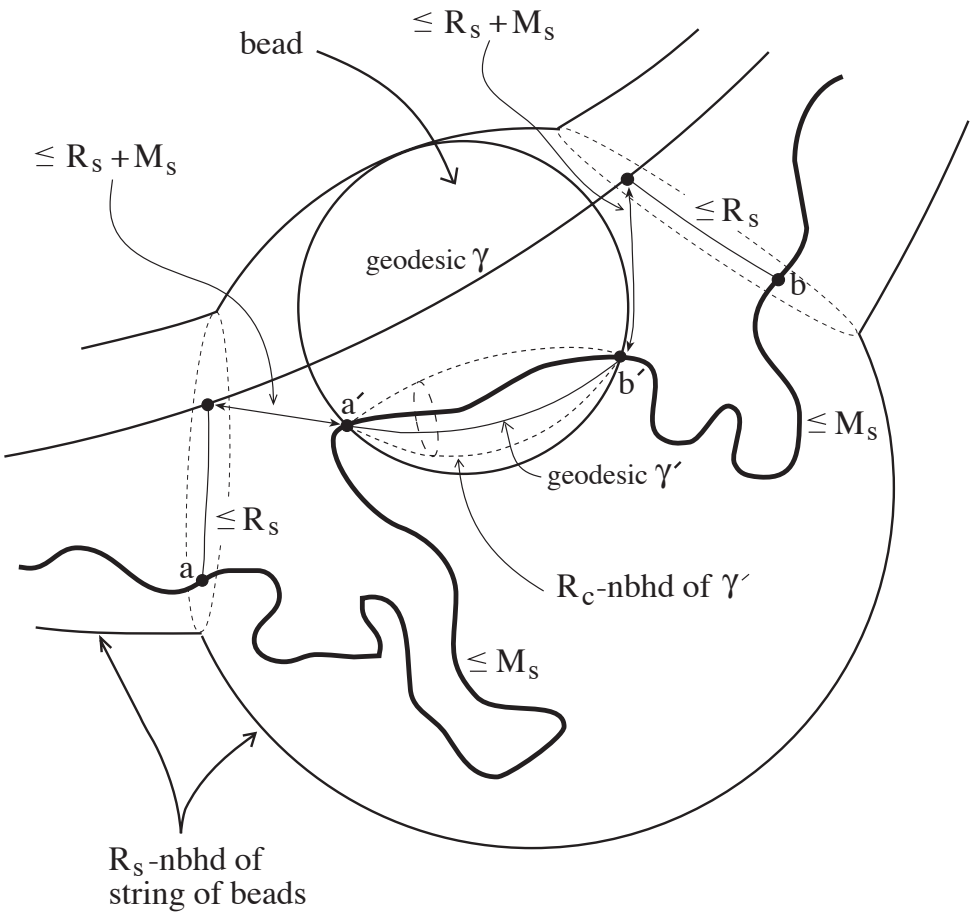

Figure 1.19: γ' is within $R_{\rm s} + M_{\rm s}$ of γ.

sociated geodesics by finding a universal constant $Q_\Phi > 0$ such that all flow lines satisfy part 2 of the definition of tracking using this Q_Φ. Thus flow lines uniformly track geodesics, and hence are uniformly quasigeodesic.

Chapter 2

Flow Lines are Quasigeodesic Inside Cusps

The singular Solv metric on a hyperbolic manifold which fibers over the circle is useful when considering the suspension flow on the manifold, for in this metric the flow lines then are simply straight vertical lines. However, the drawback to this metric is that it is not quasi-isometric to the hyperbolic metric on a cusp in the manifold, for it does not put the missing flow lines at infinity.

On the other hand, it is not practical to simply start with the original hyperbolic metric on M, because then one has no control over the path that the flow lines take through M. Starting instead with the singular Solv metric and modifying the metric in a neighborhood of the cusps, it is easy to choose coordinates so that one coordinate will parametrize the flow lines.

Therefore we will modify the singular Solv metric in each cusp to create a new metric, which we will call the **modified singular Solv metric**, or modified metric for short. This will be done by scaling the singular Solv metric on concentric tori in each cusp to make the modified metric on the cusp quasi-isometric to the hyperbolic metric on the cusp. It is in this modified metric that we will show the flow lines are uniformly quasigeodesic.

2.1 The Modified Metric

In this thesis we modify the metric in each cusp neighborhood so that it agrees with the singular Solv metric (see Section 1.2.2) on the boundary of the cusp, but gets scaled on successive tori cylinders so that the cusp is isometric to a hyperbolic cusp. The modification takes place by redefining the metric on a cusp using the pull-back of the hyperbolic metric under a cleverly defined map f of the hyperbolic metric. This f will map from the universal cover of the cusp to the standard cusp (recall that the standard cusp is everything above and including the horosphere $z = 1$ in the upper half space model of hyperbolic space). Once we have the metric in the cusps modified, we will **blend** the singular Solv and modified metrics on a $\mathbb{T}^2 \times I$ product neighborhood between the singular Solv metric on the neutered space N of the manifold and the cusp with the modified metric.

We will show the portions of the flow lines which lie in the cusps are

quasigeodesic in the modified metric by proving that their images are quasigeodesic in $\mathbb{H}^3$ under the map f to the standard cusp.

2.1.1 Quasi-Isometry Between Modified and Hyperbolic Metrics

We want to show that there exists a quasi-isometry between $\mathbb{H}^3$ and the universal cover of the M under the modified singular Solv metric, for then we will know that quasigeodesics under the modified metric correspond to quasigeodesics in $\mathbb{H}^3$. Since the metrics we are considering are Riemannian, it suffices to show that the manifolds downstairs are quasi-isometric. Thus the goal of this section is to establish that the new metric on the manifold M created by modifying the singular Solv metric in cusp neighborhoods as described above is quasi-isometric to the hyperbolic metric on M.

To do this, we will first establish a quasi-isometry between a modified cusp and a hyperbolic cusp. The neutered space of M under the modified metric (which is simply the Solv metric since we are away from the cusps) is quasi-isometric to the neutered space under the hyperbolic metric, by compactness. We then glue each (modified) cusp into the neutered space, blending the metrics on a $\mathbb{T}^2 \times I$ connector between the two pieces. The details follow below.

Definition 2.1.1 *Two metrics m_1 and m_2 on a manifold are* ***quasi-isometric*** *if there is a homeomorphism isotopic to the identity map from (M, m_1) to (M, m_2) which is bi-Lipshitz.*

The proof that the hyperbolic and modified metrics on M are quasi-isometric makes use of the following lemma.

Lemma 2.1.2 *Any two Riemannian metrics on a compact manifold are quasi-isometric.*

Proof: Let X be a compact manifold, and let ds_1^2 and ds_2^2 give the two Riemannian metrics on X. Under the identity map, the ratio $\frac{ds_1^2}{ds_2^2}$ is bounded above and below (by compactness). Thus the identity map between X and itself is bi-Lipshitz. □

The neutered space N of M is compact. Thus by Lemma 2.1.2, the singular Solv metric on the neutered space N of M is quasi-isometric to the hyperbolic metric restricted to N, with some bi-Lipshitz constant B_N. It remains to find a universal bi-Lipshitz constant so that the modified metric on every cusp of M is quasi-isometric to the hyperbolic metric on that cusp, with that bi-Lipshitz constant. Let $T_1, T_2, \ldots, T_n$ denote the cusps of M.

Lemma 2.1.3 *Any two hyperbolic metrics on a hyperbolic cusp are quasi-isometric.*

Proof: Let T be a cusp endowed with two different hyperbolic structures. The cusp T is a product of the torus $\mathbb{T}^2$ with the interval $[0, \infty)$. Any hyperbolic structure on T is given by the quotient of $\mathbb{R}^2 \times [0, \infty)$ by a group of isometries; let G_1 and G_2 be the two groups of isometries ($G_1 \cong G_2 \cong \mathbb{Z} \times \mathbb{Z}$) corresponding to the two different hyperbolic structures on T. Each group of isometries G_1, G_2 of $\mathbb{R}^2 \times [0, \infty)$ must be the extension of a pair of isometries on $\mathbb{R}^2$ which give rise to the torus.

Since the torus is compact, the geometric structures on the torus given by both groups of isometries are quasi-isometric. Thus the identity map $I_{\mathbb{T}^2} : \mathbb{T}^2 \to \mathbb{T}^2$ is a quasi-isometry with bi-Lipshitz constant $B_{\mathbb{T}^2}$.

The identity map on the cusp T can be seen as the extension of the map $I_{\mathbb{T}^2}$ to a map $I_T : \mathbb{T}^2 \times [0, \infty) \to \mathbb{T}^2 \times [0, \infty)$ by

$$I_T(x, t) = (I_{\mathbb{T}^2}(x), t).$$

Thus the map I_T is also bi-Lipshitz with bi-Lipshitz constant $B_{\mathbb{T}^2}$. Therefore the two hyperbolic metrics on T are quasi-isometric. □

Lemma 2.1.4 (Blending Lemma) *Given Riemannian metrics ds_1^2 on $\mathbb{T}^2 \times (-\epsilon, 0]$ and ds_2^2 on $\mathbb{T}^2 \times [1, 1 + \epsilon)$, there exists a Riemannian metric on*

$\mathbb{T}^2 \times (-\epsilon, 1+\epsilon)$ *extending them.*

Proof: [Blending Lemma] Use the metric $d\tau^2$: if $(x,t) \in \mathbb{T}^2 \times [0,1]$, then $d\tau^2(x,t) = (1-t)ds_1^2(x,0) + t \cdot ds_2^2(x,1)$. □

Proposition 2.1.5 *The modified singular Solv metric on M is quasi-isometric to the hyperbolic metric on M. Thus flow lines which are quasigeodesic in the modified metric will also be quasigeodesic in the hyperbolic metric.*

Proof: Attatch each cusp to the neutered space with a $\mathbb{T}^2 \times [0,1]$ neighborhood so that the metric on $\mathbb{T}^2 \times 0$ agrees with the singular Solv metric on the boundary in the neutered space and the metric on $\mathbb{T}^2 \times 1$ agrees with the modified metric on the boundary of the cusp, using the Blending Lemma above (see Figure 2.1). If $B_1, B_2, \ldots, B_n$ are bi-Lipshitz constants for the quasi-isometries between the hyperbolic metrics on the cusps $T_1, \ldots, T_n$ given by the the pull-back of the hyperbolic metric under the map f, and the hyperbolic metric on $T_1, \ldots, T_n$ inherited from M. Then if $B = \max\{B_N, B_1, B_2, \ldots, B_n\}$, the modified metric and the hyperbolic metric on M are quasi-isometric with bi-Lipshitz constant B. □

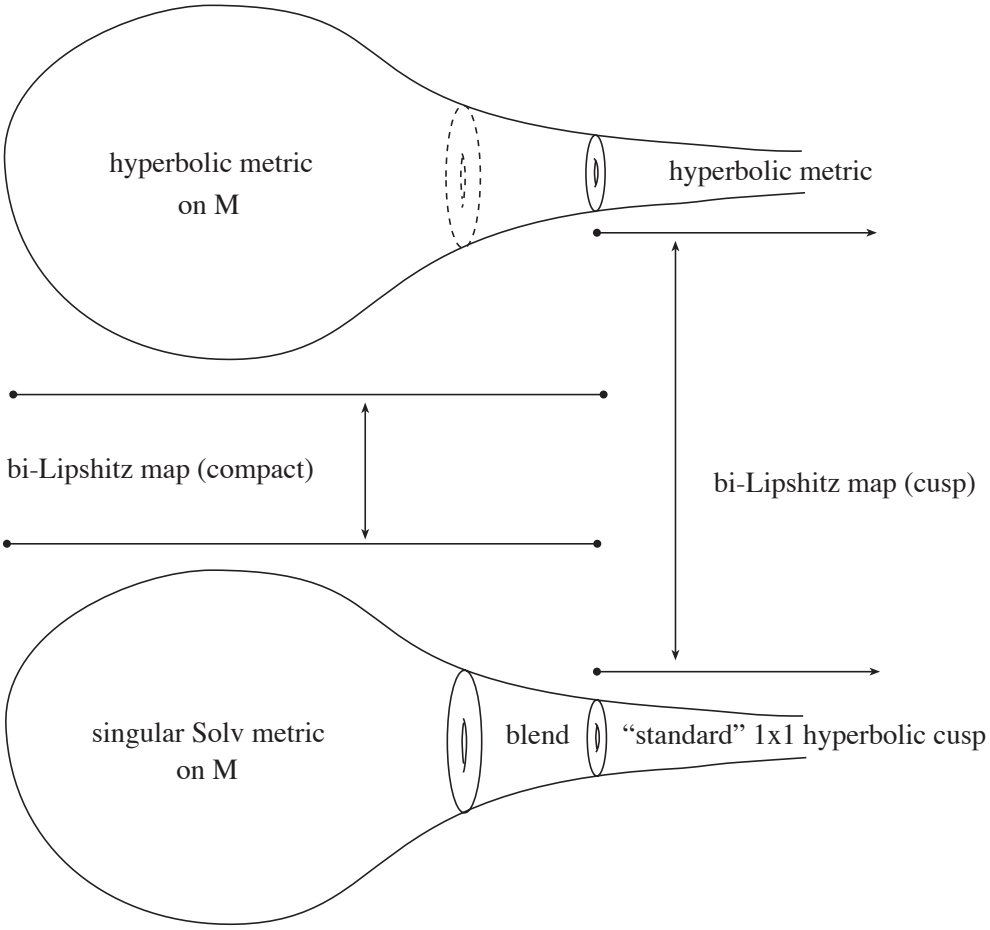

Figure 2.1: Glueing the cusps back into the neutered space, blending the metrics.

2.1.2 Preliminaries for Defining the Map f Which Modifies the Metric in a Cusp

Recall that $\widehat{M}$ denotes the particular intermediate cover of M described in Section 1.2.4: $\widehat{M}$ is the cover of M given by $\widehat{F} \times \mathbb{R}^1$, where $\widehat{F}$ is homeomorphic to a multiply punctured plane. Recall also that $T \simeq (D^2 - *) \times \mathbb{S}^1$. As before, think of the flow lines in $\widehat{M}$ as being vertical, and choose a particular preimage $\widehat{T}$ in $\widehat{M}$ of a cusp T in M. The cover $\widehat{T}$ in $\widehat{M}$ is homeomorphic to $(D^2 \setminus \{(0,0)\}) \times \mathbb{R}^1$.

The universal cover of $\widehat{T}$ (which is also the universal cover of T) is easiest to picture if we use cylindrical coordinates in a neighborhood of $\widehat{T}$. Choose local coordinates $r \in [0, \frac{1}{e})$, $\theta \in [0, n\pi]$ at an n-pronged singularity, and $t \in \mathbb{R}$, where r and θ are polar coordinates for $(D^2 \setminus \{(0,0)\})$ and t is the vertical coordinate for singular Solv, so that the preimage of the puncture in each horizontal cross section of $\widehat{T}$ occurs on the t-axis. Recall that near a singularity, the singular Solv metric consists of n copies of a vertical half space in Solv arranged like slices of a cake. The θ coordinate increases by π in each half space.

Adjust this choice of coordinates if necessary so that $\theta = 0$ corresponds to an unstable eigendirection, the unstable and stable eigendirections are evenly spaced around the origin (see Figures 2.3, 2.4 for examples), and $r = \frac{1}{e}$ gives the boundary of the disc. (The choice $r = \frac{1}{e}$ giving the boundary of the disc will later ensure that the image in $\mathbb{H}^3$ under f of the universal

cover $\widehat{T}$ will be the standard cusp in the upper half space model of $\mathbb{H}^3$: everything above and including the plane $z = 1$.) The universal cover of $\widehat{T}$ is obtained by unwrapping $\widehat{T}$ in the θ direction about the preimage of the puncture.

Each flow line which intersects $\widehat{T}$ is then given by some fixed choice of r and θ, and is parametrized by the coordinate t. For this reason it is convenient to introduce the following notation:

Notation 2.1.6 *Let $\ell(r, \theta)$ represent the flow line defined by r and θ.*

Recall that horizontal cross-sections of $\widehat{T}$, when viewed in the Euclidean metric instead of the singular Solv metric, become more eccentric as $|t| \to \infty$ (refer back to Figure 1.11, if necessary). As flow lines are vertical straight lines in these coordinates, a typical flow line which intersects $\widehat{T}$ will enter the cusp at some height t_0 and will remain inside the cusp until some height $t_1 > t_0$, where it will exit, never to return to $\widehat{T}$ again. Figure 2.2 illustrates this observation when $\widehat{T}$ is a regular cusp; an analogous picture describes the case where $\widehat{T}$ is a singular cusp.

Although the cusp T may be either a regular or a singular cusp, both types of cusps are composed of a number of identical "sections" which are glued together around the puncture. Our goal is to map T to the standard hyperbolic cusp so that flow lines (vertical geodesics in singular Solv) go to quasigeodesics. This is done by giving an equivariant map of the universal

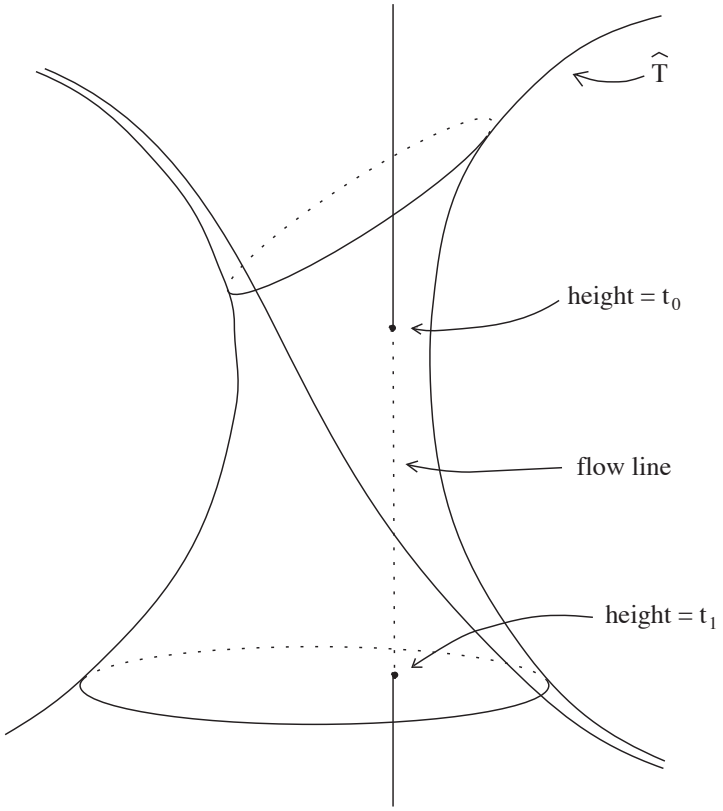

Figure 2.2: A typical flow line intersection with $\widehat{T}$

cover of T into the standard horoball in $\mathbb{H}^3$. We will do this by defining the map to the standard horoball for one section of T, and then the map from the universal cover of T onto the standard cusp will be defined by glueing together copies of this section map.

Definition 2.1.7 *Using the coordinates r, θ, and t above, the **k-th section** of the intermediate cover $\widehat{T}$ of a cusp T is the subset of $\widehat{T}$ having θ between $(k-1)\pi$ and $k\pi$. The k-th section of the cusp T is the image of the k-th section of $\widehat{T}$.*

The intersection of the singular stable and unstable foliations with a horizontal cross section of $\widehat{T}$ gives a picture similar to Figure 2.3 if $\widehat{T}$ is a regular cusp, or Figure 2.4 if $\widehat{T}$ is a singular cusp. Sections of $\widehat{T}$ are indicated on the pictures. The center is missing from each cross-section, corresponding to the missing flow line in the center of each cusp. The dynamics of the flow on the cross section of $\widehat{T}$ are indicated by arrows.

Note that under this choice of coordinates, each section is isometric to all the the others, and that a cusp with an n-prong singularity ($n = 2$ indicates a regular cusp) has n sections, with $0 \leq \theta < n\pi$. The singular Solv metric on a section is simply the (non-singular) Solv metric, since a section does not contain a singularity. Further,

Proposition 2.1.8 *Any segment of flow line which lies inside a cusp T*

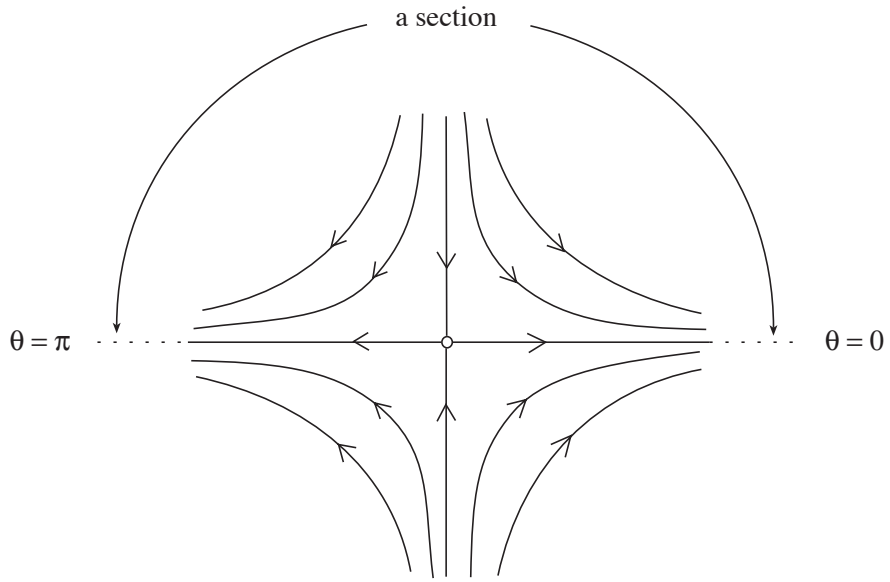

Figure 2.3: The dynamics of the flow and choice of coordinates in the cross section of a regular cusp.

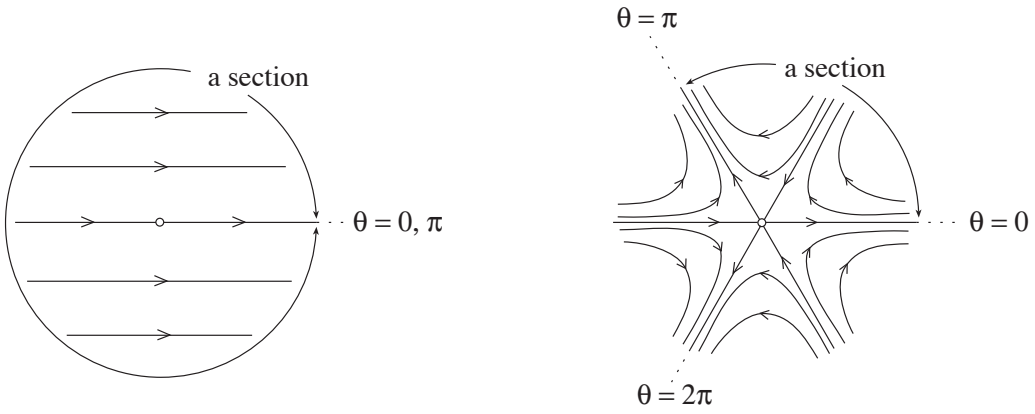

Figure 2.4: The dynamics of the flow and choice of coordinates in the cross section of singular cusps.

cannot have a change in angle, measured from the positive x-axis in Solv geometry, more than $\frac{\pi}{2}$.

Proof: Study the dynamics of the flow near a regular and singular cusp (Figures 2.3, 2.4). A flow line moves from the stable direction to the unstable direction, which is an angle $\frac{\pi}{2}$ in Solv. □

We will make extensive use of the above proposition throughout this chapter of the thesis.

2.1.3 Definition of the map f Which Modifies the Metric in a Cusp

We will map a standard section of $\widehat{T}$ to the standard cusp in $\mathbb{H}^3$ in such a way that the image flow lines are quasigeodesic in the hyperbolic metric. Figure 2.5, suggested by Thurston, is a useful picture of one section of the universal cover of $\widehat{T}$. The desired map from the universal cover of $\widehat{T}$ is then obtained by glueing together the maps on the sections of $\widehat{T}$. which indicates how the glueing should be performed.

The metric is to be altered in the cusp T so that it resembles the hyperbolic metric on T. For a sequence of points in $\widehat{T}$ such that r approaches 0, the image under f of these points should have upper half space z-coordinate

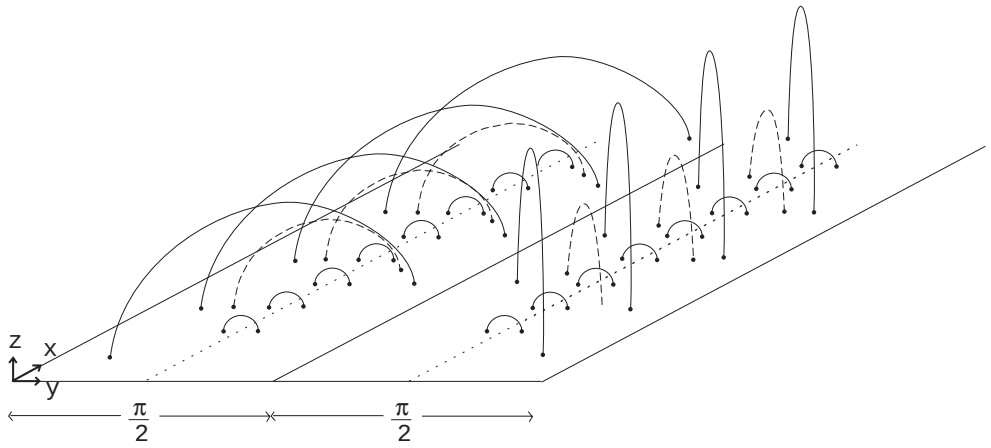

Figure 2.5: One "section" of the universal cover of a cusp neighborhood.

approaching infinity. To a first approximation, this map sends (r, θ, t) to $(x, y, z) = (t, \theta, -\ln r)$. However, we need to ensure that the Solv isometry given by vertical translation is realized as translation in the direction of the flow lines over in hyperbolic space.

Specifically, let τ_s be the singular Solv isometry which translates vertically (along the t axis) for s units. Then we want

$$f \circ \tau_s = T_s \circ f,$$

where $T_s : \mathbb{H}^3 \to \mathbb{H}^3$ is the parabolic isometry given by $T_s(a, b, c) = (s + a, b, c)$. In other words, we want f to make the diagram below commute:

$$\begin{array}{ccc} \widehat{T} & \xrightarrow{f} & \mathbb{H}^3 \\ {\scriptstyle \tau_s}\downarrow & & \downarrow{\scriptstyle T_s} \\ \widehat{T} & \xrightarrow{f} & \mathbb{H}^3 \end{array}$$

We will map the cylindrical cover of the cusp over by horizontal levels, first translating the level with $t = s$ down to level $t = 0$ by vertical translation τ_{-s}, then mapping over by (approximately) $(r, \theta, t) \mapsto (t, \theta, -\ln r)$, then translating back using T_s. Using rectangular coordinates, τ_{-s} can be seen locally as the function on Solv in standard coordinates given by the formula

$$\tau_{-s}(x, y, s) = (\lambda^{-s}x,\ \lambda^{s}y,\ 0);$$

a short calculation gives that for any point (r, θ, t) in $\widehat{T}$, the isometry τ_{-t} taking this to level 0 in cylindrical coordinates is

$$\tau_{-t}(r, \theta, t) = (r\sqrt{\lambda^{-2t}\cos^2\theta + \lambda^{2t}\sin^2\theta},\ \tan^{-1}(\lambda^{2t}\tan\theta),\ 0).$$

To define the map f, we first define a map from one section to a certain slab in $\mathbb{H}^3$. Then we extend this map to all slabs in $\mathbb{H}^3$. Thus a function which maps each section of the universal cover of $\widehat{T}$ (section by section) onto the standard cusp in $\mathbb{H}^3$ is given by the following definition.

Definition 2.1.9 *The function f which maps the universal cover $\widetilde{T}$ of a cusp T to the standard horoball in $\mathbb{H}^3$ is defined as*

$$\begin{aligned} f(r, \theta, t) &= (t,\ \tan^{-1}(\lambda^{2t}\tan\theta),\ -\ln(r\sqrt{\lambda^{-2t}\cos^2\theta + \lambda^{2t}\sin^2\theta})) \\ &= (x(r, \theta, t),\ y(r, \theta, t),\ z(r, \theta, t)) \end{aligned}$$

Thus, we'll denote the first, second, and third coordinate functions by x, y, and z, respectively. This function, which maps the universal cover of a cusp

T, section by section, to the standard horoball in $\mathbb{H}^3$, will be used to define the modified metric on the cusp T.

Under f, the image of a fundamental domain is $[0,1] \times [0, n\pi] \times [1, \infty)$.

Lemma 2.1.10 *A point (r, θ, t) on a flow line is inside the cusp exactly when*

$$r\sqrt{\lambda^{-2t}\cos^2\theta + \lambda^{2t}\sin^2\theta} < \frac{1}{e}.$$

Proof: A point (r, θ, t) on a flow line is inside the cusp whenever the z coordinate of the its image in upper half space is greater than 1; in other words, when

$$-\ln(r\sqrt{\lambda^{-2t}\cos^2\theta + \lambda^{2t}\sin^2\theta}) > 1.$$

This happens exactly when

$$r\sqrt{\lambda^{-2t}\cos^2\theta + \lambda^{2t}\sin^2\theta} < \frac{1}{e}.$$

□

In particular, when $t = 0$, we have $r < \frac{1}{e}$.

2.1.4 Trapped and Returning Flow Lines

Consider the dynamics of the flow in a cusp $\widehat{T}$, indicated by arrows on the intersection of the suspensions of the singular stable and unstable foliations

with the level of the cusp given by $t = 0$ (refer to Figures 2.3, 2.4). The dynamics can be expressed in a 2-dimensional picture by choosing a particular flow line and translating a point on that flow line at height t, using the singular Solv isometry τ_{-t}, to height 0. The coordinates r and θ remain constant on a flow line; however the angle measured in Solv geometry between a radius vector at some height t and the x-axis changes as $t \to \infty$. From the formula for the isometry τ_{-t} (see page 60), we see that this angle changes according to the formula $\tan^{-1}(\lambda^{2t} \tan\theta)$, which is monotonic in t. In other words, if you were to take successive horizontal cross sections of the cusp, and use the map τ_{-t} to map the cross section to the 0 level, then the images of a particular flow line would lie on points similar to those marked by the x's on Figure 2.6.

Clearly, there are two types of flow lines in $\widehat{T}$: those which lie along a line through the origin having θ an integer multiple of π, and those which don't. The first kind of flow line lies in the suspension of a singular leaf of one of the foliations on the fiber emanating from the missing leaf and hence spiral in towards the missing leaf in either forward or backwards time. We will refer to this type of flow line as a **trapped** flow line, for one end of the flow line becomes trapped in the cusp forever.

The second, more common type of flow line lies in the suspension of a non-singular leaf of one of the foliations on the fiber. This type will leave the cusp neighborhood $\widehat{T}$ through its boundary in finite forwards and backwards time. As these flow lines will enter the cusp and then return to

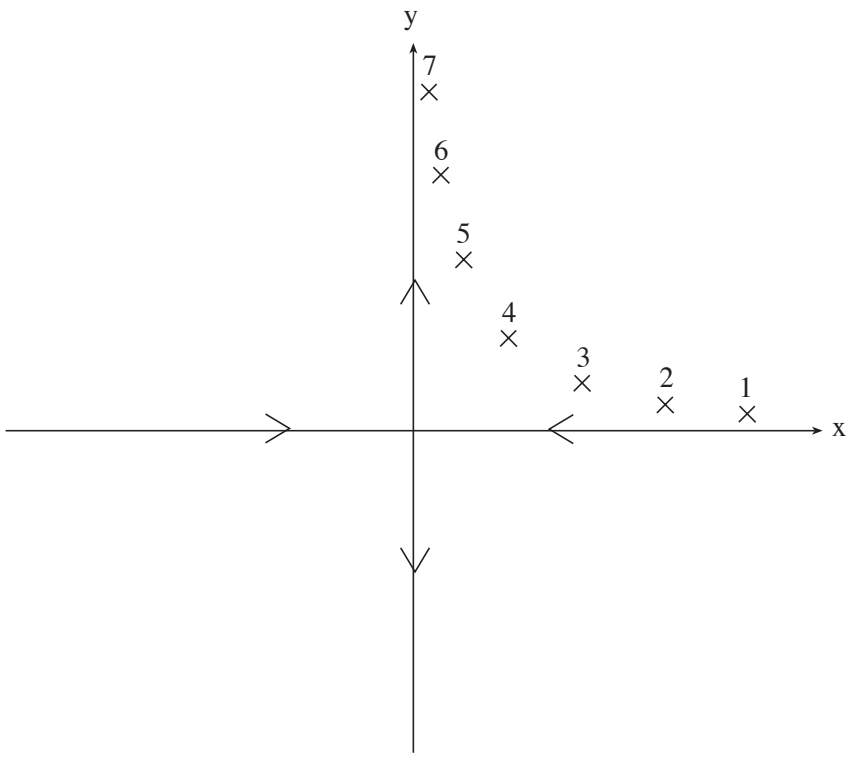

Figure 2.6: Successive hits given by the dynamics of the flow in a section of a cusp.

the compact part of the manifold, we will call them **returning** flow lines.

We will make use of the following lemma several times throughout this thesis.

Lemma 2.1.11 (At Most One Visit Lemma) *A flow line visits a covering cylinder $\widehat{T}$ in $\widehat{M}$ (and hence in $\widetilde{M}$) at most once.*

Proof: Given the intermediate cover $\widehat{T}$ of a cusp T, a flow line ℓ defines one fixed choice of r and θ. It is clear from the dynamics that a flow line may enter any given section of $\widehat{T}$ at most one time. Every returning flow line remains in the same section of $\widehat{T}$ as t grows, and every trapped flow line stays on the same line radiating from the origin. Therefore a flow line may visit a covering cylinder $\widehat{T}$ in $\widehat{M}$ at most one time. □

We will show separately that trapped and returning flow lines are quasi-geodesic.

2.2 Trapped Flow Line Segments Are Quasi-geodesic in the Cusps

Proposition 2.2.1 *There is a $K_t > 0$ such that all trapped flow line segments are uniformly K_t-quasigeodesic in the modified metric on the cusp. In fact, the image of a trapped flow line under f is a Euclidean straight line in $\mathbb{H}^3$.*

Proof: Let ℓ be any trapped flow line in the image of a section. A trapped flow line in any section is characterized by having $\theta = n\pi$, $n \in \mathbb{Z}$. In this case,

$$\begin{aligned} f(r,\theta,t) &= (t, \tan^{-1}(\lambda^{2t}\tan n\pi), -\frac{1}{2}\ln(r^2(\lambda^{-2t}\cos^2 n\pi + \lambda^{2t}\sin^2 n\pi))) \\ &= (t, 0, \ln\lambda \cdot t - \ln r). \end{aligned}$$

(Recall that r and θ are constant on a flow line.) Therefore

$$\begin{aligned} \frac{dx}{dt} &= 1 \\ \frac{dy}{dt} &= 0, \text{ and} \\ \frac{dz}{dt} &= \ln\lambda. \end{aligned}$$

So ℓ is a Euclidean straight line in the upper half space model of $\mathbb{H}^3$ with slope $\frac{dz}{dx} = \ln\lambda$, and constant y coordinate. Thus ℓ can be parametrized by

$$x = t, \qquad z = \ln\lambda \cdot t, \qquad y = \text{constant}.$$

The hyperbolic length of a segment along ℓ is then a constant multiple of the length of a vertical geodesic segment with the same starting and ending

height, since integrating the hyperbolic metric gives:

$$\begin{aligned} d_\ell(t_1,t_2) &= \int_{t_1}^{t_2} \frac{\sqrt{(\frac{dx}{dt})^2+(\frac{dy}{dt})^2+(\frac{dz}{dt})^2}}{z(t)}\,dt \\ &= \int_{t_1}^{t_2} \frac{\sqrt{1+(\ln\lambda)^2}}{\ln\lambda\cdot t}\,dt \\ &= \frac{\sqrt{1+(\ln\lambda)^2}}{\ln\lambda}\int_{t_1}^{t_2}\frac{1}{t}\,dt \\ &= \frac{\sqrt{1+(\ln\lambda)^2}}{\ln\lambda}\,d_{\mathbb{H}^3}((x,y,t_1),(x,y,t_2)) \\ &= K_{\mathrm{t}}\cdot d_{\mathbb{H}^3}((x,y,t_1),(x,y,t_2)), \end{aligned}$$

where $K_{\mathrm{t}} = \frac{\sqrt{1+(\ln\lambda)^2}}{\ln\lambda}$. Therefore,

$$d_\ell(t_1,t_2) \le K_{\mathrm{t}}\cdot d_{\mathbb{H}^3}((x,y,t_1),(x,y,t_2)).$$

Thus trapped flow lines are uniformly K_{t}-quasigeodesics. □

2.3 Returning Flow Lines are Quasigeodesic in the Cusps

Recall that a returning leaf is a flow line segment inside the cusp which eventually exits the cusp in both forwards and backwards directions. To see that a returning leaf is quasigeodesic, we will first show that its image in $\mathbb{H}^3$ under f travels monotonically in the x and y directions, and increases

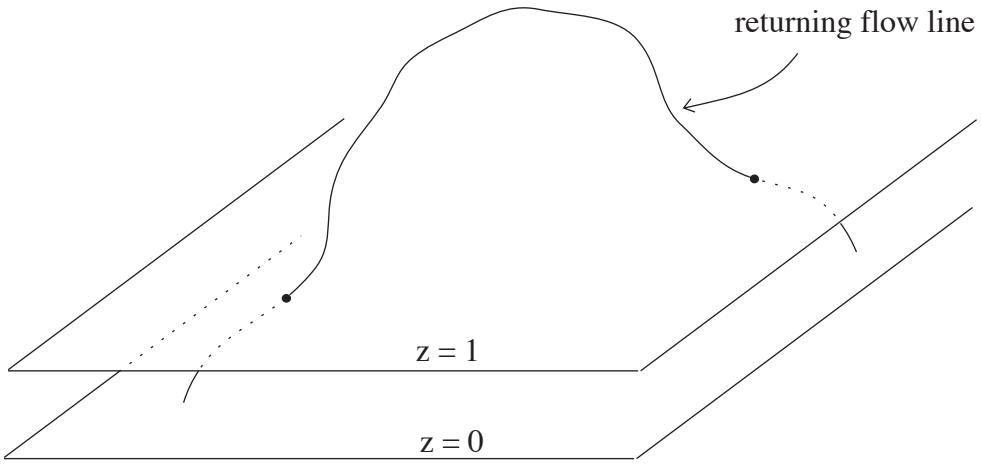

Figure 2.7: The image under f of a returning flow line segment inside a cusp.

monotonically in the z direction until it reaches a peak, then decreases monotonically until it exits the cusp again. Thus the image of a typical returning flow line in $\mathbb{H}^3$ looks like Figure 2.7. We want to compare the length of a returning flow line segment which lies inside the cusp to the length of the geodesic connecting its endpoints

First, we will show that the hyperbolic length of a returning flow line segment is no more than a fixed multiple of the hyperbolic length of a vertical line segment v from the highest point of the flow line to the boundary of the cusp, as follows:

Divide the returning flow line segment at half its Euclidean height into a top half, called the **crown**, and two bottom pieces, called **legs**, as in Figure 2.8.

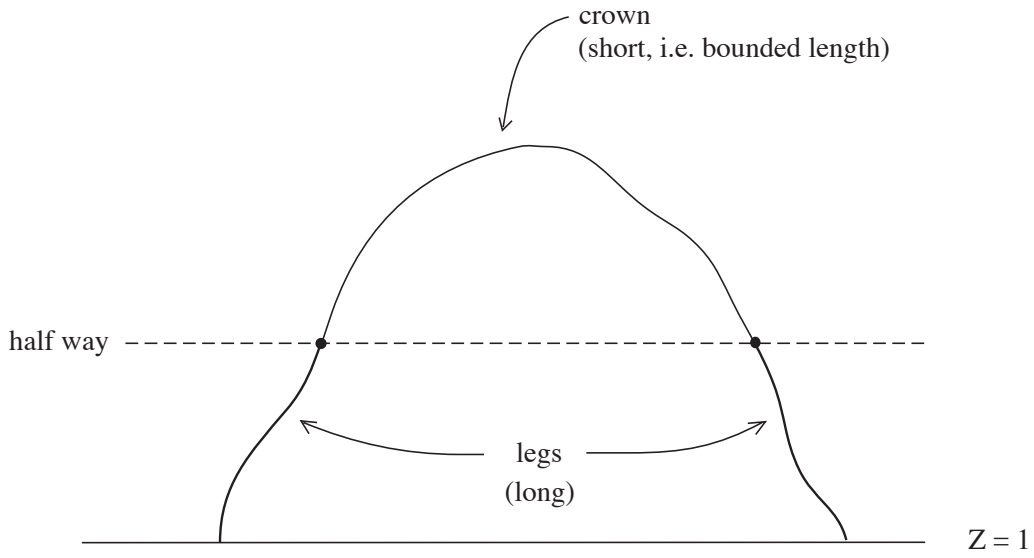

Figure 2.8: The crown and legs of a returning flow line.

We will show that the length of the crown is a small bounded number, so that the length of a returning flow line segment can be approximated by the sum of the lengths of its legs. Furthermore, we show that the slopes of the legs of sufficiently long returning flow lines are uniformly bounded below, therefore the length of a leg is comparable to the length of the vertical segment from the boundary of the cusp to the top of the leg (see Figure 2.9). Thus the length of a returning flow line segment is no more than a fixed multiple of the hyperbolic length of the vertical line segment v.

A direct calculation from the parametrization f of the flow lines gives that the z-value at the peak of a flow line (which is approximately the Euclidean length of the line segment v) is no more than a fixed multiple

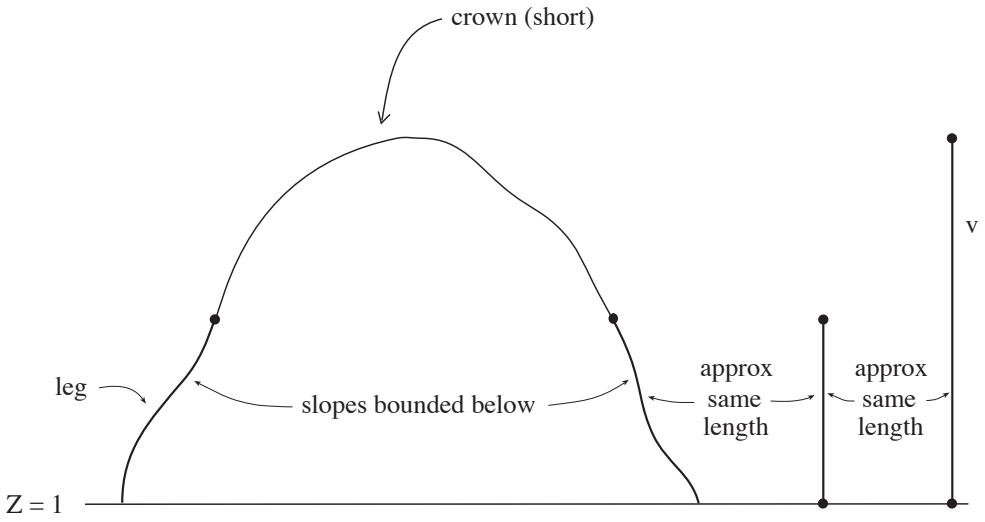

Figure 2.9: The length of a leg is comparable to the length of the vertical segment v.

of the Euclidean distance between the points a and b where the flow line enters and exits the cusp, as in Figure 2.10. As we are only considering long returning flow lines, we may take natural logs to obtain a comparison between the hyperbolic length of v and the natural log of the Euclidean distance between the points a and b.

Finally, a calculation from hyperbolic geometry relates the natural log of the Euclidean distance between the points a and b to the length of the geodesic connecting these endpoints.

2.3.1 Monotonicity of the Map Defining the Metric

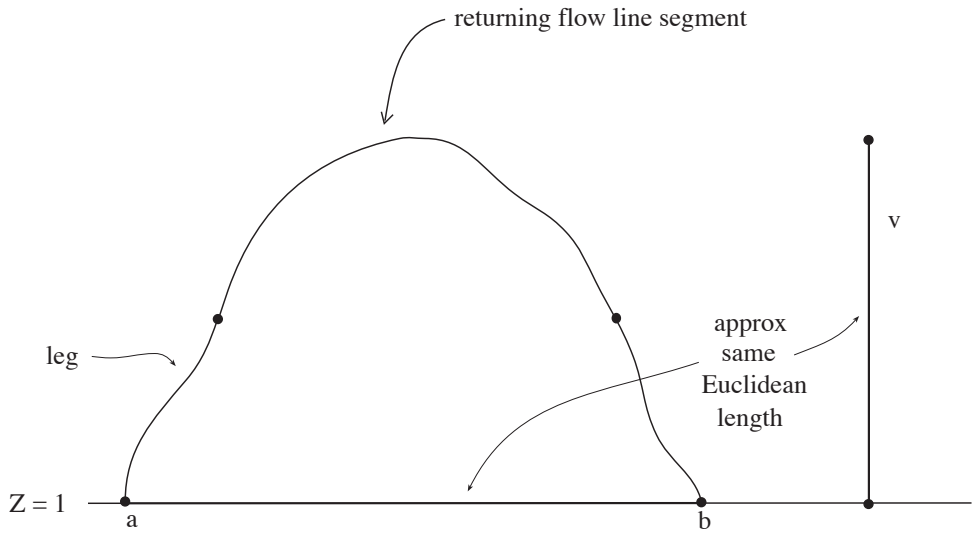

Figure 2.10: The Euclidean length of v is comparable to the Euclidean horizontal distance between a and b.

Lemma 2.3.1 *If* $0 < \theta < \frac{\pi}{2}$, *the coordinate functions* $x(r, \theta, t)$ *and* $y(r, \theta, t)$ *of* f *are monotonic with respect to the parameter* t, *and the coordinate function* $z(r, \theta, t)$ *is piecewise monotonic with respect to* t *before and after one critical point* t_c, *where* t_c *depends on* θ *but not* r.

Proof: Monotonicity follows by examining each coordinate function's derivative with respect to t. Recall that these coordinate functions are

defined as

$$\begin{aligned} x(r,\theta,t) &= t \\ y(r,\theta,t) &= \tan^{-1}(\lambda^{2t}\tan\theta) \\ z(r,\theta,t) &= -\frac{1}{2}\ln(r^2(\lambda^{-2t}\cos^2\theta + \lambda^{2t}\sin^2\theta)). \end{aligned}$$

Clearly $\frac{\partial x}{\partial t} > 0$, so x is everywhere increasing.

Next,

$$\frac{\partial y}{\partial t} = \frac{2\ln\lambda \cdot \lambda^{2t}\tan\theta}{1+\lambda^{4t}\tan^2\theta}.$$

This derivative always exists, and is zero only when $\tan\theta = 0$. But we are in the case $0 < \theta < \pi/2$, therefore y has no critical points. Thus y is also monotonic with respect to t.

Finally,

$$\frac{\partial z}{\partial t} = \ln\lambda \cdot \frac{(\lambda^{-2t}\cos^2\theta - \lambda^{2t}\sin^2\theta)}{(\lambda^{-2t}\cos^2\theta + \lambda^{2t}\sin^2\theta)}.$$

Since the denominator is always strictly positive, the derivative always exists. Further, $\frac{\partial z}{\partial t} = 0$ whenever $\lambda^{-2t}\cos^2\theta = \lambda^{2t}\sin^2\theta$; i.e., whenever $\lambda^{4t} = \cot^2\theta$. Thus the one critical point is at

$$t_c = \frac{1}{2}\log_\lambda \cot\theta.$$

Further,

$$\begin{aligned} t < t_c &\Rightarrow \frac{\partial z}{\partial t} > 0, \text{ and} \\ t > t_c &\Rightarrow \frac{\partial z}{\partial t} < 0. \end{aligned}$$

Thus z is piecewise monotonic before and after the its one critical point t_c, growing up to t_c and then shrinking past t_c. $\square$

2.3.2 Reparametrization of f

The rest of the calculations will be simpler if we create a new map F which is a reparametrization of f with the critical point of each leaf at $t = 0$. Since F is merely a reparametrization of f along each leaf, F and f will draw out flow lines of the same length. Thus we may carry out the rest of our length calculations using the map F in place of the map f.

Recall that a given flow line ℓ is specified by a fixed choice of r and θ. Therefore, it is only a slight abuse of notation to treat r and θ as constants, and think of our reparametrized function F as merely a function of t. This shift of perspective should not create any problems as long as we ensure that all our bounds in the ensuing calculations are independent of r and θ.

For a flow line ℓ which defines a fixed choice of r, θ, and critical point $t_c = \frac{1}{2}\log_\lambda \cot\theta$, define a function $F(t)$ as follows:

$$\begin{aligned} F(t) &= f(r, \theta, t + t_c) \\ &= (t + t_c, \tan^{-1}(\lambda^{2t}), -\ln(r\sqrt{\sin\theta\cos\theta(\lambda^{-2t} + \lambda^{2t})})), \end{aligned}$$

Denote the new coordinate functions for F by $X(t), Y(t)$, and $Z(t)$.

2.3.3 Bound on the Length of the Crown of a Flow Line

Away from the critical point of a returning flow line segment, we can easily show that the absolute values of the derivatives $\frac{dZ}{dX}$ and $\frac{dZ}{dY}$ are bounded below (Section 2.3.4). In a neighborhood of the critical point of the flow line segment in $\mathbb{H}^3$, the derivatives are clearly not bounded below, but very little length is picked up, because the metric on hyperbolic space makes lengths of paths relatively small when they have large Z-coordinate.

In order to consider a neighborhood of a critical point of a flow line segment inside the cusp separately from the rest of the segment, we will cut a flow line segment into a "top half" and a "bottom half". In this section we will find a number A which uniformly bounds the lengths of the top halves of (sufficiently long) flow line segments.

Each flow line reaches its maximum height at $t = 0$ by the way we've chosen F. Denote the Z value at this peak (where $t = 0$) by Z_{p}; plugging $t = 0$ into the formula for Z gives $Z_{\mathrm{p}} = -\ln(r\sqrt{\sin 2\theta})$. Recall $r < \frac{1}{e}$, so $Z_{\mathrm{p}} > 0$. Then the top half of a flow line, or the crown, will be the portion of flow line for which the $Z \geq \frac{1}{2}(1 + Z_{\mathrm{p}})$; the rest, the bottom half, breaks up into two pieces called the legs.

The Z value midway between $Z = 1$ and Z_{p} is where Z has value $Z_{\mathrm{m}} = \frac{1}{2}(1 - \ln(r\sqrt{\sin 2eta}))$. Therefore the crown and legs of a flow line segment in the cusp are defined as follows:

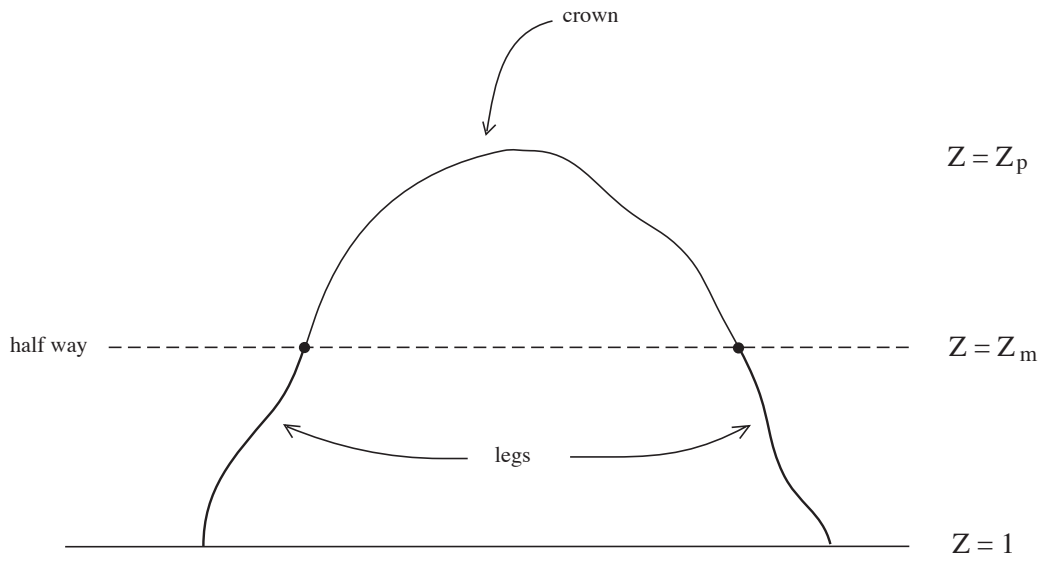

Figure 2.11: The legs and crown of a returning flow line, with Z-values labeled.

Definition 2.3.2 *The **crown** of any returning flow line segment of the suspension flow is the neighborhood of its critical point that has Z coordinate at least $Z_m = \frac{1}{2}(1 - \ln(r\sqrt{\sin 2\theta}))$.*

Definition 2.3.3 *The **legs** of any returning flow line segment inside the cusp are the segments of flow line whose Z coordinate is between 1 and Z_m.*

The two corresponding values of the flow parameter t where $Z = Z_{\mathrm{m}}$ (in other words, the values of t where the legs meet the crown) are found

by solving the equation

$$-\ln(r\sqrt{\sin\theta\cos\theta(\lambda^{-2t}+\lambda^{2t})}) = \frac{1}{2}(1-\ln(r\sqrt{\sin 2\theta}))$$

for t. This calculation is detailed in the appendix in Section A.1. The two solutions are $\pm t_{\mathrm{m}}$, where

$$t_{\mathrm{m}} = +\frac{1}{2}\log_\lambda(\frac{1+\sqrt{1-e^2r^2\sin 2\theta}}{er\sqrt{\sin 2\theta}}).$$

It is not surprising that both t values lie the same distance from $t=0$, for the map F draws the flow lines in hyperbolic space symmetrically. We will often take advantage of this symmetry by performing calculations on only one half of a leaf (one of the sides from $Z=1$ to Z_{p}) and use symmetry to comment on the other half.

A similar calculation gives $\pm t_{\mathrm{h}}$ as the two t values where the flow line intersects the horosphere $Z=1$, where

$$t_{\mathrm{h}} = \frac{1}{2}\log_\lambda(\frac{1+\sqrt{1-e^4r^4\sin^2 2\theta}}{e^2r^2\sin 2\theta}).$$

For reference, below is a table of constants and their values for a flow line segment ℓ which lies inside the cusp:

Name	**Description**	**Value**
Z_{p}	Z value at the peak	$-\ln(r\sqrt{\sin 2\theta})$
Z_{m}	Z value midway between Z_p and $Z=1$	$\frac{1}{2}(1-\ln(r\sqrt{\sin 2\theta}))$
t_{m}	Positive t value giving $Z=Z_{\mathrm{m}}$	$\frac{1}{2}\log_\lambda(\frac{1+\sqrt{1-e^2r^2\sin 2\theta}}{er\sqrt{\sin 2\theta}})$

t_{h}	Positive t value giving $Z = 1$	$\frac{1}{2}\log_\lambda(\frac{1+\sqrt{1-e^4r^4\sin^2 2\theta}}{e^2r^2\sin 2\theta})$

The following shows that the crown of a flow line behaves like the crown of a geodesic, namely, it has bounded length.

Lemma 2.3.4 *For the eigenvalue λ of the pseudo-Anosov map Ψ, there exists a uniform constant $A > 0$ depending only on λ such that the hyperbolic length of the crown of every returning flow line at most A.*

Proof: Let ℓ be a returning flow line segment which lies inside the cusp. Note that the functions X,Y, and Z are symmetric with respect to t. Further, X,Y, and Z are monotonic on each half of the crown, and the smallest Z value in the crown occurs when $Z = Z_{\mathrm{m}}$. Thus by the Taxicab Lemma (Lemma B.4.1),

$$\begin{aligned} d_\ell(F(-t_{\mathrm{m}}), F(t_{\mathrm{m}})) &= 2\, d_\ell(F(0), F(t_{\mathrm{m}})) \quad \text{by symmetry} \\ &\leq \frac{2(\Delta X + \Delta Y + \Delta Z)}{Z_{\mathrm{m}}} \quad \text{by the Taxicab Lemma} \end{aligned}$$

where $\Delta X = |X(t_{\mathrm{m}}) - X(0)|$, and so on. By a calculation detailed in the

appendix in Section A.2, for any returning flow line,

$$\begin{aligned}\frac{\Delta X}{Z_{\mathrm{m}}} &\leq \frac{2+\ln 2}{\ln \lambda},\\ \frac{\Delta Y}{Z_{\mathrm{m}}} &\leq \frac{\pi}{2}, \text{ and}\\ \frac{\Delta Z}{Z_{\mathrm{m}}} &\leq 1.\end{aligned}$$

Thus

$$\begin{aligned}d_\ell(F(-t_{\mathrm{m}}), F(t_{\mathrm{m}})) &\leq 2(\frac{\Delta X}{Z_{\mathrm{m}}} + \frac{\Delta Y}{Z_{\mathrm{m}}} + \frac{\Delta Z}{Z_{\mathrm{m}}})\\ &\leq 2(\frac{2+\ln 2}{\ln \lambda} + \frac{\pi}{2} + 1)\\ &= A,\end{aligned}$$

where A is independent of r and θ, thus independent of choice of flow line. □

2.3.4 Uniform Lower Bound for Slope of Legs of Returning Flow Line Segments

Lemma 2.3.5 *There exist constants B, C_x, and C_y depending only on λ so that in the legs of any returning flow line segment which is longer than B, $|\frac{dZ}{dX}| \geq C_x$ and $|\frac{dZ}{dY}| \geq C_y$.*

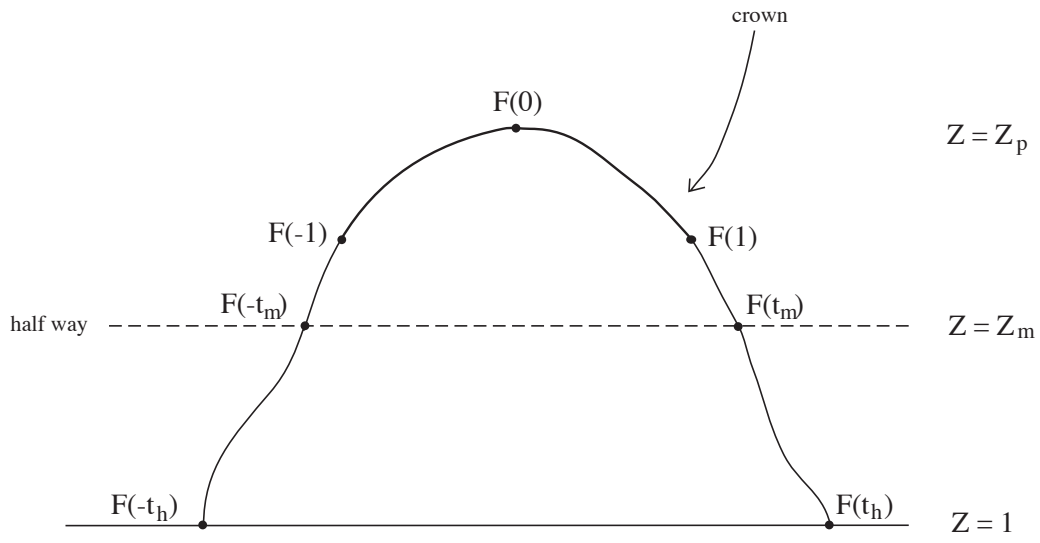

Figure 2.12: A flow line containing $F([-1,1])$ in its crown.

This lemma is clearly false if we don't require the lengths of the returning flow line segments to be bounded below, for one may take shorter and shorter flow line segments which enter the cusp more and more shallowly, in which case the legs would be more and more horizontal, and then these slopes would not be bounded below. But we are only interested in the behavior of the leaves over the long haul; thus we will only consider segments of flow lines in the cusp which are longer than some fixed number B. The actual value we choose for B is rather arbitrary; we shall choose a B so that if the length of the part of a leaf that lies in the cusp is larger than B, then all values of the parameter $t \in [-1,1]$ give points in the crown of the leaf, as in Figure 2.12.

We will find an actual value of B which ensures that all values of the

parameter $t \in [-1,1]$ give points in the crown of the leaf before proceeding with the proof of Lemma 2.3.5.

Claim 2.3.6 *If ℓ is a leaf such that $r\sqrt{\sin 2\theta} \leq \frac{2}{e(\lambda^{-2}+\lambda^2)}$, then $F([-1,1])$ is contained in the crown of the leaf ℓ.*

Proof: By symmetry, we only need to ensure that $Z(1) \geq Z(t_{\mathrm{m}})$. But from the formula for Z,

$$\begin{aligned}
Z(1) \geq Z(t_{\mathrm{m}}) &\Leftrightarrow -\ln(r\sqrt{\sin 2\theta \cos 2\theta(\lambda^{-2}+\lambda^2)}) \geq \frac{1}{2}(1 - \ln(r\sqrt{\sin 2\theta})) \\
&\Leftrightarrow 2\ln(r\sqrt{\sin 2\theta \cos 2\theta(\lambda^{-2}+\lambda^2)}) \leq \ln(r\sqrt{\sin 2\theta}) - 1 \\
&\Leftrightarrow \ln(r^2 \sin\theta\cos\theta(\lambda^{-2}+\lambda^2)) \leq \ln(r\sqrt{\sin 2\theta}) - 1 \\
&\Leftrightarrow r^2 \sin 2\theta \cdot \frac{1}{2}(\lambda^{-2}+\lambda^2) \leq \frac{r\sqrt{\sin 2\theta}}{e} \\
&\Leftrightarrow r\sqrt{\sin 2\theta} \leq \frac{2}{e(\lambda^{-2}+\lambda^2)}.
\end{aligned}$$

□

Claim 2.3.7 *If the length of a segment ℓ of a returning flow line which lies inside the cusp is at least B, where*

$$B = \log_\lambda\left(\frac{(\lambda^{-2}+\lambda^2)^2 + \sqrt{(\lambda^{-2}+\lambda^2)^4 - 16}}{4}\right) - 2\ln\left(\frac{2}{\lambda^{-2}+\lambda^2}\right) + \pi,$$

then the values of r and θ defined by ℓ satisfy $r\sqrt{\sin 2\theta} \leq \frac{2}{e(\lambda^{-2}+\lambda^2)}$, and hence $F([-1,1])$ is contained in its crown.

Proof: [Claim 2.3.7] Suppose $r\sqrt{\sin 2\theta} > \frac{2}{e(\lambda^{-2}+\lambda^2)}$. Recall that each half of each leaf is monotonic in X, Y and Z with respect to t. Thus the hyperbolic length of the crown of the leaf is given by

$$
\begin{aligned}
& d_{\mathbb{H}^3}(F(-t_{\mathrm{h}}), F(t_{\mathrm{h}})) \\
&\quad \leq \; 2 \cdot d_{\mathbb{H}^3}(F(0), F(t_{\mathrm{h}})) \\
&\quad \leq \; 2 \cdot [\tfrac{\Delta X+\Delta Y+\Delta Z}{1}] && \text{Taxicab Lemma} \\
&\quad = \; 2 \cdot (|X(t_{\mathrm{h}}) - X(0)| + |Y(t_{\mathrm{h}}) - Y(0)| + |Z(t_{\mathrm{h}}) - Z(0)|) \\
&\quad \leq \; 2 \cdot (t_{\mathrm{h}} + \tfrac{\pi}{2} + (Z_{\mathrm{p}} - 1)) \\
&\quad = \; 2t_{\mathrm{h}} + 2Z_{\mathrm{p}} + \pi - 2 \\
&\quad = \; \log_\lambda(\tfrac{1+\sqrt{1-e^4 r^4 \sin^2 2\theta}}{e^2 r^2 \sin 2\theta}) - 2\ln(r\sqrt{\sin 2\theta}) + \pi - 2 && \text{def of } t_{\mathrm{h}}, Z_{\mathrm{p}} \\
&\quad < \; \log_\lambda(\tfrac{1+\sqrt{1-\frac{16}{(\lambda^{-2}+\lambda^2)^4}}}{\frac{4}{(\lambda^{-2}+\lambda^2)^2}}) - 2\ln(\tfrac{2}{e(\lambda^{-2}+\lambda^2)}) + \pi - 2 \\
&\quad = \; \log_\lambda(\tfrac{(\lambda^{-2}+\lambda^2)^2+\sqrt{(\lambda^{-2}+\lambda^2)^4-16}}{4}) - 2\ln(\tfrac{2}{\lambda^{-2}+\lambda^2}) + \pi \\
&\quad = \; B.
\end{aligned}
$$

□

This constant B motivates the following definition:

Definition 2.3.8 *A **long returning leaf segment** is a finite segment of a flow line with both endpoints on the boundary of a cusp and length at least B.*

We now prove lemma 2.3.5.

Proof: (Lemma 2.3.5) We want to show that for long returning flow line segments, the absolute value of the functions $\frac{dZ}{dX}$ and $\frac{dZ}{dY}$ are uniformly bounded below in the legs (i.e for t between t_{m} and t_{h}). The bound will be uniform for all choices of r, θ which give rise to a long returning leaf segment.

Recall that $F(t) = (t + t_0, \tan^{-1}(\lambda^{2t}), -\ln(r\sqrt{\sin\theta\cos\theta(\lambda^{-2t} + \lambda^{2t})}))$. Calculation gives

$$\begin{aligned} \frac{dX}{dt} &= 1, \\ \frac{dY}{dt} &= \frac{2\ln\lambda \cdot \lambda^{2t}}{1+\lambda^{4t}}, \text{ and} \\ \frac{dZ}{dt} &= \frac{(\ln\lambda)(\lambda^{-2t} - \lambda^{2t})}{\lambda^{-2t} + \lambda^{2t}}. \end{aligned}$$

Therefore

$$\begin{aligned} \frac{dZ}{dX} &= \frac{dZ}{dt} \cdot \frac{dt}{dX} \\ &= \frac{(\ln\lambda)(\lambda^{-2t} - \lambda^{2t})}{\lambda^{-2t} + \lambda^{2t}}, \text{ and} \end{aligned}$$

$$\begin{aligned} \frac{dZ}{dY} &= \frac{dZ}{dt} \cdot \frac{dt}{dY} \\ &= \frac{(\ln\lambda)(\lambda^{-2t} - \lambda^{2t})}{\lambda^{-2t} + \lambda^{2t}} \cdot \frac{1+\lambda^{4t}}{2\ln\lambda \cdot \lambda^{2t}} \\ &= \frac{(\lambda^{-2t} - \lambda^{2t})(1+\lambda^{4t})}{2(1+\lambda^{4t})} \\ &= \frac{1}{2}(\lambda^{-2t} - \lambda^{2t}). \end{aligned}$$

We want to bound the absolute values of both of these derivatives below in the legs. Note that they are already independent of r and θ, thus any bound on these derivatives will be a uniform bound valid for all long returning leaf segments. Taking advantage of symmetry, we will show that the absolute values of the derivatives are bounded below for $t_{\mathrm{m}} < t < t_{\mathrm{h}}$, and the same result will immediately follow for $-t_{\mathrm{h}} < t < -t_{\mathrm{m}}$.

Since we are only considering leaves which contain $F([-1,1])$ in their crown, the legs of such a leaf are subsets of the sections of the leaf for which $|t| > 1$. Therefore, a bound on the derivatives when $|t| > 1$ is a bound on the derivatives in the legs of the leaves.

Now

$$\frac{d}{dt}(\frac{dZ}{dX}) \;=\; \frac{2(\ln\lambda)^2}{(\lambda^{-2t}+\lambda^{2t})^2}\cdot[(\lambda^{-2t}-\lambda^{2t})^2-(\lambda^{-2t}+\lambda^{2t})^2]$$

This derivative is always negative; therefore the function $\frac{dZ}{dX}$ is monotonically decreasing. Further, $|\frac{dZ}{dX}| = 0$ when $t = 0$ and increases as $|t|$ approaches infinity. So if $|t| > 1$,

$$|\frac{dZ}{dX}| = \frac{(\ln\lambda)|\lambda^{-2t}-\lambda^{2t}|}{\lambda^{-2t}+\lambda^{2t}} = \frac{(\ln\lambda)(\lambda^{2|t|}-\lambda^{-2|t|})}{\lambda^{-2|t|}+\lambda^{2|t|}} \geq \frac{(\ln\lambda)(\lambda^2-\lambda^{-2})}{\lambda^{-2}+\lambda^2} = C_x.$$

Similarly, $|\frac{dZ}{dY}|$ is bounded below by the constant $C_y = \frac{(\ln\lambda)(\lambda^2-\lambda^{-2})}{2}$ whenever $|t| > 1$. □

2.3.5 Proof That Returning Flow Lines Are Quasigeodesic in the Cusp

Proposition 2.3.9 *There exists a constant K_r depending only on λ such that all long returning leaf segments are uniformly K_r-quasigeodesic in the hyperbolic metric.*

Proof: We need to show that all returning leaf segments are quasigeodesic. Let ℓ be a long returning flow line segment (in other words, ℓ is a returning flow line segment in the cusp whose length is greater than B). Let γ be the geodesic connecting the points $a = F(-t_{\mathrm{h}})$ and $b = F(t_{\mathrm{h}})$ where ℓ enters and exits the cusp. We want to find a number $K_{\mathrm{r}} > 1$ so that $d_\ell(a,b) \leq K_{\mathrm{r}} \cdot d_\gamma(a,b)$, for then it is trivial that $\frac{1}{K_{\mathrm{r}}} \cdot d_\gamma(a,b) \leq d_\ell(a,b)$, because $d_\gamma(a,b)$ is the geodesic, and therefore the shortest, distance between a and b. The actual calculations for this proof appear in the appendix (Section 2.3.9); however, an outline of the proof is given below:

1. The distance along the flow line ℓ between a and b, $d_\ell(a,b)$, is at most a multiple of $\ln(Z_{\mathrm{p}})$, the vertical hyperbolic distance from the plane $Z = 1$ to the peak of the flow line. This gives equation (A.1) in the appendix:

   $$d_\ell(a,b) \leq P \cdot \ln(Z_{\mathrm{p}})$$

   (refer to Figure 2.9 for a picture of what this calculation means).

2. A short calculation gives a constant Q so equation (A.3) in the appendix holds:

$$Z_{\mathrm{p}} \leq Q \cdot t_{\mathrm{h}}$$

(refer to Figure 2.10).

3. From this it immediately follows that $\ln(Z_{\mathrm{p}}) \leq \ln(Q) + \ln(t_{\mathrm{h}})$. However, since we are only considering long returning leaf segments, $\ln(t_{\mathrm{h}})$ is bounded below by a constant R (equation (A.4)), thus $\ln(Q) \leq \frac{\ln(Q)}{R} \cdot \ln(t_{\mathrm{h}})$. This gives equation (A.5) in the proof in the appendix,

$$\ln(Z_{\mathrm{p}}) \leq (\frac{\ln(Q)}{R} + 1) \cdot \ln(t_{\mathrm{h}}).$$

4. The number t_{h} is half the difference in X-coordinates between a and b. But (half) the difference in X-coordinates between a and b is less than (half) the Euclidean distance between a and b by the triangle inequality. Finally, $2\ln$(half the Euclidean distance between a and b) $\leq d_\gamma(a, b)$, the distance along the geodesic γ between a and b. Thus

$$2\ln(t_{\mathrm{h}}) \leq 2\ln(\text{half the Euclidean distance between } a \text{ and } b) \leq d_\gamma(a, b),$$

which is equation (A.6) in the proof in the appendix.

Putting steps 1, 3, and 4 together gives

$$\begin{aligned} d_\ell(a,b) &\leq P \cdot \ln(Z_{\mathrm{p}}) \\ &\leq P \cdot [(\frac{\ln(Q)}{R} + 1) \cdot \ln(t_{\mathrm{h}})] \\ &\leq \frac{P}{2} \cdot (\frac{\ln(Q)}{R} + 1) \cdot (2\ln(t_{\mathrm{h}})) \\ &\leq \frac{P}{2} \cdot (\frac{\ln(Q)}{R} + 1) \cdot d_\gamma(a,b). \end{aligned}$$

Let $K_{\mathrm{r}} = \frac{P}{2} \cdot (\frac{\ln(Q)}{R} + 1)$. Then

$$\frac{1}{K_{\mathrm{r}}} \cdot d_\gamma(a,b) \leq d_\ell(a,b) \leq K_{\mathrm{r}} \cdot d_\gamma(a,b),$$

as desired. □

2.4 Flow Line Segments in the Cusp are Quasigeodesic

Theorem 2.4.1 *There exists a constant $K_c > 0$ depending only on λ such that every segment of flow line inside the cusp is a K_c-quasigeodesic.*

Proof: Let $K_{\mathrm{c}} = \max\{K_{\mathrm{t}}, K_{\mathrm{r}}\}$. If ℓ is any segment of flow line which lies inside the cusp, then ℓ is either a trapped leaf or a returning leaf. If ℓ is a trapped flow line, ℓ is a K_{t}-quasigeodesic by proposition 2.2.1. If ℓ

is a returning flow line, then the segment of returning flow line which lies inside the cusp is either longer or shorter than B. If it is shorter, then it is vacuously quasigeodesic. On the other hand, if it is longer than B, then ℓ is a K_{r}-quasigeodesic by proposition 2.3.9. $\square$

Chapter 3

Flow Lines Lie Inside Neighborhoods of Geodesics

We will show that the flow lines of the suspension flow on M are uniformly quasigeodesic using the fact that a path is quasigeodesic if and only if it tracks a genuine geodesic (Proposition 3.1.1). For convenience, the definition of tracking is repeated below.

Definition 1.3.2 *A path c **tracks** a geodesic segment γ in $\mathbb{H}^3$ if*

1. *There exists $R > 0$ so that c lies within a neighborhood of radius R of γ.*

2. *There exists $Q > 0$ such that if the length of a subpath of c with endpoints a and b is at least Q, then the distance between $\pi(a)$ and*

$\pi(b)$ along γ is at least 1, where π denotes orthogonal projection onto γ.

Thus we will find constants R_Φ and Q_Φ so that each flow line tracks a geodesic with tracking constants R_Φ and Q_Φ. In this section we will show that flow lines satisfy part 1 of the definition of tracking; in Chapter 4 we will show that they satisfy part 2 of the definition. Refer to Section 1.4 for an outline of the proof to take place in this chapter.

3.1 A Path Is Quasigeodesic If and Only If It Tracks a Geodesic

First we must establish that tracking is equivalent to being quasigeodesic.

Proposition 3.1.1 *A path is a quasigeodesic if and only if it tracks a geodesic.*

Proof: $\Rightarrow$) First, we will show that if q is a K-quasigeodesic, then it tracks a geodesic. To prove that q tracks a geodesic, we will show that q satisfies parts 1 and 2 of the definition.

1. Suppose a path q is a K-quasigeodesic in $\widetilde{M} = \mathbb{H}^3$, with endpoints on the sphere at infinity, $\mathbb{S}^2_\infty$. It is well known that a quasigeodesic has

2 distinct limit points on $\mathbb{S}^2_\infty$; let γ be the geodesic connecting these endpoints. We will show that there exists R so that q lies inside the neighborhood of radius R about γ.

Let $R = 6K^2$. Then q lies inside the neighborhood of radius R about γ, for suppose $y \in q$ falls outside this neighborhood. Then there is a long subsegment c of q, with endpoints a and b on the boundary of a smaller neighborhood of γ of radius $r = 2K$, so that the interior of c falls entirely outside this smaller neighborhood. Denoting the length of c by $|c|$ and so on, we have

$$|c| \geq 2(R - r). \tag{3.1}$$

We will see the path obtained by traveling from a straight to the geodesic γ, across γ, and back up to b is more than a factor of K shorter than c, which contradicts that c is a subsegment of a K-quasigeodesic.

Let π_γ denote orthogonal projection onto γ. Construct a new, shorter path s from a to b by connecting a to $a' = \pi_\gamma(a)$ by dropping orthogonally onto γ using a path of length r, then following along γ from $a' = \pi_\gamma(a)$ to $b' = \pi_\gamma(b)$, and finally passing orthogonally back up from b' to b by another path of length r. By the Geodesic Projection Lemma (Lemma B.1.1),

$$|c| \geq \frac{e^r}{2} \cdot |\pi_\gamma(c)|. \tag{3.2}$$

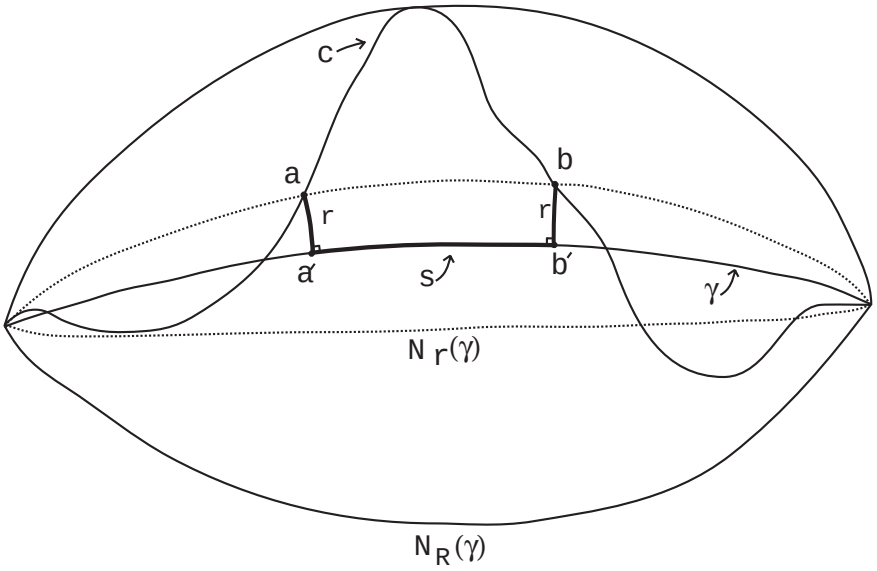

Figure 3.1: K-Quasigeodesics lie within $R = 6K^2$ neighborhoods of geodesics.

Comparing half the length of c with K times the length of the projection of c, and the other half the length of c with K times the length of the two paths connecting c to the geodesic, we get

$$\begin{aligned}
|c| &= \tfrac{1}{2}|c| + \tfrac{1}{2}|c| \\
&\geq [R - r] + [\tfrac{1}{4}e^r \cdot |\pi_\gamma(c)|] && \text{by equations (1) and (2)} \\
&= [3Kr - r] + [\tfrac{1}{4}e^{2K} \cdot |\pi_\gamma(c)|] && \text{since } R = 6K^2 \text{ and } r = 2K \\
&> [3Kr - Kr] + [\tfrac{1}{4}e^{2K} \cdot |\pi_\gamma(c)|] && \text{since } K > 1 \\
&\geq [2Kr] + [K \cdot |\pi_\gamma(c)|] && \text{since } K > 1, \text{ thus } e^{2K} > 4K \\
&= K(2r + |\pi_\gamma(c)|) && \text{factoring} \\
&= K \cdot |s|
\end{aligned}$$

which contradicts that c is a subsegment of q, a K-quasigeodesic.

2. Again, suppose a path q is a K-quasigeodesic in $\widetilde{M} = \mathbb{H}^3$, with endpoints on the sphere at infinity, and let γ be the geodesic connecting these endpoints. We will show that the projection of q onto γ makes reasonable progress along γ.

   Let $Q = 2KR + 2K$. Suppose points a and b on q denote endpoints of a subsegment c of q of length $|c| \geq Q$. Let s be the subpath between a and b of the geodesic γ' connecting those two points. If $|\pi_\gamma(c)|$

   is the length of the image of c under projection by π_γ onto γ, we want to show that $|\pi_\gamma(c)| > 1$.

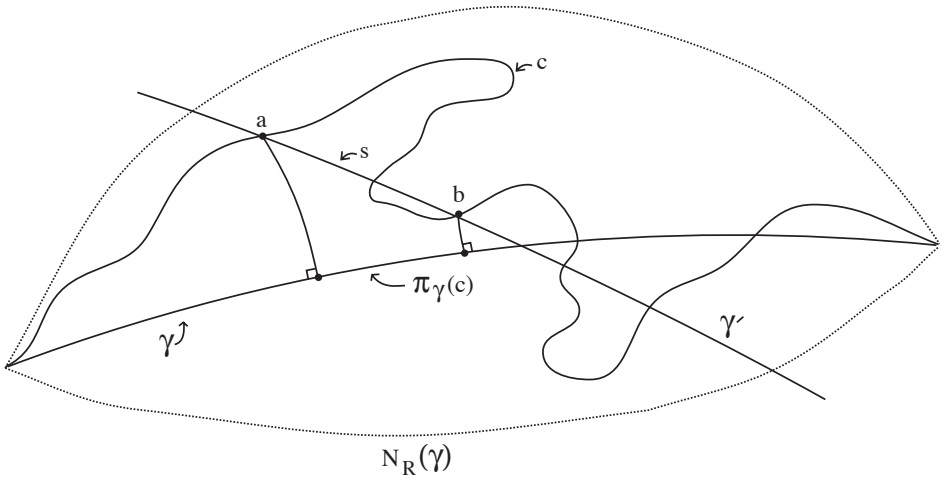

Figure 3.2: K-Quasigeodesics make reasonable progress along the geodesic connecting its endpoints.

Now

$$\begin{aligned} 2KR + 2K &= Q \\ &\leq |c| \\ &\leq K \cdot |s| && \text{since } q \text{ is a } K\text{-quasigeodesic} \\ &\leq K \cdot (2R + |\pi_\gamma(c)|) && \text{since } \gamma' \text{ is a geodesic} \\ &= 2KR + K|\pi_\gamma(c)|. \end{aligned}$$

Subtracting $2KR$ from both sides and dividing by K gives $2 \leq |\pi_\gamma(c)|$, therefore $|\pi_\gamma(c)| > 1$, as desired.

Therefore, if q is a K-quasigeodesic, then q tracks the geodesic γ connecting its endpoints at the sphere at infinity, with tracking constants $R = 6K^2$ and $Q = 2KR + 2K$.

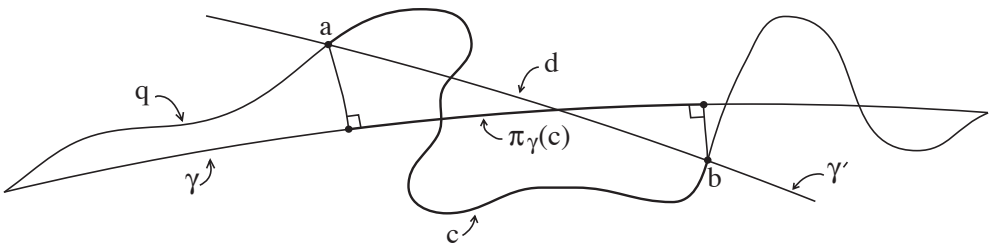

Figure 3.3: A path which R, Q-tracks a geodesic is a $(Q \cdot \frac{4}{e^R})$-quasigeodesic.

$\Leftarrow$) Now suppose a path q tracks a geodesic γ, with tracking constants R and Q, with γ connecting the endpoints of q on the sphere at infinity. Define $K = Q \cdot \frac{4}{e^R}$ and $L = Q$.

Let a and b be any two points on q such that $d_q(a, b) > Q$, and denote the subpath of q between a and b by c. Thus $|c| > Q$. Let γ' be the geodesic connecting a and b, and let d denote the subpath of γ' between a and b, so that $|d|$ is the distance between a and b (see Figure3.3).

Since $|c| > Q$ there is an integer $n \geq 1$ so that

$$nQ < |c| \leq (n+1)Q. \tag{3.3}$$

Splitting c up into n segments of length greater than Q and applying property 2 of the definition of tracking to each of the n segments gives

$|\pi_\gamma c| > n \cdot 1 = n$. Then

$$\begin{aligned}
|c| &\leq (n+1)Q && \text{by equation (3.3)} \\
&\leq 2nQ && \text{since } n \geq 1 \\
&< 2|\pi_\gamma c|Q && \text{since } |\pi_\gamma c| > n \\
&< 2 \cdot (\tfrac{2}{e^R} \cdot |d|) \cdot Q && \text{by the Geodesic Projection Lemma (Lemma B.1.1)} \\
&= K \cdot |d| && \text{by definition of } K.
\end{aligned}$$

Thus q is a K-quasigeodesic. □

Thus flow lines track geodesics if they make reasonable progress along a neighborhood of a geodesic.

3.2 Flow Lines Lie Inside Neighborhoods of Strings of Beads

To see that flow lines lie near geodesics, we will first establish that finite segments of flow lines lie uniformly near the string of beads along the geodesic passing through the endpoints of the segment. Thus flow lines follow along geodesics, at least outside of cusps.

3.2.1 Pushed Flow Line Segments Are Neutered Space Quasigeodesics

This argument takes place in the infinite cyclic cover N_∞ of the neutered space N. The outline of the argument found below precedes the formal proof.

If $p_1, p_2, \ldots, p_j$ are the punctures of F and $\overset{\circ}{\eta}(p_i)$ is an open neighborhood of p_i, then N can be thought of as

$$((F \smallsetminus \{\overset{\circ}{\eta}(p_1), ..., \overset{\circ}{\eta}(p_j)\}) \times [0,1])/(x,1) \sim (\Psi x, 0).$$

The infinite cyclic cover of N, N_∞, thus consists of infinitely many copies of $(F \smallsetminus \{\overset{\circ}{\eta}(p_1), ..., \overset{\circ}{\eta}(p_j)\}) \times [0,1]$ glued together top to bottom (see Figure 3.4). Note $N_\infty \subseteq M_\infty$, where M_∞ is the infinite cyclic cover of M.

If we consider $\mathbb{R}^1$ direction as being horizontal in M_∞, then a flow line travels exactly horizontally in M_∞, typically entering, passing through, and leaving several of the cylinders in M_∞ which cover cusps in M. Furthermore, because of the dynamics of the map Ψ, a flow line may enter each covering cylinder at most once (refer to the Limited Visit Lemma, Lemma 2.1.11).

To create a pushed flow line, a flow line is pushed out to the nearest point on the boundary of each cylinder it enters. Thus pushed flow lines spiral around the perimeter of each cylinder covering a cusp in M_∞ monotonically with respect to the horizontal coordinate θ.

By Proposition 2.1.8, we know that each flow line, when intersecting any cusp in the infinite cyclic cover M_∞ of M, can rotate through an angle at

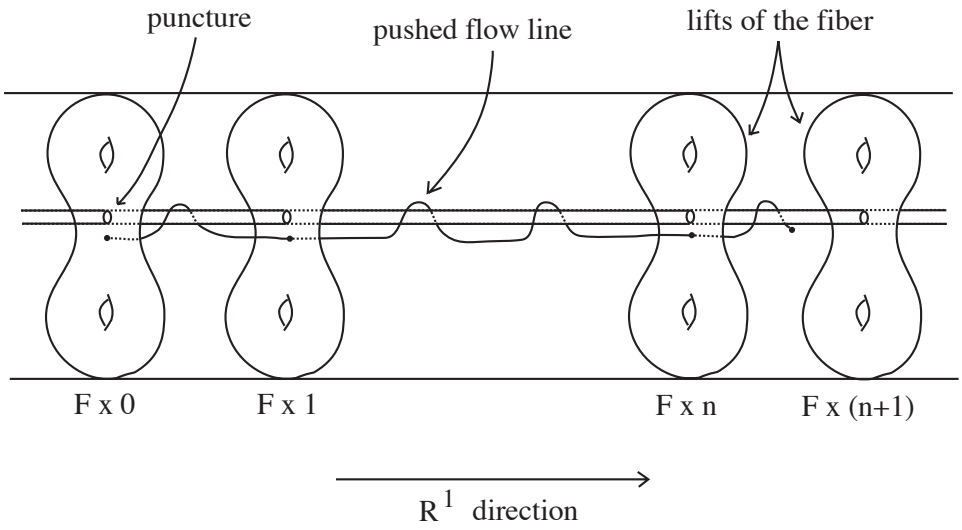

Figure 3.4: The infinite cyclic cover of the neutered space, N_∞

most $\frac{\pi}{2}$. This limited rotation coupled with the monotone vertical progress causes the pushed flow lines to be quasigeodesic in the neutered space.

A formal proof follows:

Proposition 3.2.1 (Pushed Flow Lines are Quasigeodesic) *There exists a constant $K_p > 0$ such that every pushed flow line $\overline{\ell}$ is a K_p-quasigeodesic in the inherited metric on the infinite cyclic cover N_∞ of the neutered space N of M, and hence a K_p quasigeodesic in the universal cover of N.*

Proof: [Proposition 3.2.1] We want to compare the distance between two points along a pushed flow line with the geodesic distance between the two points. In fact, we will compare a number which is greater than the distance

between two points along the pushed flow line to a number which is less than the geodesic distance between the two points. The calculation boils down to showing that the maximum length of a pushed flow line between successive lifts of F is no more than a bounded multiple of the minimum (neutered space) distance between the lifts.

Let $F_N = (F \setminus \{\mathring{\eta}\,(p_1), ..., \mathring{\eta}\,(p_j)\})$, so that the infinite cyclic cover of N is given by $N_\infty \simeq F_N \times \mathbb{R}$. If we let π_2 be the map $\pi_2 : N_\infty \simeq F_N \times \mathbb{R} \to \mathbb{R}$ given by projection onto the second coordinate, then π_2 restricted to any pushed flow line is monotone, by the discussion above. Therefore, once any pushed flow line passes through one copy of the fiber $F_N \times \{t\}$ for $t \in \mathbb{R}$, it never returns. Thus, the length of a pushed flow line can be approximated by the maximum length a pushed flow line spends between successive integral copies of $F_N \times \{t\}$ multiplied by the number of integral copies of $F_N \times \{t\}$ the pushed flow line passes through.

To find an upper bound for the length of a pushed flow line segment between the surfaces $F_N \times \{0\}$ and $F_N \times \{1\}$, define a function $g : F_N \to \mathbb{R}$ as follows: let $g(x)$ be the length of the pushed flow line in N_∞ starting at the point x in $F_N \times 0$ and ending at $F_N \times 1$. Then g is a continuous function (because the flow is continuous) on the compact set F_N, therefore its image is bounded above by some constant A.

Let ϵ be the minimum distance between the compact surfaces $F_N \times 0$ and $F_N \times 1$ in N_∞. Choose $K_\mathrm{p} > \frac{2A}{\epsilon}$ and $L_p = 1$. Let $\overline{\ell}$ be a pushed flow line, and let a and b be endpoints of some finite segment of $\overline{\ell}$ such that

$d_{\overline{\ell}}(a,b) > L_p$. The length $d_{\overline{\ell}}(a,b)$ lies between two consecutive integers; let n be an integer so that $n < d_{\overline{\ell}}(a,b) \leq n+1$ (in particular, $n \geq 1$). Then since the distance along any flow line between consecutive (integral) copies of the fiber is at most A,

$$d_{\overline{\ell}}(a,b) \leq A(n+1), \tag{3.4}$$

since $\overline{\ell}$ passes through no more than $n+1$ copies of the preimage of F_N. Furthermore, since ϵ is a lower bound for the distance between two consecutive (integral) copies of the fiber F_N, we know

$$d_{N_\infty}(a,b) \geq \epsilon n, \tag{3.5}$$

(see Figure 3.5).

Thus

$$\begin{aligned}
d_{\overline{\ell}}(a,b) &\leq A(n+1) && \text{by equation (3.4)} \\
&\leq A \cdot 2n && \text{since } n \geq 1 \\
&< \tfrac{1}{2} K_{\mathrm{p}} \epsilon \cdot 2n && \text{by definition of } K_{\mathrm{p}} \\
&= K_{\mathrm{p}}(\epsilon n) && \\
&< K_{\mathrm{p}} \cdot d_{N_\infty}(a,b) && \text{by equation (3.5).}
\end{aligned}$$

Therefore every pushed flow line $\overline{\ell}$ is an (L_p, K_{p})-quasigeodesic. □

Thus pushed flow lines are uniformly K_{p}-quasigeodesic in the neutered space. We want to show that a pushed flow line segment remains inside a

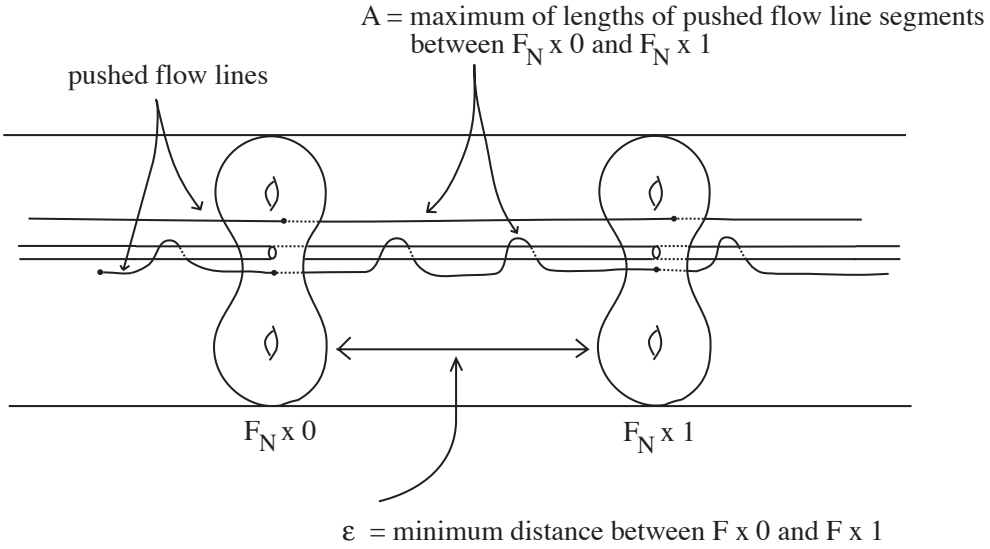

Figure 3.5: Distance comparison in the infinite cyclic cover of N.

uniform (hyperbolic space) neighborhood of the string of beads connecting its endpoints.

Consider a pushed flow line segment in $\mathbb{H}^3$ with endpoints a and b and the string of beads connecting these endpoints. We will show that the pushed flow line segment cannot stray very far away from this string of beads, for if it does, a path in the neutered space which follows the string of beads will be much shorter than the path along the pushed flow line, which will contradict that the pushed flow line is quasigeodesic in the neutered space. To make this comparison, we will first need to know how much distance along a neutered space path is decreased when the path is projected onto a string of beads.

3.2.2 Projecting Onto Strings of Beads Decreases Distance

Definition 3.2.2 *For a string of beads γ_+ along a geodesic γ, define the* ***string of beads projection*** *onto γ_+, denoted $\pi_{\gamma_+} : \mathbb{H}^3 \to \gamma_+$, by*

$$\pi_{\gamma_+}(x) = \text{ nearest point projection of } x \text{ to } \gamma_+.$$

In the case where there is more than one nearest point to x, in other words, in case x is equidistant from the string and one or more beads, project x onto the string.

It is of course possible that a point is equally close to two beads, but not all that close to the string (see Figure 3.6). However, we may choose the beads to be far enough apart so that this can't happen.

To reduce notational complexity, the projection π_{γ_+} will be denoted simply by π when the string of beads we are projecting onto is clear from the context.

Note that nearest point projection from any point in $\mathbb{H}^3$ onto a string of beads γ_+ will project that point orthogonally onto either the geodesic γ or onto one of the beads along the geodesic. This projection function will be used to project a pushed flow line segment onto a string of beads γ_+. The String of Beads Projection Lemma (Lemma 3.2.3) will establish that the image of a pushed flow line under π will be substantially shorter than the original pushed flow line.

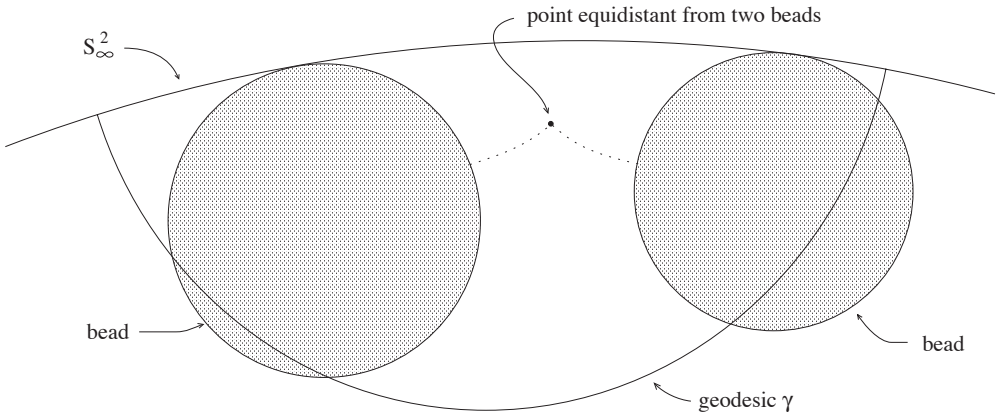

Figure 3.6: A point which is equally close to two beads but not close to the string.

Lemma 3.2.3 (String of Beads Projection Lemma) *Let c be a segment of path whose endpoints lie on the boundary of a neighborhood of radius r of a string of beads γ_+, and whose interior lies completely outside this neighborhood. Then projecting c onto γ_+ decreases distance by a multiplicative factor of at least $\frac{e^r}{2}$. That is,*

$$|c| \geq \frac{e^r}{2} \cdot |\pi c|.$$

Remark 3.2.4 *Note that for any path c, πc is a union of (usually disjoint) arcs $c_1, ..., c_n$, lying alternately along a bead and along the string (see Figure 3.7). Thus the length $|\pi c| = \Sigma |c_i|$.*

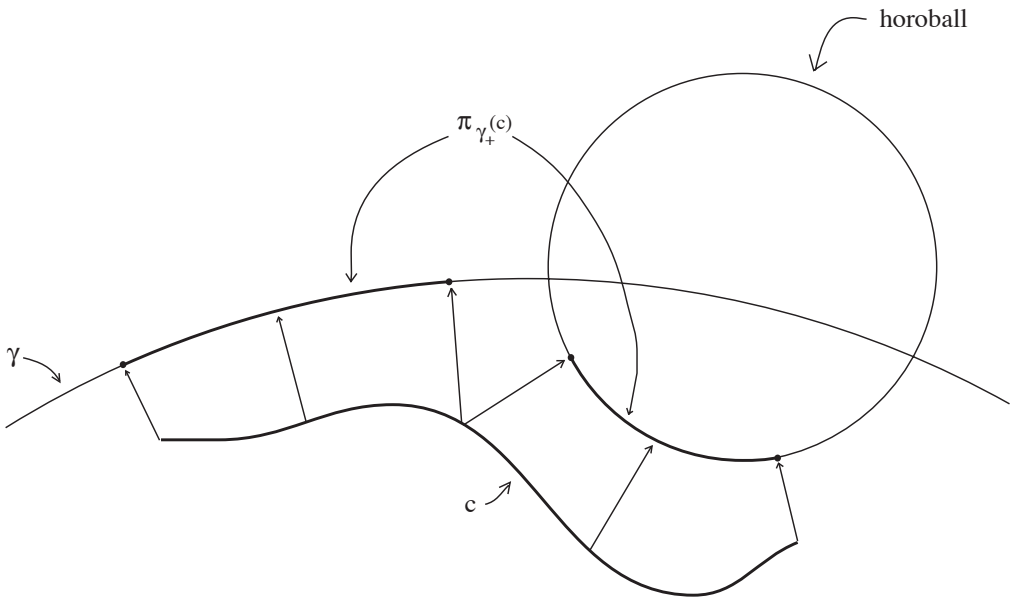

Figure 3.7: The image of a path under π_{γ_+} need not be connected.

Proof: [String of Beads Projection Lemma] Let c be a segment of path whose endpoints lie on the boundary of a neighborhood of radius r of a string of beads γ_+, and whose interior lies completely outside this neighborhood. Then c can be broken up into subpaths $c_1, \ldots, c_n$ which project alternately onto the geodesic γ and onto a horosphere that γ intersects.

Let $|c_i|$ be the length of path subsegment c_i, and let $|\pi c_i|$ be the length of the image πc_i. Then, if c_i projects onto the geodesic γ under π,

$$|c_i| \geq \frac{1}{2}(e^r + e^{-r}) \cdot |\pi c_i| \geq \frac{e^r}{2} \cdot |\pi c_i|$$

by the Geodesic Projection Lemma (Lemma B.1.1). On the other hand, if

c_i projects onto the one of the horoballs that γ intersects under π, then

$$|c_i| \geq e^r \cdot |\pi c_i| \geq \frac{e^r}{2} \cdot |\pi c_i|$$

by the Horosphere Projection Lemma (Lemma B.2.1). Therefore

$$|c| \geq \frac{e^r}{2} \cdot |\pi c|,$$

as desired. □

3.2.3 Creating a (Potentially) Shorter Path

Recall that our goal is to show that a pushed flow line segment must remain inside a neighborhood of the string of beads along the geodesic connecting its endpoints. To do this, we will see that if a pushed flow line segment strays too far away from the string of beads connecting its endpoints, we can produce a much shorter path by following its image along the string of beads instead. This will contradict the fact that a pushed flow line is a K_{p}-quasigeodesic in the neutered space.

We have seen that the length of a path far from string of beads is significantly longer than its image under π. However, the image of a path under projection by π_{γ_+} need not be connected (recall Figure 3.7). Therefore, to create a true path along the string of beads, we will need to connect these disconnected pieces. A priori, these extra connector pieces may be so large

as to negate the savings gained by projecting onto the string of beads. However, we will see that that is not the case, for the length of these joining paths is bounded above by some constant J. As long as we ensure that the horoballs are placed a distance at least $2J$ apart (which we may easily accomplish by choosing slightly smaller cusps, if necessary), then we will see that this extra length no more than doubles the overall length of the path along the string of beads.

Suppose c is a path with endpoints a and b, and let γ_+ be the string of beads connecting a to b. Let π denote projection onto the string of beads γ_+. We will create another connected path s from a to b along the string of beads (which we will show is a shorter path if c strays too far away from γ_+). To create s, project c onto the string of beads. Thus we obtain a sequence of (likely disjoint) path segments on γ_+. These correspond to the c_i's in Lemma 3.2.3. To be more specific, denote the subsegments which lie along the geodesic by g_i's and the ones lying along one of the horospheres the geodesic γ intersects by h_i's, with lengths $|g_i|$ and $|h_i|$ respectively. Since these subpaths do not necessarily form a connected path along γ_+, let j_i's be the (shortest) paths along the string of beads joining images lying on the string and images lying on a bead (see Figure 3.8). Proposition 3.2.5 shows that the length of the connector pieces j_i is bounded above.

Proposition 3.2.5 *There is a universal constant $J > 0$ so that any two consecutive subsegments (one projecting onto the string and the other pro-*

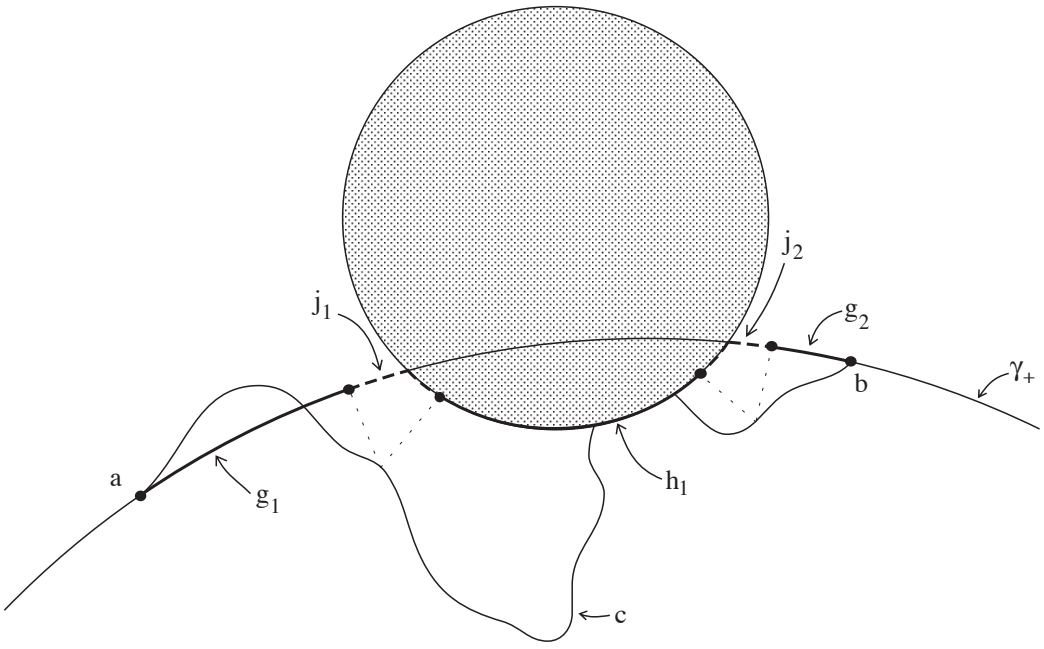

Figure 3.8: Creating a new path $s = g_1 \cup j_1 \cup h_1 \cup j_2 \cup g_2$ from c.

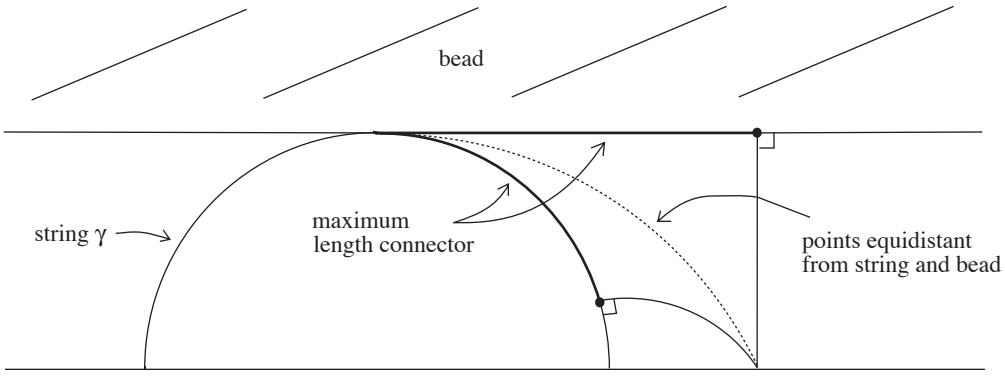

Figure 3.9: The maximum length of a connector.

jecting onto a bead) of the projection of a segment of path onto the string of beads connecting its endpoints can be connected by a path with length at most J.

Proof: The longest connector will occur when the string just touches the bead (see Figure 3.9). The curve of points equidistant from the string and the bead divides any path into segments which project onto the string and onto the bead. The length of the required connector increases as the path being projected move further and further away from the string and bead along the curve of equidistant points. Figure 3.9 exhibits the upper bound for such a connector; call it J. □

3.2.4 Pushed Flow Line Segments Lie Inside Neighborhoods of Strings of Beads

Assume we have chosen our cusps so that any two horoballs are at least $2J$ apart. In this section we will show that a pushed flow line segment in N, in fact, any K-quasigeodesic segment in N, lies within a neighborhood of a string of beads along a genuine geodesic segment in $\mathbb{H}^3$. Note that this proof is similar in spirit to the proof that a K-quasigeodesic lies inside an R-neighborhood of a geodesic (Proposition 3.1.1), except that this time we must take the geodesic and the horoballs it intersects into account.

Proposition 3.2.6 *Choose $K > 0$. Then there exists $R > 0$ (depending on K) such that if q is any K-quasigeodesic segment in the neutered space N, and γ is the hyperbolic geodesic segment passing through the endpoints of q, then q lies within a (hyperbolic) distance R of the string of beads along γ.*

Proof: [Proposition 3.2.6] Define $R = 9K^2$. Then q lies completely inside the regular neighborhood $N_R(\gamma_+)$ of the string of beads along γ, for suppose $y \in q$ falls outside this neighborhood. Then there is a long subsegment c of q, with endpoints a and b on the boundary of a smaller neighborhood of radius $r = 3K$, so that the interior of c falls entirely outside this smaller

neighborhood of the string of beads (see Figure 3.10). Thus

$$|c| \geq 2(R - r). \tag{3.6}$$

We will see that a factor of K shortcut can be taken by traveling from a straight to the string of beads along γ, across the string of beads, and back up to b, which contradicts that q is a K-quasigeodesic.

Let π denote projection onto the string of beads γ_+. Connect a to $a' = \pi(a)$ and b to $b' = \pi(b)$ using paths orthogonal to γ_+ of length r. If we project c onto the string of beads, we obtain a sequence of (potentially disjoint) paths on γ_+, beginning at a' and ending at b'. As before, label these subpaths using g_i's and h_i's depending on whether π projects them onto the geodesic γ or a bead along γ. Again, let j_i's be the connectors between consecutive g_i's and h_i's. Let s be the path thus obtained, by traveling from a to a' along the orthogonal path, then traveling along the string of beads γ_+ to b' using the now connected path which alternates between g_i's and h_i's connected together by j_i's, and finally passing up from b' to b using the second orthogonal path (again, see Figure 3.10).

Note that each horoball along the string of beads between a' and b' requires the addition of two connector paths, one on each side of the horoball. Thus by Proposition 3.2.5, each horoball along the string of beads adds length $2J$ to the length of the projected subpaths. By assumption, the horoballs are at least a distance $2J$ from each other, therefore at most 2 connectors are needed for each $2J$ distance traveled along the geodesic γ.

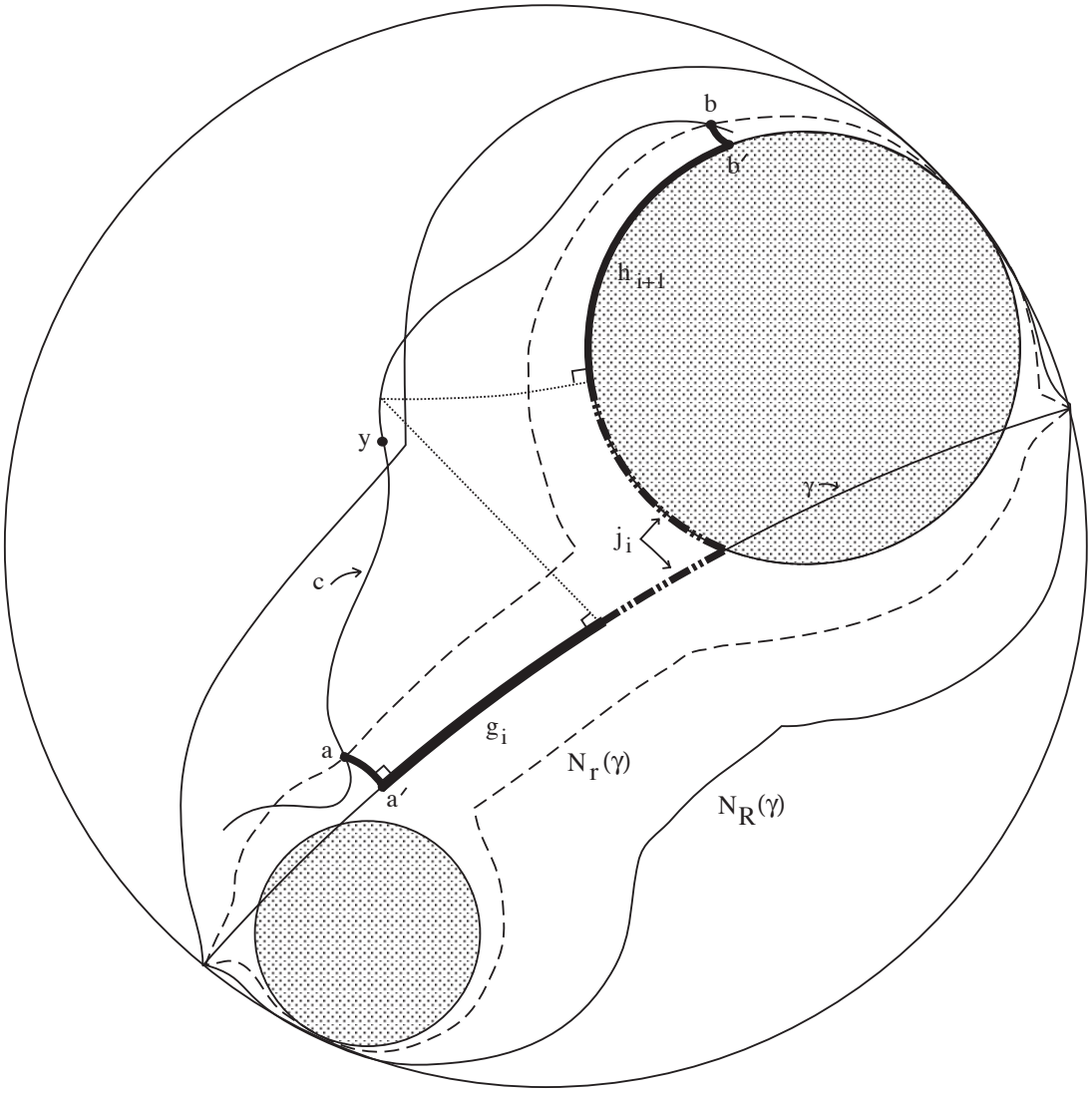

Figure 3.10: Quasigeodesic segments lie inside neighborhoods of strings of beads

Thus we need at most $(\Sigma|g_i|)/(2J)$ connectors added, for an additional length due to connectors of at most

$$\Sigma|j_i| \leq 2J \cdot \frac{\Sigma|g_i|}{2J} = \Sigma|g_i|. \tag{3.7}$$

Let $|s|$ be the length of s and $|c|$ be the length of c. The following computation shows that $K \cdot |s| \leq |c|$:

$$\begin{aligned}
K \cdot |s| &= K \cdot (2r + \Sigma|g_i| + \Sigma|h_i| + \Sigma|j_i|) \\
&\leq K \cdot (2r + \Sigma|g_i| + \Sigma|h_i| + \Sigma|g_i|) && \text{by equation (3.7)} \\
&\leq K \cdot (2r + 2(\Sigma|g_i| + \Sigma|h_i|)) \\
&\leq K \cdot (2r + 2|\pi c|) \\
&= 2Kr + 2K|\pi c| \\
&\leq 2Kr + 2K \cdot \tfrac{2}{e^r} \cdot |c| && \text{by Proposition 3.2.3} \\
&= 6K^2 + 2K \cdot \tfrac{2}{e^{3K}} \cdot |c| && \text{since } r = 3K \\
&= 6K^2 + 4K\tfrac{1}{e^{3K}} \cdot |c| \\
&\leq 6K^2 + \tfrac{e^{3K}}{2} \cdot \tfrac{1}{e^{3K}} \cdot |c| && \text{since } 1 < K \text{ thus } 4K < \tfrac{e^{3K}}{2} \\
&= 6K^2 + \tfrac{1}{2}|c| \\
&\leq (R - r) + \tfrac{1}{2}|c| && \text{since } R = 9K^2,\ r = 3K,\ K > 1 \\
&\leq \tfrac{1}{2}|c| + \tfrac{1}{2}|c| && \text{by equation 3.6} \\
&= |c|
\end{aligned}$$

Recall that at the beginning we assumed that a portion of the K-quasigeodesic c lies outside the neighborhood of radius R of the string of beads. However, we just found a path s so that $K \cdot |s| \leq |c|$ – a contradiction. $\square$

Corollary 3.2.7 *There exists a constant $R_p > 0$ so that every pushed flow line segment lies within a neighborhood of radius R_p of the string of beads connecting its endpoints.*

3.2.5 Flow Line Segments Lie Inside Neighborhoods of Strings of Beads

We know that a pushed flow line segment lies in a neighborhood of the string of beads along the geodesic connecting its endpoints. A pushed flow line is just a flow line which has been pushed out of all the cusps; thus a pushed flow line agrees with the original flow line outside the cusps. Therefore we only need to see that the segments of flow line which lie inside a cusp lies close to the string of beads.

Note that this does not follow automatically from what we have already done, for cusps come in two flavors: beads and non-beads. A segment of flow line which lies inside one of the beads trivially lies inside a neighborhood of the string of beads, but the flow line may enter non-beads as well (refer to Figure 3.11).

Proposition 3.2.8 (Flow Line Segments Lie in String of Beads Nbhds) *There exists $R_s > 0$ such that if ℓ is a flow line segment, then ℓ lies within*

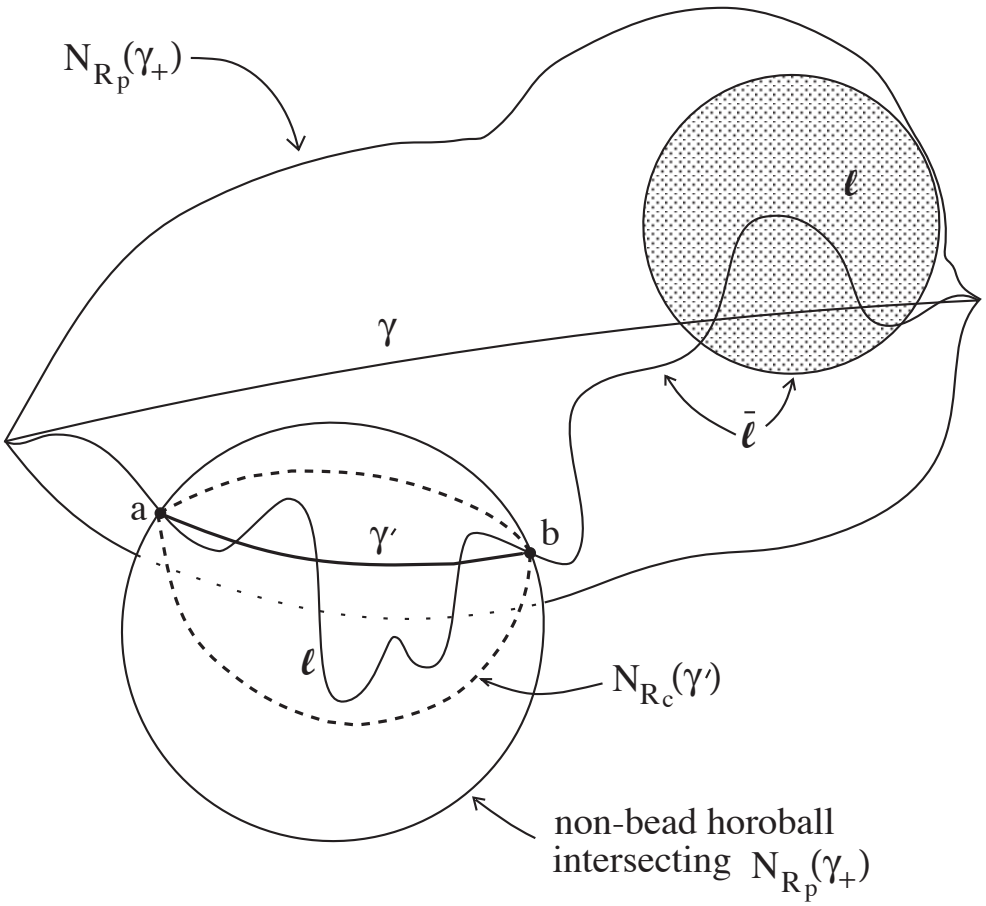

Figure 3.11: Flow line segments lie inside $R_{\rm s} = R_{\rm p} + R_{\rm c}$ neighborhoods of strings of beads.

a neighborhood of radius R_s about the string of beads along the geodesic connecting its endpoints.

Proof: Let ℓ be a flow line segment. This flow line segment is either part of a trapped flow line (one which spends infinite backwards or forwards time in a cusp) or it isn't.

Case 1: Suppose ℓ is not a subsegment of a trapped flow line. Extend ℓ a bit further if necessary so that the endpoints of ℓ lie outside the cusps. Then if $\overline{\ell}$ is the associated pushed flow line, $\overline{\ell}$ has the same endpoints as ℓ. Let γ be the geodesic connecting these endpoints.

The flow line ℓ agrees with $\overline{\ell}$ outside the cusps, thus $\ell \cap \overline{\ell}$ lies within a neighborhood of radius R_{p} about the string of beads along γ by Corollary 3.2.7. So consider a subsegment of ℓ which lies inside a cusp, with endpoints a and b on the boundary of the cusp (see Figure 3.11). Since the a and b are points on the pushed flow line, they lie within a distance R_{p} of the string of beads along the geodesic. In fact, since horoballs do not intersect, these points a and b must lie within radius R_{p} of the geodesic γ. By Convexity of Tubes (Lemma B.3.1), then, the entire geodesic segment γ' connecting these endpoints lies within a distance R_{p} of γ. But a flow line is quasigeodesic inside the cusps, therefore ℓ lies within a neighborhood of some radius R_{c} of γ'. Hence, the portions of flow line inside the cusp (and thus the entire flow line segment) lie within a neighborhood of radius $R_{\mathrm{s}} = R_{\mathrm{p}} + R_{\mathrm{c}}$ of the string of beads along γ.

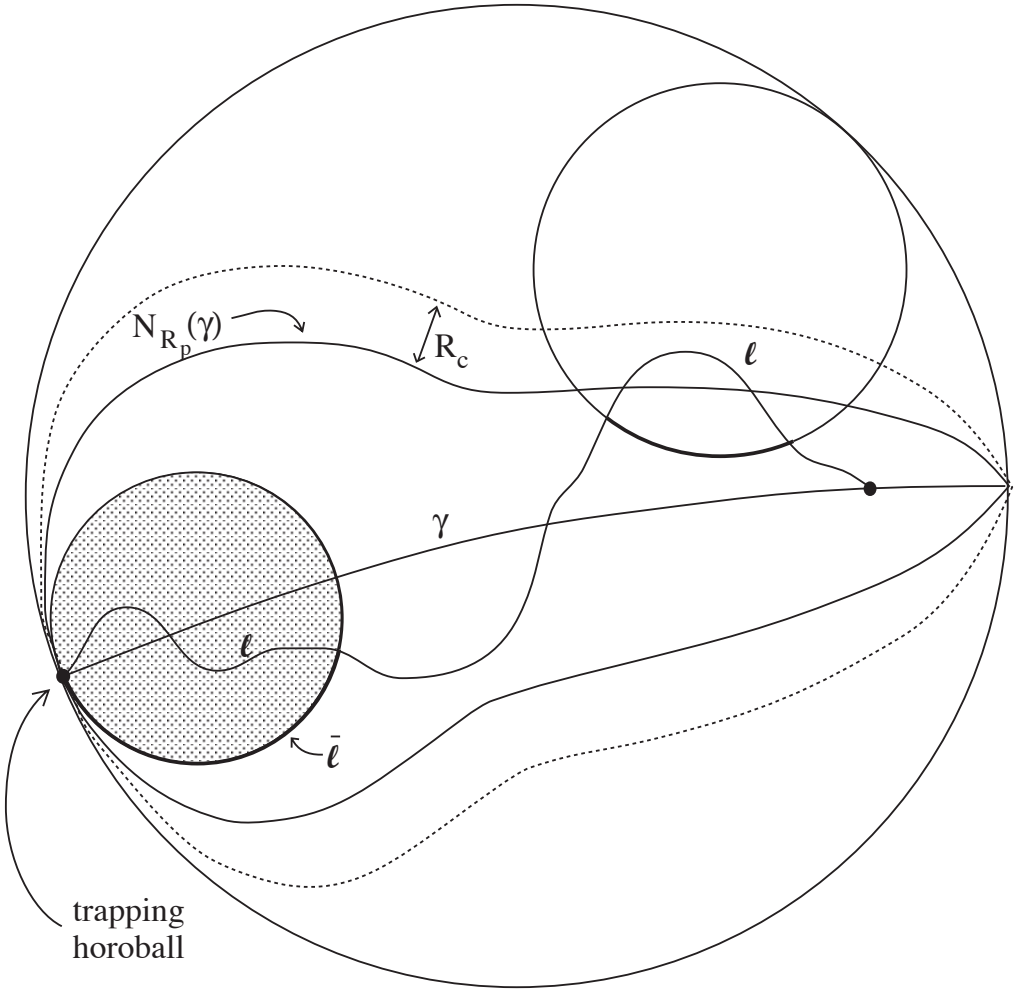

Figure 3.12: Trapped flow line segments lie inside $R_s = R_p + R_c$ neighborhoods of strings of beads.

□Case 1

Case 2: Suppose now that ℓ is a subsegment of a trapped flow line (see Figure 3.12). (If this is the case, then the trapping horoball *is* a bead of the string of beads connecting the endpoints of the *entire flow line*). Extend this flow line segment all the way to its end, where the trapping horoball meets the sphere at infinity. Let $\overline{\ell}$ be the associated pushed flow line; then again $\overline{\ell}$ has the same endpoints as ℓ, with at least one of these endpoints lying on the sphere at infinity. Let γ be the geodesic connecting these endpoints. Then the trapping horoball(s) are beads on the the string of beads along γ, so it is immediate that the portion of ℓ inside the trapping horoball lies within the string of beads, and hence any neighborhood of the string of beads, along γ. The argument for the rest of ℓ follows exactly as above.

Therefore, every flow line segment lies within a neighborhood $R_{\mathrm{s}} = R_{\mathrm{p}} + R_{\mathrm{c}}$ of the string of beads connecting its endpoints. □Case 2 □

3.3 Flow Lines Lie In Neighborhoods of Geodesics

Overall, then, a flow line segment tracks a fixed geodesic when it is away from the beads along the geodesic. The goal of this section is to show that a flow line segment tracks a geodesic in a neighborhood of the beads as well.

The proof proceeds as follows: Consider a flow line segment which lies near a bead. If the flow line segment does not enter the bead, we will show that it will spend only a bounded amount of time near the bead, and therefore will not be such a poor judge of distances overall. If, on the other hand, the segment does enter the bead, then since flow lines are quasigeodesic inside cusps, it must track some other geodesic. We'll see that since the flow line segment must enter and exit the bead near the original geodesic, the flow line segment must track the original geodesic as well.

3.3.1 Flow Line Behavior Near Beads

In this section we will find an upper bound to the length of a flow line segment that can lie in a neighborhood of a cusp in the string of beads without diving into the cusp. Specifically, we'll show that if a portion of a flow line segment lies within some radius R of a bead, then the length of that portion can be at most $12e^M$, where M is the maximum length a geodesic can spend in an R-neighborhood of a horoball without entering the horoball.

Consider the geodesic between the points where the flow line segment first enters and last exits the neighborhood of radius R around some particular bead. This geodesic is likely to pass through many cusps, as the radius R may be quite large and thus the neighborhood of radius R around the bead may intersect a significant number of other cusps. However, we will

show that this geodesic must be at least half the length of the flow line segment. To see this, we will push this geodesic out of all of the cusps except (possibly) the bead itself. This will indeed lengthen the original geodesic considerably, but by a predictable amount, as shown in Lemma 3.3.1 below. The length of the flow line segment inside the neighborhood cannot be much larger than this lengthened path, for we will show that distance cannot be significantly shortened by a path passing through only one cusp (Lemma 3.3.3). Thus we will obtain an upper bound for the length of a flow line segment which lies inside an R-neighborhood of a bead without entering the bead.

The following lemma addresses how the length of a path going through a cusp compares to the length of the path obtained once the path has been pushed out of the cusp to the boundary. In particular, the length of the path increases greatly after being pushed, but it becomes no longer than the exponential of its original length.

Lemma 3.3.1 (Pushing Lemma) *Let γ be a geodesic in $\widetilde{M}$, the universal cover of M, passing into and out of a cusp at points a and b, and let d be the distance along the horosphere between a and b. Then $d < e^{d_\gamma(a,b)}$.*

Proof: [Pushing Lemma] Given the hypotheses,

$$\begin{aligned} e^{d_\gamma(a,b)} &= \{\sqrt{1+(\tfrac{d}{2})^2}+\tfrac{d}{2}\}^2 \qquad \text{by Proposition B.6.1} \\ &= d\sqrt{1+(\tfrac{d}{2})^2}+\tfrac{d^2}{2}+1 \\ &\geq d\sqrt{1+(\tfrac{d}{2})^2} \\ &\geq d \end{aligned}$$

as desired. □

Lemma 3.3.2 (No Cusp Lemma) *If ℓ is a segment of flow line which lies outside the cusps, then any path c with the same endpoints which travels through no cusps will have length at least $|\ell|$. Thus distance between points on a flow line cannot be shortened by a path which does not enter any cusps.*

Proof: [No Cusp Lemma] Let ℓ be a segment of flow line with endpoints a and b which lies outside all cusps. Flow lines are vertical in the singular Solv metric on the universal cover of M, with the scaling and shrinking which come from the pseudo-Anosov monodromy map occurring horizontally. Vertical lines in the singular Solv metric *are* the shortest paths between any pair of points on them, because the projection function proj : $\mathbb{R}^3 \to \mathbb{R}^1$ given by projecting onto the z-coordinate is distance non-increasing.

The modified singular Solv metric (which is quasi-isometric to the hyperbolic metric on M) is identical to the singular Solv metric as long as

we stay outside the cusps. Therefore, distance between points on a flow line segment which does not enter any cusps cannot be shortened by a path which does not enter any cusps. □

Lemma 3.3.3 (One Cusp Lemma) *There exists $L > 0$ such that if ℓ is a segment of flow line of length at least L which lies outside the cusps, then any path c with the same endpoints which travels through exactly one cusp will have length at least $\frac{1}{2}|\ell|$.*

Thus distance between points on a flow line cannot be shortened dramatically by a path which enters only one cusp.

Proof: [One Cusp Lemma] The basic idea is that if a flow line ℓ is long, then at least one endpoint of ℓ must be at a height far away from level 0. Since Solv scales distances dramatically as $t \to \infty$, this endpoint will lie a large horizontal Solv distance from the cusp, from the scaling in either the x or the y direction. Hence travel to the cusp itself is comparable in distance to the vertical travel along ℓ (see Figure 3.13). For simplicity, we prove the case where the cusp is a regular cusp. The case where the cusp is a singular cusp is similar.

Let $\widehat{T}$ be the intermediate cover of a regular cusp T in M, and let ℓ be a segment of flow line (lifted to $\widehat{M}$) with endpoints a and b. If π_x and π_y are projections of $\widehat{M}$ onto the xz and yz-planes respectively, then the flow

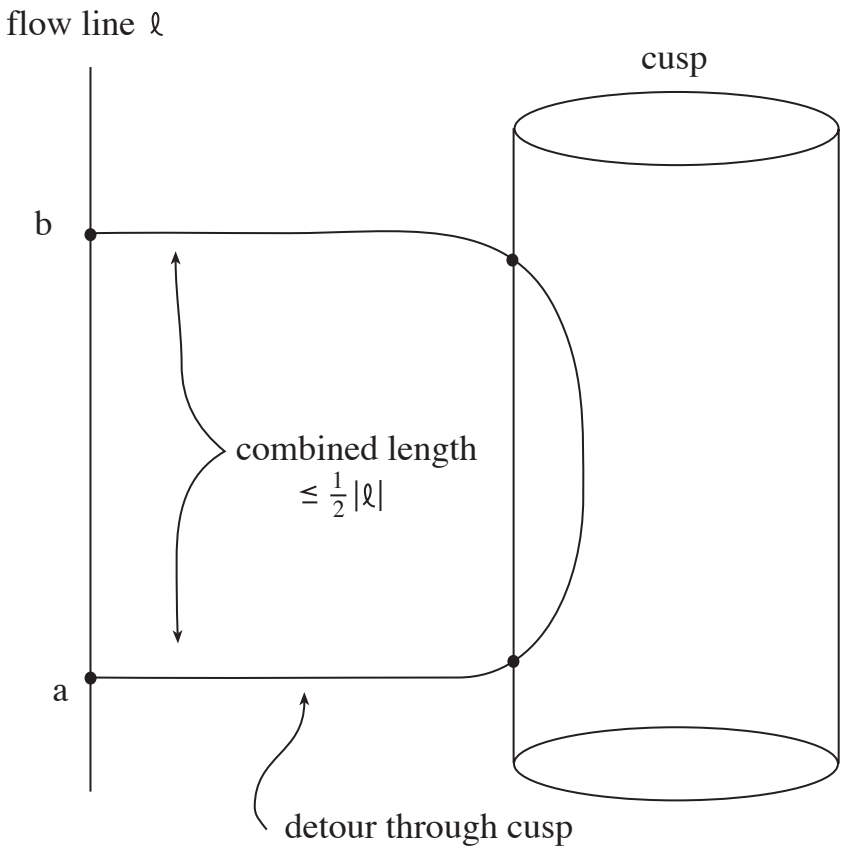

Figure 3.13: A detour through a cusp is not much shorter than the flow line segment between two points.

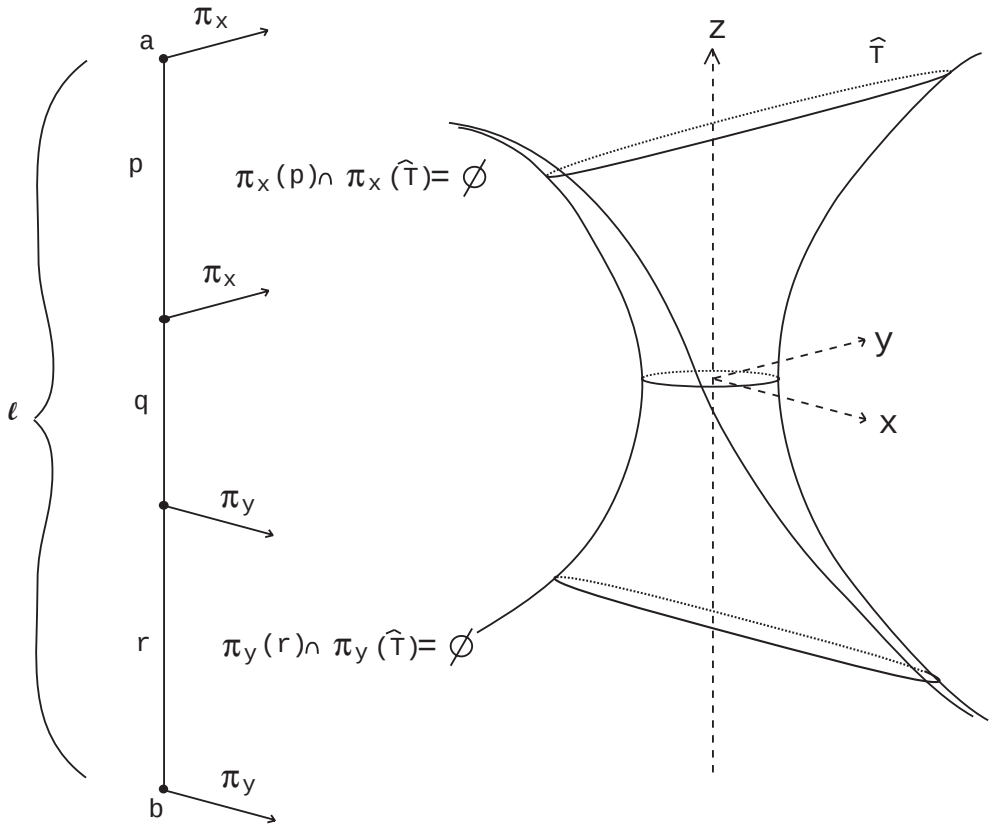

Figure 3.14: A flow line segment ℓ split up into the three segments p, q, and r.

line segment ℓ can be split up into three segments (some possibly empty): one segment p whose projection under π_x lies entirely outside of $\pi_x(\widehat{T})$, one segment r whose projection under π_y lies entirely outside of $\pi_y(\widehat{T})$, and one segment q whose endpoints lie inside or on the boundary of either $\pi_x(\widehat{T})$ or $\pi_y(\widehat{T})$ (see Figure 3.14).

The length of the segment q is bounded above by some constant B_q.

The Key Inequality in the following claim will be used to contend with segments p and r. The claim says, essentially, that whenever a flow line segment projects outside the cusp $\widehat{T}$, "horizontal" travel over from the flow line segment to the cusp is approximately as costly as "vertical" travel up the flow line segment.

Claim 3.3.4 *There exists $L_1 > 0$ such that the following holds for all flow line segments: Let ℓ be a segment of flow line with $|\ell| > L_1$ which projects entirely outside the cusp $\widehat{T}$ under π_x. Denote the endpoints of ℓ by a and b in such a way that under projection by π_x, the image of a is the further of the two endpoints from the image of $\widehat{T}$ (see Figure 3.15). Let H be the (horizontal) hyperbolic distance between $\pi_x(a)$ and $\widehat{T}$. Then*

$$H > .9|\ell|.$$

In other words, if an endpoint of such a flow line segment is far away from level 0, then the distance from that endpoint to the cusp is not much shorter than the length of the flow line segment.

Proof of Claim: Note that the modified metric on the xz-plane outside the cusps is simply the Solv metric, which is isometric to the hyperbolic metric on the xz-plane outside the cusps (take (x, z) in the space with the Solv metric to $(\lambda^{-z}x, e^z)$ in the upper half space model of hyperbolic space). Figure 3.15 depicts the upper half space model of $\mathbb{H}^2$, where it is

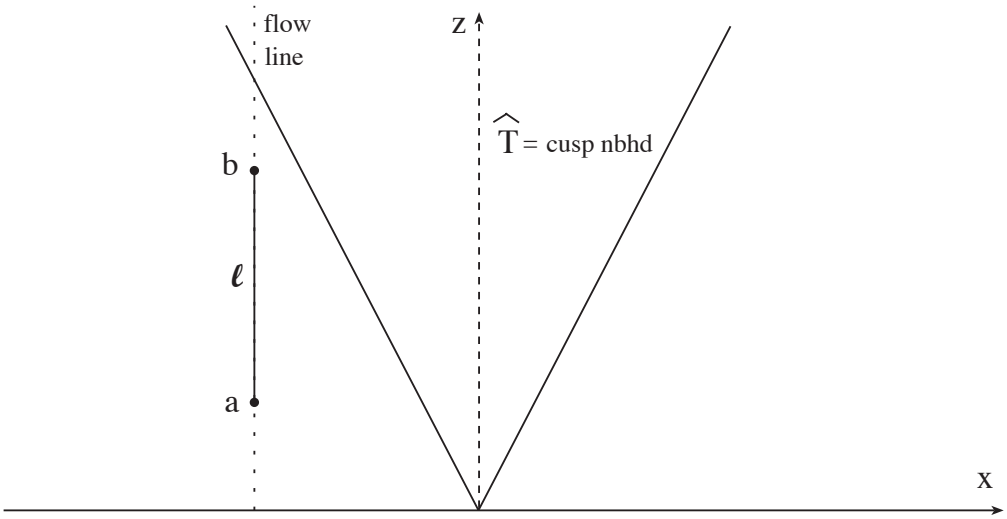

Figure 3.15: A flow line segment which projects outside $\widehat{T}$ under π_x.

easier to describe geodesics. In this model, flow lines in the Solv xz-plane are (vertical) geodesics in $\mathbb{H}^2$, a Solv cusp is a V-shaped region in $\mathbb{H}^2$, and projection from $\mathbb{R}^3$ to $\mathbb{R}^2$ (with the Solv metric restricted) which takes a point $(x, y, z) \mapsto (x, z)$ is distance non-increasing.

Let ℓ be a flow line segment with endpoints a and b which projects entirely outside the cusp $\widehat{T}$ under π_x, as in Figure 3.16. Let γ be the geodesic through a which is orthogonal to the boundary of $\widehat{T}$, and let c, d and e denote the points indicated in the figure. Throughout this proof, let bc denote the path in the figure between points b and c (and so on), and let $|bc|$ denote the length of such a path. Then the horizontal distance between the endpoint a and the cusp $\widehat{T}$ is given by $H = |ae|$, where distance is measured in $\mathbb{H}^2$. We will show that if ℓ is long enough (greater than some

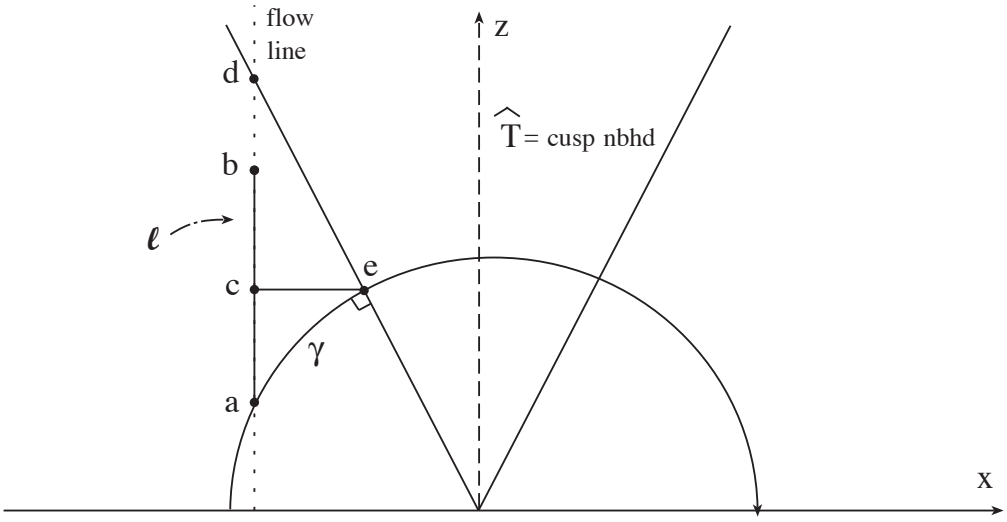

Figure 3.16: Set-up for Claim 3.3.4.

constant L to be defined below), then $H > .9|\ell|$.

Although the lengths of the paths ce and cd in the figure depend on the length of the flow line segment ℓ, they are bounded above, by constants B_{ce} and B_{cd} (see Figure 3.17). Further, B_{ce} and B_{cd} are independent of where ℓ is in relation to the cusp $\widehat{T}$, for if ℓ' is another flow line, then there is an isometry of the xz-plane taking ℓ' to ℓ, and sending $\widehat{T}$ to itself.

Let $L_1 = 10(B_{ce} + B_{cd})$, and suppose $|\ell| > L_1$. We will show that

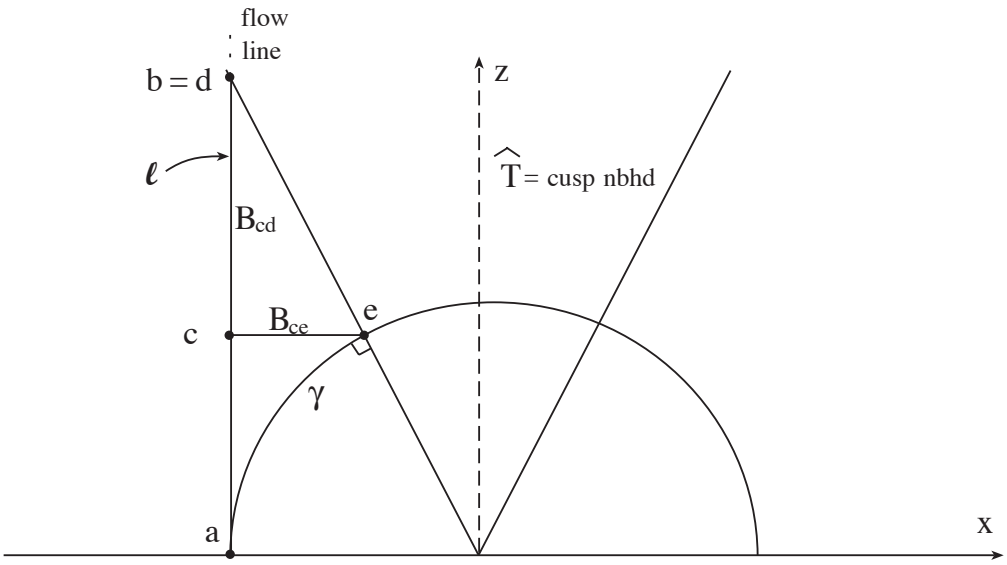

Figure 3.17: The limiting case, providing upper bounds for lengths $|cd|$ and $|ce|$.

$H > .9|\ell|$. By the triangle inequality, $H + |ce| > |ac|$; therefore

$$\begin{aligned}
H &> |ac| - |ce| \\
&= (|ad| - |cd|) - |ce| \quad \text{since } |ad| = |ac| + |cd| \\
&= |ad| - (|cd| + |ce|) \\
&\geq |\ell| - (|cd| + |ce|) \quad \text{since } \pi_x(b) \cap \pi_x(\widehat{T}) = \emptyset \\
&\geq |\ell| - (B_{ce} + B_{cd}) \\
&> |\ell| - \tfrac{1}{10}|\ell| \quad \text{since } |\ell| > 10(B_{ce} + B_{cd}) \\
&= .9|\ell|.
\end{aligned}$$

□Claim

Now we are ready to approach the general case, where the flow line ℓ splits up into the three segments p, q, and r (refer again to Figure 3.14). Let $L = 25(B_{ce} + B_{cd} + M_q)$, and suppose $|\ell| > L$. This length will force at least one of the endpoints to be far away from level 0. In particular, since $|\ell| > 25(B_{ce} + B_{cd} + M_q)$, at least one of p or r must have length at least $L_1 = 10(B_{ce} + B_{cd})$. There are two cases:

1. Both segments p and r have length at least $L_1 = 10(B_{ce} + B_{cd})$. In this case the combined distance from a to the cusp and from b to the cusp will be at least half the length of ℓ.

2. One of the segments p, r has length less than $L_1 = 10(B_{ce} + B_{cd})$; the other has length at least L_1. In this case, the furthest endpoint (the one corresponding to either p or r, whichever is longer) is even

further away from the cusp than those in case 1, so the distance from that endpoint to the cusp alone will be at least half the length of ℓ.

In either case, then, travel to and from the cusp is nearly as costly as travel up the flow line. The details follow:

Case 1: Suppose both $|p| > L_1 = 10(B_{ce} + B_{cd})$ and $|r| \geq L_1$. If α is any path in the modified solv metric passing through exactly one cusp $\widehat{T}$, starting at a and ending at b, then α must be at least as long as the minimum distance H_a from a to $\widehat{T}$ and H_b from $\widehat{T}$ to b. Further, since $|p| + |q| + |r| = \ell > L > 25M_q$ and $|q| \leq B_q$, at least one of p, r has length at least $10M_q$; without loss of generality, assume $|p| > 10M_q$. Therefore,

$$\begin{aligned}
|\alpha| &\geq H_a + H_b \\
&\geq .9|p| + .9|r| && \text{by Claim 3.3.4} \\
&= [.5|p| + .4|p|] + .9|r| \\
&> .5|p| + .4(10|q|) + .9|r| && \text{since } |p| > 10M_q \geq 10|q| \\
&= .5|p| + 4|q| + .9|r| \\
&> .5|p| + .5|q| + .5|r| \\
&= .5|\ell|.
\end{aligned}$$

□Case 1

Case 2: Without loss suppose $|p| > L_1$ but $|r| < L_1$. We know that

$$|p| + |q| + |r| = |\ell| \geq L = 25(B_{ce} + B_{cd} + M_q) = 2.5L_1 + 25B_q,$$

with $|r| < L_1$ and $|q| < B_q$. Therefore it follows that

$$|p| \geq 1.5L_1 + 24B_q \tag{3.8}$$

Now, if α is any path starting at a and ending at b, traveling through exactly one cusp $\widehat{T}$, then α must be at least as long as the minimum distance H_a from a to $\widehat{T}$. Therefore,

$$\begin{aligned}
|\alpha| &\geq H_a \\
&\geq .9|p| && \text{by Claim 3.3.4} \\
&= .5|p| + .4|p| \\
&> .5|p| + .4(1.5L_1 + 24B_q) && \text{by equation (3.8)} \\
&= .5|p| + .6L_1 + 9.6B_q \\
&> .5|p| + .5L_1 + .5B_q \\
&> .5|p| + .5|r| + .5|q| && \text{since } L_1 > |r| \\
&= .5|\ell|.
\end{aligned}$$

□Case 2

Thus, as long as a segment of flow line $|\ell| > L = 25(B_{ce} + B_{cd} + M_q)$, if α is any other path in modified Solv connecting the endpoints of ℓ which enters exactly one cusp, then $|\alpha| > .5|\ell|$, as desired. □

Lemma 3.3.5 (Limited Time Lemma) *There exists a constant $M > 0$, depending only on the constant R, such that if a and b are endpoints of a flow line segment ℓ which lies entirely inside the neighborhood of radius R of a horoball, yet outside the horoball itself, then $|\ell| < M$.*

In other words, if a flow line segment spends a long time near a cusp,

then it must enter that cusp.

Proof: [Lemma 3.3.5] Let a and b be endpoints of a flow line segment ℓ which lies entirely inside the neighborhood of radius R of a horoball H yet outside the horoball itself, and let γ be the geodesic segment connecting a and b (see Figure 3.18). Either γ misses the horoball H or it enters H.

Case 1: Suppose the geodesic segment γ does not enter the horoball H at all. Then $|\gamma|$ is bounded above by some constant $B > 0$ which depends only on R (see Figure 3.19). Although this geodesic segment γ does not enter the horoball H, it may enter other horoballs on its way from a to b. If $\overline{\gamma}$ denotes the path obtained by pushing γ out of all the cusps it passes through, then by the Pushing Lemma (Lemma 3.3.1)

$$|\overline{\gamma}| \leq e^{|\gamma|} \leq e^{B}.$$

However, $\overline{\gamma}$ is a path connecting the endpoints of ℓ which does not enter any cusps. Thus by the No Cusps Lemma (Lemma 3.3.2),

$$|\ell| \leq |\overline{\gamma}|.$$

Therefore

$$|\ell| \leq e^{B}$$

for some constant B. □Case 1

Case 2: Suppose the geodesic segment γ connecting a and b passes through the horoball H. Let a' and b' be the points near endpoints a and b where γ

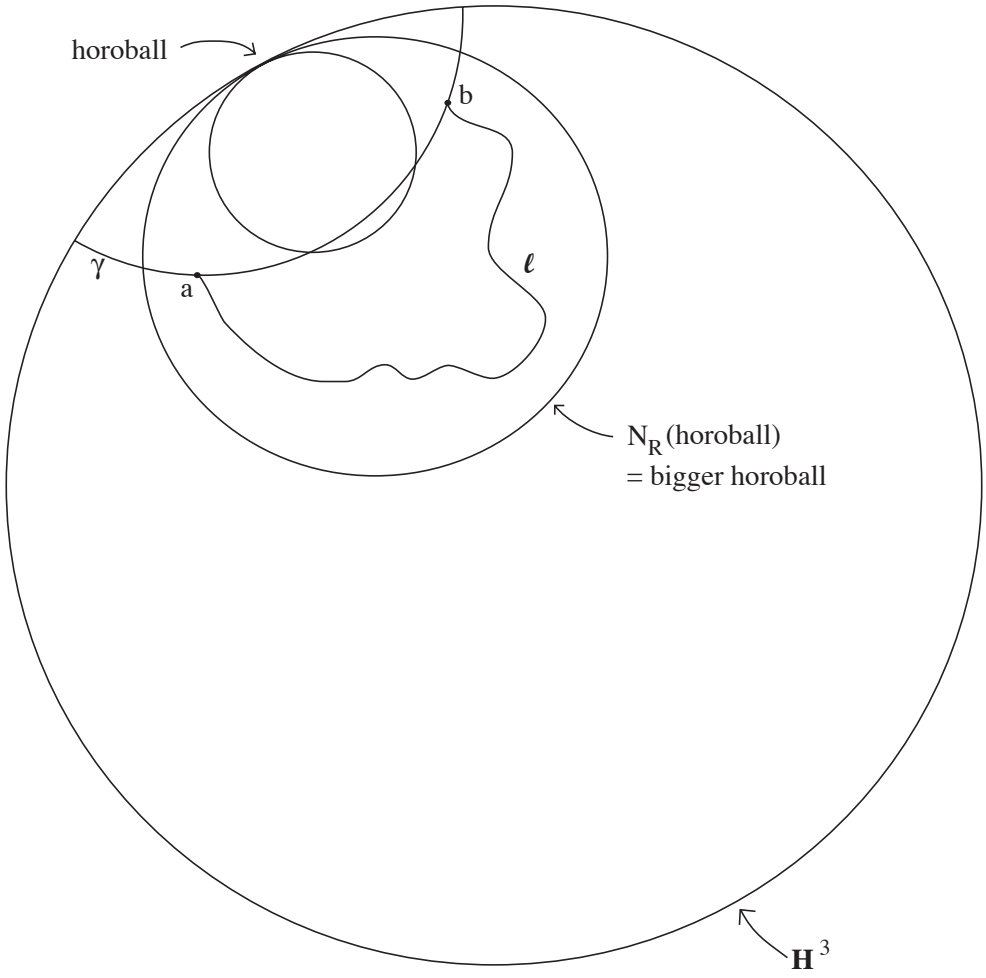

Figure 3.18: A flow line outside yet hovering near a horoball.

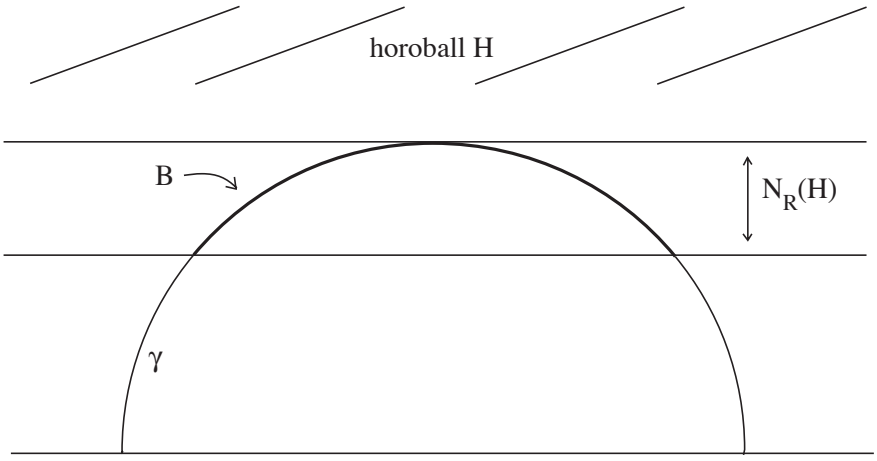

Figure 3.19: An upper bound for the length of a subsegment of γ outside H yet inside $N_R(H)$.

intersects H (see Figure 3.20). The lengths of the segments of γ between a and a' and between b and b' are geodesic segments outside of H yet inside $N_R(H)$, and hence both are bounded above by the constant B found in Case 1. As before, these segments may enter other cusps which intersect the neighborhood of radius R about H. Let $\overline{\gamma}$ be the path γ pushed out of all the cusps it passes through *except* H. Then $\overline{\gamma}$ is made up of three subpaths α, β, and δ, where α and β are obtained by pushing the segment of γ between a and a' and between b and b' out of all the cusps, and δ is the subsegment of γ inside H connecting a' to b'. By the Pushing Lemma again (Lemma 3.3.1), we know $|\alpha|, |\beta| \leq e^B$, thus

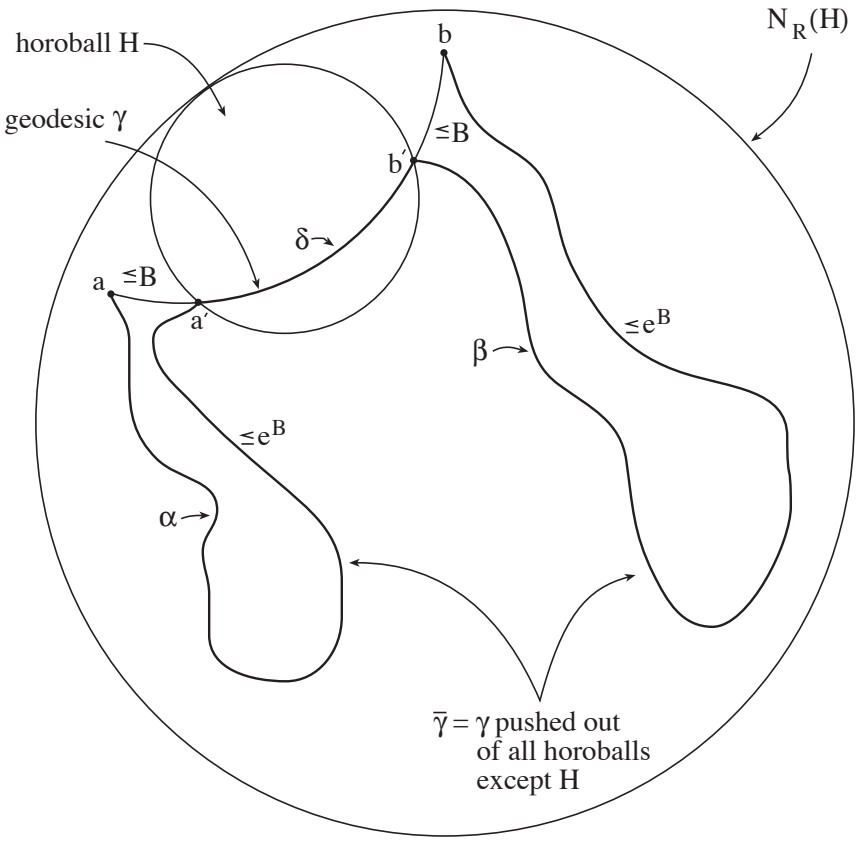

Figure 3.20: An upper bound for the length of α and β.

$$\begin{aligned} |\overline{\gamma}| &= |\alpha| + |\delta| + |\beta| \\ &\leq 2e^B + |\delta|. \end{aligned}$$

However, by Proposition B.6.1 which expresses the relationship between distance through a cusp and distance around the boundary of the cusp, if d is the length of the shortest path along the boundary of the horoball H connecting a' to b', then

$$\begin{aligned} |\delta| &= 2\ln(\sqrt{1+(\frac{d}{2})^2} + \frac{d}{2}) \\ &\leq 2\ln(1+(\frac{d}{2})^2 + \frac{d}{2}) \\ &= 2\ln(1+\frac{d^2}{4} + \frac{d}{2}) \\ &= 2\ln(\frac{1}{4}\cdot(4+d^2+2d)) \\ &\leq 2\ln(\frac{1}{4}\cdot(d^2+d^2+d^2)) \\ &= 2\ln(\frac{3}{4}d^2) \\ &< 2\ln(d^2) \\ &= 4\ln d, \end{aligned}$$

The distance d along the horosphere between a' and b' is at most the distance along ℓ between a and b, as a' and b' are closer together than a and b, and the distance along the horosphere is closer to the geodesic γ (containing all 4 points) than ℓ is to γ. Therefore

$$|\delta| \leq 4\ln|\ell|.$$

On the other hand, the path $\overline{\gamma}$ connects a to b by traveling through exactly one cusp. Therefore by the One Cusp Lemma (Lemma 3.3.3),

$$.5|\ell| \leq |\overline{\gamma}|.$$

Putting all this together, we obtain

$$\begin{aligned} .5|\ell| &\leq |\overline{\gamma}| \\ &\leq 2e^B + |\delta| \\ &\leq 2e^B + 4\ln|\ell|, \end{aligned}$$

Since this equation is not satisfied for $|\ell| \geq 12e^B$, we must have $|\ell| < 12e^B$. □Case 2

Recall that in Case 1, where γ did not enter H, we obtained $|\ell| \leq e^B$. Thus, whether γ goes through the horoball H or not, we have a constant $M = 12e^B$ such that $|\ell| < M$, as desired. □

3.3.2 Flow Line Segments Lie Inside Neighborhoods

Proposition 3.3.6 *There is a constant $R_{fs} > 0$ such that every segment of flow line of the suspension flow on M lies within the neighborhood of radius R_{fs} of the geodesic connecting its endpoints.*

Proof: Let R_{s} be the constant from Proposition 3.2.8, so that every flow line segment lies within a neighborhood of radius R_{s} of a string of beads along the geodesic connecting its endpoints. Away from the beads, the flow lines lie inside the radius R_{s} of the string, the original geodesic. So we only need to consider the portions of flow line which lie within a neighborhood of a bead.

Let ℓ be a flow line, and let a and b be endpoints of a segment of ℓ which lies inside a neighborhood of radius R_{s} of a bead. Then a and b lie within R_{s} of the original geodesic, for they are at the edge of the tube of radius R_{s} around the string.

Let M_{s} be the constant that comes from the Limited Time Lemma (Lemma 3.3.5) for $R = R_{\mathrm{s}}$. This segment we just created is either shorter than or longer than M_{s}. If the segment is shorter than M_{s}, then the entire segment is within $R_{\mathrm{s}} + M_{\mathrm{s}}$ of the geodesic, by measuring along the segment back to endpoint a (at most M_{s}), then joining up to the string with a path of length at most R_{s}.

So assume that the segment is longer than M_{s}. Then by the Limited Time Lemma, the flow line segment must enter the cusp. (See Figure 3.21, a reproduction of Figure 1.19, repeated here for reference.) The flow line segment does not enter the cusp more than once, however, by Lemma 2.1.11. Therefore this flow line segment consists of a segment from a to the point a' where the flow line meets the cusp (of length at most M_{s}), connected to a segment from a' to b' which lies entirely within the cusp, connected to a

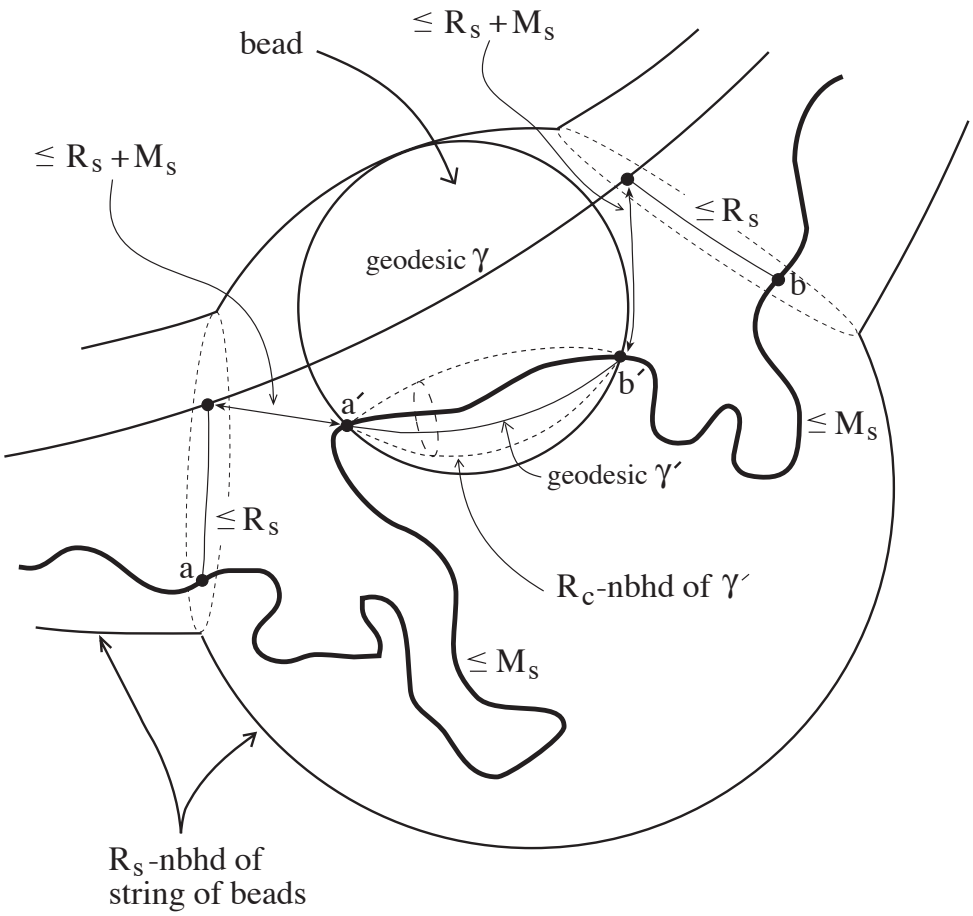

Figure 3.21: The flow line segment ℓ lies within $R_{\rm fs} = R_{\rm c} + R_{\rm s} + M_{\rm s}$ of γ.

segment from b' to b of length at most M_{s}. As above in the case of the short flow line segment, the subsegments between a and a' and between b and b' are within $R_{\mathrm{s}} + M_{\mathrm{s}}$ of the geodesic, by measuring along the subsegments. It remains only to consider the portion of the flow line inside the cusp.

The flow lines are quasigeodesic in the cusp, therefore they lie within a neighborhood of radius R_{c} of the geodesic connecting its endpoints a' and b'; call it γ'. By Convexity of Tubes, the maximum distance between γ and γ' occurs at one of the endpoints a' or b'. Thus the entire geodesic segment γ' lies within a $R_{\mathrm{s}} + M_{\mathrm{s}}$ neighborhood of γ. Therefore, every point on the flow line between a' and b' lies within a distance of $R_{\mathrm{c}} + R_{\mathrm{s}} + M_{\mathrm{s}}$ of γ (for they lie at most R_{c} from γ', which is at most $R_{\mathrm{s}} + M_{\mathrm{s}}$ from γ). Taking $R_{\mathrm{fs}} = R_{\mathrm{c}} + R_{\mathrm{s}} + M_{\mathrm{s}}$ gives the desired result. □

3.3.3 Passing From Segments to the Entire Flow Line

Theorem 3.3.7 (Flow lines lie inside neighborhoods of geodesics) *There exists $R_\Phi > 0$ such that if ℓ is a flow line, then there is a unique geodesic γ such that ℓ lies within a neighborhood of radius R_Φ about γ.*

Proof: Let ℓ be a flow line in $\widetilde{M}$, and choose a point p on ℓ. For each $n \in \mathbb{N}$, choose points a_n and b_n on ℓ at unit intervals on either side of p, so

that the distance along ℓ between p and a_n and between p and b_n is n, and so that p is contained in the interval between a_n and b_n.

Consider the ball of radius $2R_{\text{fs}}$ about p. By Proposition 3.3.6, p lies within a distance R_{fs} of the geodesic γ_n connecting a_n and b_n for all n. Therefore, each γ_n meets the ball of radius R_{fs} about p, and further each geodesic γ_n intersects the ball of radius $2R_{\text{fs}}$ about p in a geodesic segment.

For each n, let x_n and y_n be the endpoints of these segments of γ_n. In other words, x_n and y_n are the two points where the geodesic γ_n meets the sphere of radius $2R_{\text{fs}}$ about p (see Figure 3.22). Since the sphere is compact, there is a subsequence γ_{n_i} of γ_n such that endpoints x_{n_i} converge to a limit point x on the sphere and endpoints y_{n_i} converge to a limit point y on the sphere. This selects a geodesic in $\widetilde{M}$; let γ denote the geodesic connecting x to y. We will see that every point q on the flow line ℓ lies within a distance $R_\Phi = R_{\text{fs}} + 1$ of this geodesic γ.

Choose a point q on ℓ, and consider the ball of radius $d(p,q) + R_{\text{fs}} + 1$ around p. This ball is then a neighborhood of q. Let w_{n_i} and z_{n_i} denote the points where γ_{n_i} intersect this ball. These intersection points converge to points w and z on γ. Thus there exists an N_1 so large that if $n_i > N_1$, then $d(w_{n_i}, w) < 1$ and $d(z_{n_i}, z) < 1$. By Convexity of Tubular Neighborhoods of Geodesics, if $n_i > N_1$, then the segment of γ_{n_i} between w_{n_i} and z_{n_i} lies inside the neighborhood of radius 1 of the geodesic γ.

The sequences $\{a_{n_i}\}$ and $\{b_{n_i}\}$ make at least unit distance progress along ℓ from p. Thus there exists an $N_2 > 0$ ($N_2 = d(p,q) + R_{\text{fs}} + 1$ will do) such

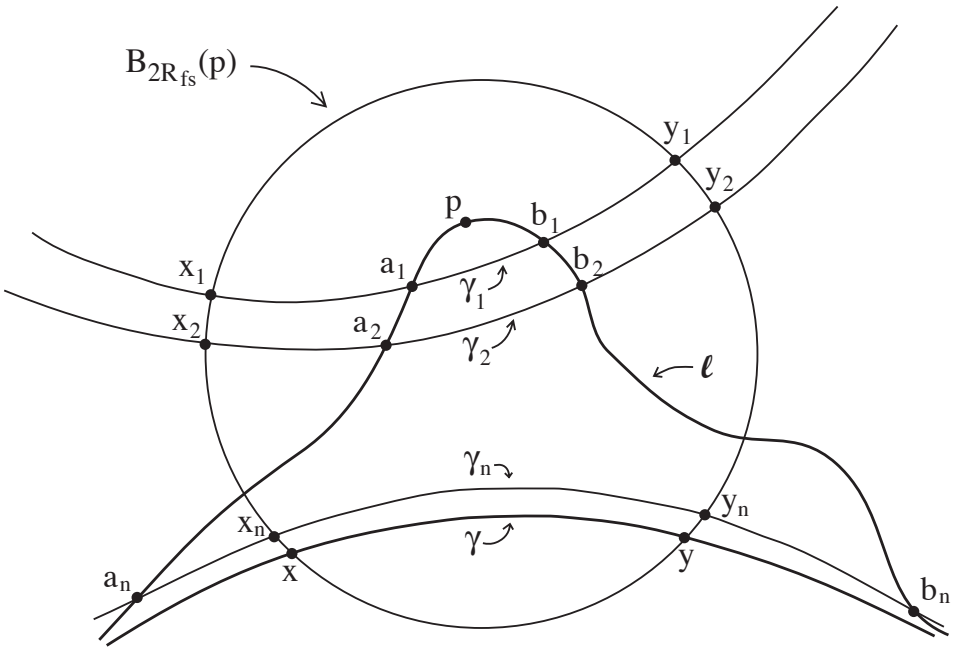

Figure 3.22: The sequence of geodesics $\gamma_1, \gamma_2, \ldots$, and the geodesic γ.

that if $n_i > N_2$, then the point q must lie between points a_{n_i} and b_{n_i} on ℓ. Then by Proposition 3.3.6 again, q lies within distance R_{fs} of the geodesic γ_{n_i}.

Let $N = \max\{N_1, N_2\}$ and choose $n_i > N$. Since $n_i > N_2$, q lies within distance R_{fs} of some point r, on the geodesic γ_{n_i}, which lies inside the ball of radius $d(p,q)+R_{\text{fs}}+1$ about p (see Figure 3.23). Since $n_i > N_1$, the segment of γ_{n_i} which lies inside $B_{d(p,q)+R_{\text{fs}}+1}(p)$ must fall inside the neighborhood of radius 1 of the geodesic γ. Hence r lies no more than 1 unit away from γ. Thus, the point q lies within distance $R_\Phi = R_{\text{fs}} + 1$ of the geodesic γ.

□

Corollary 3.3.8 *A flow line in $\widetilde{M} = \mathbb{H}^3$ has two distinct endpoints on the sphere at infinity.*

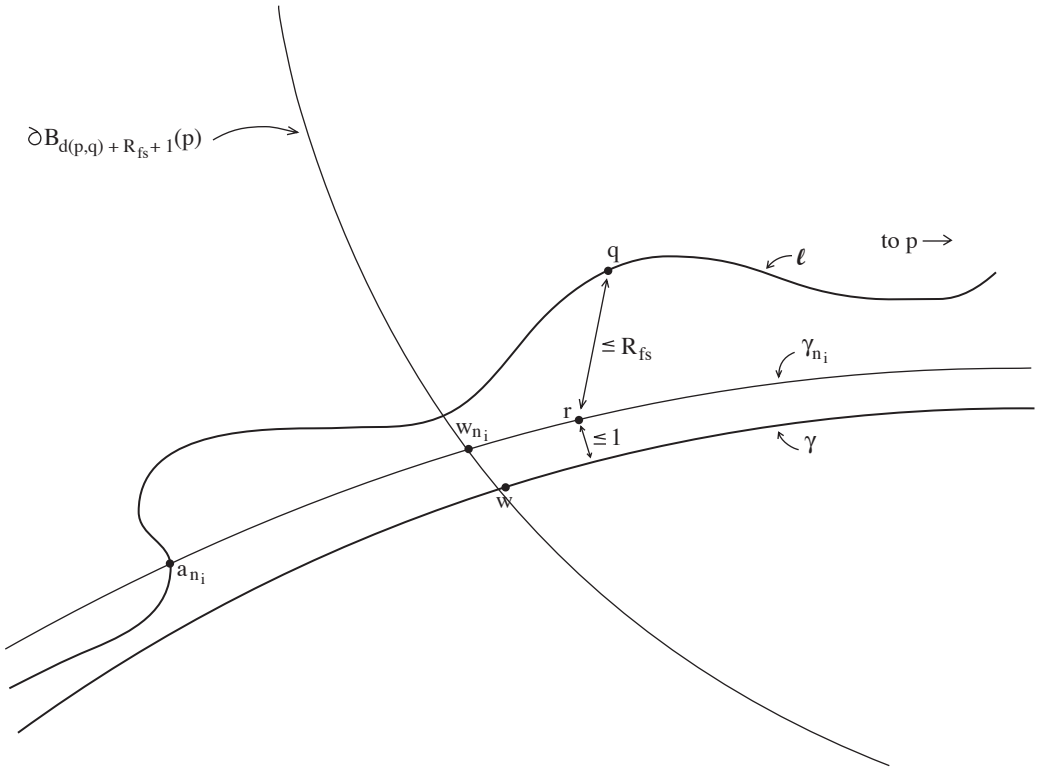

Figure 3.23: The point q lies within $R_\Phi = R_{\text{fs}} + 1$ of γ.

Chapter 4

Flow Line Progress Through Neighborhoods

In Chapter 3 we proved the existence of a number $R_\Phi > 0$ so that every flow line lies within the neighborhood of radius R_Φ of the geodesic connecting its endpoints on the sphere at infinity. Thus we have shown that flow lines satisfy part 1 of the definition of tracking. In this chapter, we prove that flow lines satisfy part 2 of the definition: that inside this neighborhood of the geodesic, flow lines make reasonable progress from one end of the tube to the other. More formally, we show

Theorem 4.0.1 *There exists $Q_\Phi > 0$ such that if ℓ is any flow line such that the length of a subpath of ℓ with endpoints a and b is at least $Q_\Phi > 0$, then the distance between $\pi(a)$ and $\pi(b)$ along γ is at least 1, where π*

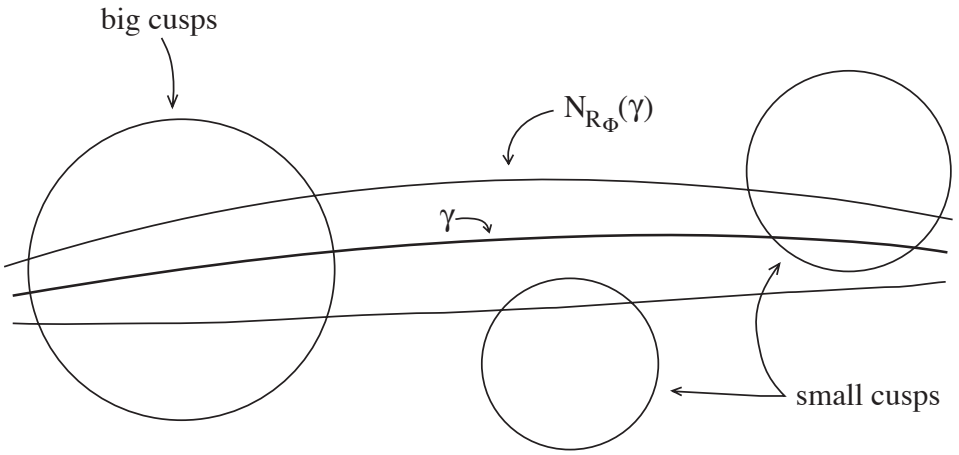

Figure 4.1: Big and small cusps intersecting $N_{R_\Phi}(\gamma)$.

denotes orthogonal projection onto γ.

We will use the following definitions:

Definition 4.0.2 *Let* ℓ *be a flow line and let* γ *be the geodesic connecting its endpoints, so that* $\ell \subset N_{R_\Phi}(\gamma)$. *Consider the set of all cusps meeting* $N_{R_\Phi}(\gamma)$. *These can be split into two types:* ***big cusps****, which disconnect the neighborhood* $N_{R_\Phi}(\gamma)$, *and* ***small cusps****, which do not (see Figure 4.1).*

The big cusps split the neighborhood $N_{R_\Phi}(\gamma)$ up into segments. The dynamics of the flow dictate that a flow line may enter a cusp in $\widetilde{M}$ only once. Therefore, since the flow line has two distinct endpoints, it must enter a big cusp from one side of the neighborhood (one segment), and emerge from the big cusp on the other side (a different segment).

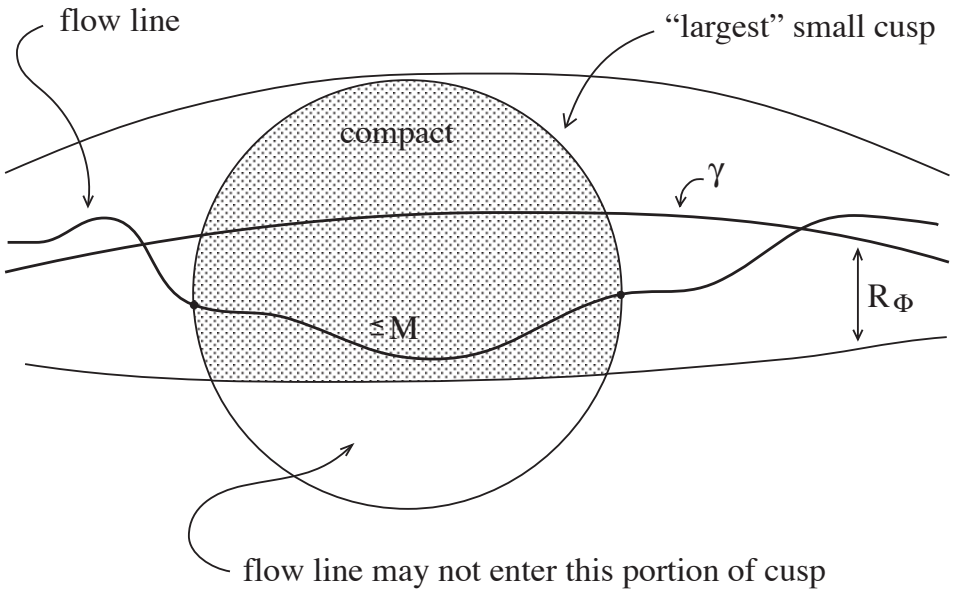

Figure 4.2: The maximum length a flow line can spend inside a small cusp.

Lemma 4.0.3 *There is a constant M so that the distance any flow line travels inside a small cusp is less than M.*

Proof: There is a maximum intersection between a small cusp and the tube of radius R_Φ (beyond which the small cusp becomes a big cusp) (see Figure 4.2). Therefore there is a maximum distance a flow line can travel inside a small cusp, given by the quasigeodesic constant K_c in the cusp times the maximum geodesic distance across a small bead. Let M be this maximum distance a flow line can travel inside a small cusp. □

Proof: [Theorem 4.0.1] Let ℓ be a flow line and let γ be the geodesic connecting its endpoints, so that $\ell \subset N_{R_\Phi}(\gamma)$. We may split this flow line into segments at the boundaries of the big cusps, so that some segments lie entirely inside a big cusp, and the rest of the segments lie between big cusps.

Let β be a segment of ℓ which lies entirely within a big cusp. Then β is a quasigeodesic segment, as we established in Chapter 2 of this thesis. Therefore, β tracks the geodesic segment γ' connecting its endpoints on the boundary of the big cusp; let R', Q' be the tracking constants given in the definition of tracking. Thus if the distance between two points a and b along β is at least Q', then we have

$$d(\pi_{\gamma'}(a), \pi_{\gamma'}(b)) > 1.$$

Now ℓ may enter this big cusp at most once by Lemma 2.1.11, therefore one endpoint of β must lie on one side of the big cusp (towards one endpoint of γ on the sphere at infinity), and the other endpoint of β must lie on the other side of the big cusp (see Figure 4.3).

Each endpoint of the quasigeodesic segment γ' lies within R_Φ of γ, thus the entire segment γ' lies within R_Φ of γ by Convexity of Tubes (Lemma B.3.1). Thus there is a constant $K > 1$ so that

$$K \cdot d(\pi a, \pi b) \geq K \cdot d(\pi(\pi_{\gamma'}(a)), \pi(\pi_{\gamma'}(b))) \geq d(\pi_{\gamma'}(a), \pi_{\gamma'}(b)) > 1;$$

in other words,

$$d(\pi a, \pi b) \geq \frac{1}{K} \cdot d(\pi_{\gamma'}(a), \pi_{\gamma'}(b)) > \frac{1}{K}.$$

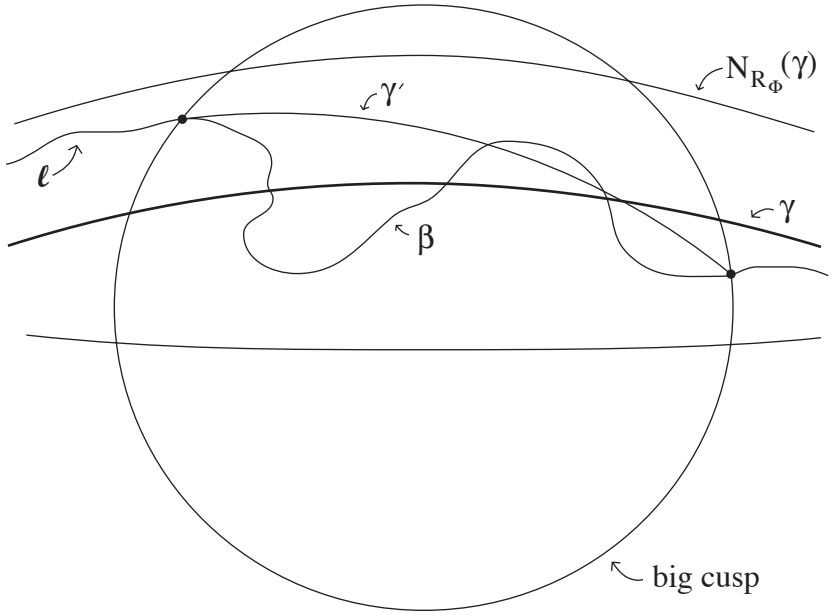

Figure 4.3: The segments of flow line ℓ inside a big cusp track the geodesic γ.

So choosing $Q_{\mathrm{b}} > K \cdot Q'$ guarantees that whenever a and b are boundary endpoints of a flow line inside a big cusp whose distance along that flow line is at least Q_{b}, then we are guaranteed $d(\pi a, \pi b) > 1$.

Therefore, the problem is reduced to showing that flow lines make reasonable progress along the segments between the big cusps. Suppose a and b are two points on a segment λ of flow line ℓ which lie in the same segment of $N_{R_\Phi}(\gamma)$. Let D_a and D_b denote the meridian disks of the tube about γ of radius R_Φ which contains the points a and b respectively (see Figure 4.4). Then the distance between D_a and D_b is $d(\pi a, \pi b)$. Since both a and b lie inside $N_{R_\Phi}(\gamma)$, we know that the

$$d(a, b) \leq 2R_\Phi + d(\pi a, \pi b).$$

Our original neutered space N consists of $\mathbb{H}^3$ with all its horoballs removed, where the size of the horoball corresponding to each cusp was chosen once and for all in the beginning of this thesis. We define a new, larger neutered space, LN, as follows: shrink all the original horoballs so that if a new shrunken horoball meets the tube of radius R_Φ about γ, then it was originally a "big" cusp. In other words, we shrink all the horoballs until no original small cusp still intersects the tubular neighborhood of γ after shrinking. Then λ passes through no shrunken horoballs, and therefore λ is contained inside LN. This means that $\lambda = \overline{\lambda}$, where $\overline{\lambda}$ is the segment λ pushed into the large neutered space LN. Note that since we have shrunk all the original small horoballs out of $N_{R_\Phi}(\gamma)$, LN-neutered space distance

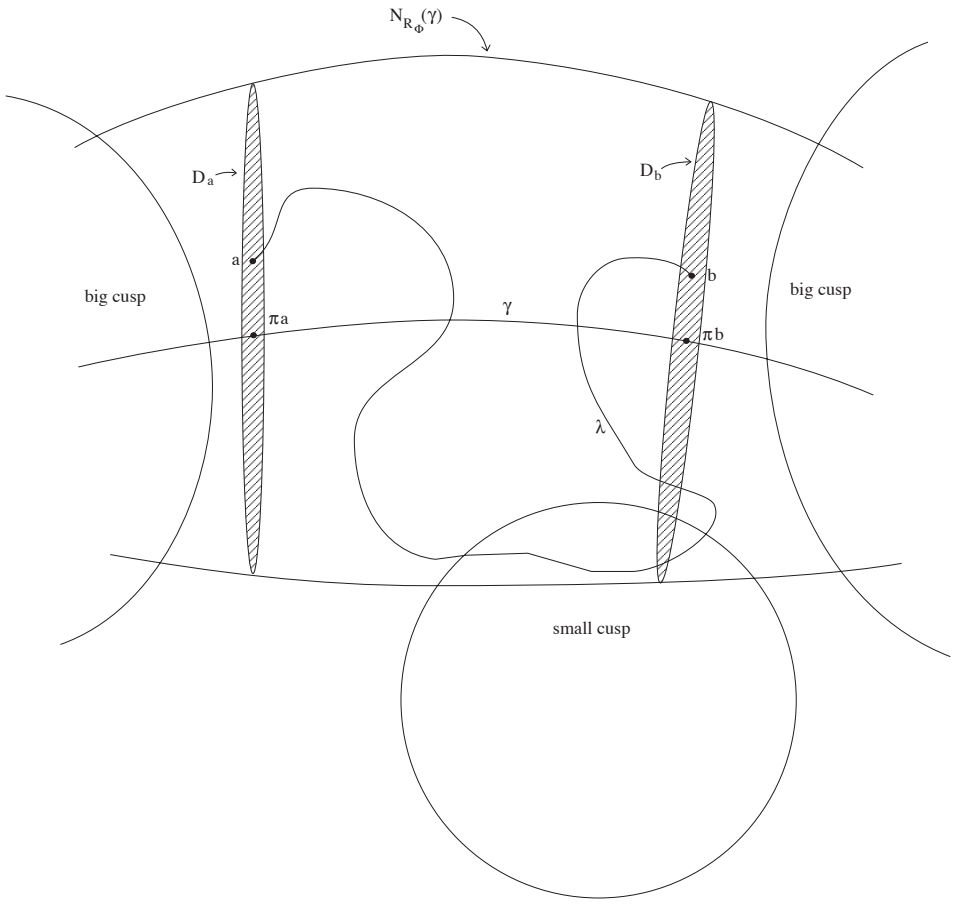

Figure 4.4: Flow line segments in regions of $N_{R_\Phi}(\gamma)$ between big cusps.

inside the convex set $N_{R_\Phi}(\gamma)$ is the same as hyperbolic distance.

Pushed flow lines are quasigeodesic in neutered spaces; let $R_{\mathrm{LN}}, Q_{\mathrm{LN}}$ be the tracking constants for pushed flow lines in LN. Thus if $|\lambda| = |\overline{\lambda}| > Q_{\mathrm{LN}}$, then $d(a,b) > 1$. In fact, applying this quasigeodesic constant Q_{LN} over and over down the length of λ, if $|\lambda| > (2R_\Phi + 1) \cdot Q_{\mathrm{LN}}$, then $d(a,b) > (2R_\Phi + 1)$. Therefore

$$2R_\Phi + 1 < d(a,b) \leq d(\pi a, \pi b) + 2R_\Phi,$$

so $d(\pi a, \pi b) > 1$, as desired.

Taking $Q_\Phi = \max\{Q_{\mathrm{b}}, (2R_\Phi + 1) \cdot Q_{\mathrm{LN}}\}$ gives the result. □

Appendix A

Technical Calculations

A.1 Values of t where $Z(t) = Z_{\mathbf{m}}$

We need to find t values such that $Z(t) = Z_{\mathrm{m}}$; i.e., the t value at the start of the crown:

$$
\begin{aligned}
Z(t) = Z_{\mathrm{m}} \quad &\Leftrightarrow \quad -\ln(r\sqrt{\sin\theta\cos\theta(\lambda^{-2t}+\lambda^{2t})}) = \frac{1}{2}(1-\ln(r\sqrt{\sin 2\theta})) \\
&\Leftrightarrow \quad 2\ln(r\sqrt{\sin\theta\cos\theta(\lambda^{-2t}+\lambda^{2t})}) = \ln(r\sqrt{\sin 2\theta}) - 1 \\
&\Leftrightarrow \quad \frac{1}{2}r^2\sin 2\theta(\lambda^{-2t}+\lambda^{2t}) = \frac{r\sqrt{\sin 2\theta}}{e} \\
&\Leftrightarrow \quad er^2\sin 2\theta(\lambda^{-2t}+\lambda^{2t}) = 2r\sqrt{\sin 2\theta} \\
&\Leftrightarrow \quad (er^2\sin 2\theta)\lambda^{4t} - (2r\sqrt{\sin 2\theta})\lambda^{2t} + (er^2\sin 2\theta) = 0 \\
&\Leftrightarrow \quad \lambda^{2t} = \frac{2r\sqrt{\sin 2\theta} \pm \sqrt{4r^2\sin 2\theta - 4e^2r^4\sin^2 2\theta}}{2er^2\sin 2\theta}.
\end{aligned}
$$

Simplifying this expression gives

$$\begin{aligned}
\lambda^{2t} &= \frac{2r\sqrt{\sin 2\theta} \pm \sqrt{4r^2 \sin 2\theta - 4e^2 r^4 \sin^2 2\theta}}{2er^2 \sin 2\theta} \\
&= \frac{2r\sqrt{\sin 2\theta} \pm \sqrt{(4r^2 \sin 2\theta)(1 - e^2 r^2 2 \sin 2\theta)}}{2er^2 \sin 2\theta} \\
&= \frac{(2r\sqrt{\sin 2\theta})(1 \pm \sqrt{1 - e^2 r^2 \sin 2\theta})}{2er^2 \sin 2\theta} \\
&= \frac{1 \pm \sqrt{1 - e^2 r 2 \sin 2\theta}}{er\sqrt{\sin 2\theta}}
\end{aligned}$$

Note that these two solutions are reciprocals of each other:

$$(\frac{1 + \sqrt{1 - e^2 r^2 \sin 2\theta}}{er\sqrt{\sin 2\theta}})(\frac{1 - \sqrt{1 - e^2 r^2 \sin 2\theta}}{er\sqrt{\sin 2\theta}}) = \frac{1 - 1 + e^2 r^2 \sin 2\theta}{e^2 r^2 \sin 2\theta} = 1.$$

We will denote

$$a = \frac{1 + \sqrt{1 - e^2 r^2 \sin 2\theta}}{er\sqrt{\sin 2\theta}},$$

then

$$\lambda^{2t} = a^{\pm 1}.$$

Therefore the t values at the ends of the crown of a leaf occur when $t = \pm\frac{1}{2}\log_\lambda(a)$.

A.2 Calculation for Lemma 2.3.4

We desire an upper bound for the quantities $\frac{\Delta X}{Z_{\mathrm{m}}}$, $\frac{\Delta Y}{Z_{\mathrm{m}}}$, and $\frac{\Delta Z}{Z_{\mathrm{m}}}$, where $\Delta X = X(t_{\mathrm{m}}) - X(0)$, and so on. We will restrict our attention to the case $0 \leq$

$\theta \leq \frac{\pi}{2}$; the argument generalizes to all θ by symmetry. Now,

$$\begin{aligned}
\frac{\Delta X}{Z_{\mathrm{m}}} &= \frac{|X(t_{\mathrm{m}}) - X(0)|}{Z_{\mathrm{m}}} \\
&= \frac{2t_{\mathrm{m}}}{(1 - \ln(r\sqrt{\sin 2\theta}))} \\
&= \frac{\log_\lambda c}{(1 - \ln(r\sqrt{\sin 2\theta}))} \\
&= (\frac{1}{\ln \lambda})\frac{\ln(1 + \sqrt{1 - e^2 r^2 \sin 2\theta}) - \ln(er\sqrt{\sin 2\theta})}{(1 - \ln(r\sqrt{\sin 2\theta}))} \\
&= (\frac{1}{\ln \lambda})(\frac{\ln(1 + \sqrt{1 - e^2 r^2 \sin 2\theta})}{(1 - \ln(r\sqrt{\sin 2\theta}))} + \frac{\ln(r\sqrt{\sin 2\theta}) + 1}{\ln(r\sqrt{\sin 2\theta}) - 1})
\end{aligned}$$

Since $0 < r\sqrt{\sin 2\theta} < \frac{1}{e}$,

$\ln(r\sqrt{\sin 2\theta}) < -1 \;\Rightarrow\; 2 < 1 - \ln(r\sqrt{\sin 2\theta})$, and

$e^2 r^2 \sin 2\theta > 0 \;\Rightarrow\; 1 - e^2 r^2 \sin 2\theta < 1 \Rightarrow \ln(1 + \sqrt{1 - e^2 r^2 \sin 2\theta}) < \ln 2.$

Therefore,

$$\begin{aligned}
\frac{\Delta X}{Z_{\mathrm{m}}} &= (\frac{1}{\ln \lambda})(\frac{\ln(1 + \sqrt{1 - e^2 r^2 \sin 2\theta})}{(1 - \ln(r\sqrt{\sin 2\theta}))} + \frac{\ln(r\sqrt{\sin 2\theta}) + 1}{\ln(r\sqrt{\sin 2\theta}) - 1}) \\
&< \frac{1}{\ln \lambda}[\frac{\ln 2}{2} + \frac{-\ln(r\sqrt{\sin 2\theta}) - 1}{-\ln(r\sqrt{\sin 2\theta}) + 1}].
\end{aligned}$$

Also, $0 < r\sqrt{\sin 2\theta} < \frac{1}{e} \Rightarrow 1 < -\ln(r\sqrt{\sin 2\theta})$, thus $-\ln(r\sqrt{\sin 2\theta}) - 1$ is a smaller positive number than $-\ln(r\sqrt{\sin 2\theta}) + 1$, so it follows that

$$\frac{-\ln(r\sqrt{\sin 2\theta}) - 1}{-\ln(r\sqrt{\sin 2\theta}) + 1} < 1.$$

So finally,

$$\begin{aligned}
\frac{\Delta X}{Z_{\mathrm{m}}} &< \frac{2}{\ln\lambda}[\frac{\ln 2}{2} + \frac{-\ln(r\sqrt{\sin 2\theta}) - 1}{-\ln(r\sqrt{\sin 2\theta}) + 1}] \\
&< \frac{2}{\ln\lambda}[\frac{\ln 2}{2} + 1] \\
&= \frac{2 + \ln 2}{\ln\lambda}.
\end{aligned}$$

Similarly,

$$\begin{aligned}
\frac{\Delta Z}{Z_{\mathrm{m}}} &= \frac{|Z(t_{\mathrm{m}}) - Z(0)|}{Z_{\mathrm{m}}} \\
&= \frac{Z_{\mathrm{p}} - Z_{\mathrm{m}}}{Z_{\mathrm{m}}} \\
&= \frac{-\ln(r\sqrt{\sin 2\theta}) - \frac{1}{2}(1 - \ln(r\sqrt{\sin 2\theta}))}{\frac{1}{2}(1 - \ln(r\sqrt{\sin 2\theta}))} \\
&= \frac{-\ln(r\sqrt{\sin 2\theta}) - 1}{-\ln(r\sqrt{\sin 2\theta}) + 1} \\
&\leq 1.
\end{aligned}$$

To bound $\frac{\Delta Y}{Z_{\mathrm{m}}}$, recall that over the life of any particular leaf, the y value changes less than $\pi/2$. Therefore, over the life of its crown,

$$\frac{\Delta Y}{Z_{\mathrm{m}}} \leq \frac{\pi/2}{\frac{1}{2}(1 - \ln(r\sqrt{\sin 2\theta}))} = \frac{\pi}{(1 - \ln(r\sqrt{\sin 2\theta}))} \leq \frac{\pi}{2}.$$

A.3 Proof of Proposition 2.3.9

Proof: [Proposition 2.3.9] Recall that we want to find a number $K_{\mathrm{r}} > 1$ such that if ℓ is a long returning flow line (in other words, if ℓ is a returning flow line segment whose length inside the cusp is greater than B) and γ is the geodesic connecting the points $a = F(-t_{\mathrm{h}})$ and $b = F(t_{\mathrm{h}})$ where ℓ enters the cusp, then

$$d_\ell(a, b) \leq K_{\mathrm{r}} \cdot d_\gamma(a, b).$$

The proof will follow the outline given in the main body of this thesis, on page 83.

1. First we must show that $d_\ell(a, b) \leq P \cdot \ln(Z_{\mathrm{p}})$ for some constant P. Note that

$$\begin{aligned} d_\ell(a, b) &= 2 \cdot (\text{length of one leg}) + (\text{length of crown}) && \text{by symmetry of the leaf } \ell \\ &\leq 2 \cdot (\text{length of one leg}) + A && \text{since } \ell \text{ is a long returning flow line,} \end{aligned}$$

where A is the maximum hyperbolic length of a crown of a long re-

turning flow line (Lemma 2.3.4). Therefore

$$\begin{aligned}
d_\ell(a,b) &\leq 2\int_1^{t_{\rm h}} \frac{\sqrt{[\frac{dX}{dt}]^2+[\frac{dY}{dt}]^2+[\frac{dZ}{dt}]^2}}{Z(t)}\,dt + A \\
&= -2\int_{Z(1)}^{Z(t_{\rm h})} \frac{\sqrt{[\frac{dX}{dZ}]^2+[\frac{dY}{dZ}]^2+[\frac{dZ}{dZ}]^2}}{Z}\,dZ + A, \text{ since } \tfrac{dt}{dZ} \text{ is negative on } [1,t_h] \\
&\leq -2\int_{Z(1)}^{Z(t_{\rm h})} [|\frac{dX}{dZ}|+|\frac{dY}{dZ}|+|\frac{dZ}{dZ}|]\cdot\frac{1}{Z}\,dZ + A, \text{ by the triangle inequality} \\
&\leq -2[\frac{1}{C_x}\int_{Z(1)}^{Z(t_{\rm h})}\frac{1}{Z}\,dZ + \frac{1}{C_y}\int_{Z(1)}^{Z(t_{\rm h})}\frac{1}{Z}\,dZ + \int_{Z(1)}^{Z(t_{\rm h})}\frac{1}{Z}\,dZ] + A \\
&= 2[\frac{1}{C_x}+\frac{1}{C_y}+1]\int_{Z(t_{\rm h})}^{Z(1)}\frac{1}{Z}\,dZ + A \\
&\leq D_1\int_{Z(t_{\rm h})}^{Z(0)}\frac{1}{Z}\,dZ + A \\
&= D_1\int_1^{Z_{\rm p}}\frac{1}{Z}\,dZ + A \\
&= D_1(\ln(Z_{\rm p})-\ln(1)) + A \\
&= D_1\ln(Z_{\rm p}) + A
\end{aligned}$$

where $D_1 = 2[\frac{1}{C_x}+\frac{1}{C_y}+1] > 0$. Since we are only considering long returning leaf segments, this constant A must be shorter than some multiple of $\ln(Z_{\rm p})$, the vertical hyperbolic distance from the plane $Z = 1$ to the peak of the flow line. The fact that ℓ is a long leaf

guarantees:

$$\begin{aligned}
\ln(Z_{\mathrm{p}}) &= (\ln(-\ln(r\sqrt{\sin 2\theta}))), \text{ by definition of } Z_{\mathrm{p}} \\
&\geq \ln(-\ln(\frac{2}{e(\lambda^{-2}+\lambda^{2})})) \\
&= \ln(\ln(\frac{e(\lambda^{-2}+\lambda^{2})}{2})) \\
&= D_2,
\end{aligned}$$

where $D_2 > 0$. Thus A is smaller than $\frac{A}{D_2} \cdot \ln(Z_{\mathrm{p}})$, so

$$\begin{aligned}
d_\ell(a,b) &\leq D_1(\ln(Z_{\mathrm{p}})) + A \\
&\leq D_1(\ln(Z_{\mathrm{p}})) + \frac{A}{D_2}(\ln(Z_{\mathrm{p}})) \\
&= (D_1 + \frac{A}{D_2})(\ln(Z_{\mathrm{p}})).
\end{aligned}$$

Hence we have $d_\ell(a,b)$ bounded above by a multiple of $\ln(Z_{\mathrm{p}})$ (by definition of Z_{p}):

$$d_\ell(a,b) \leq P \cdot \ln(Z_{\mathrm{p}}), \tag{A.1}$$

where $P = D_1 + \frac{A}{D_2}$.

2. In this part we will show that $Z_{\mathrm{p}} \leq Q \cdot t_{\mathrm{h}}$, for some constant Q. Now

by the definition of t_{h},

$$\begin{aligned}(\ln\lambda)\cdot t_{\mathrm{h}} &= \frac{1}{2}\ln\left(\frac{1+\sqrt{1-e^4r^4\sin^2 2\theta}}{e^2r^2\sin 2\theta}\right)\\ &\geq \frac{1}{2}\ln\left(\frac{1}{e^2r^2\sin 2\theta}\right)\\ &= -\ln(er\sqrt{\sin 2\theta})\\ &= -1-\ln(r\sqrt{\sin 2\theta})\\ &= -1+Z_{\mathrm{p}}.\end{aligned}$$

Adding 1 to both sides gives

$$Z_{\mathrm{p}} \leq 1+(\ln\lambda)\cdot t_{\mathrm{h}}.$$

We will find a constant D_3 so that $1 < \frac{1}{D_3}\cdot t_{\mathrm{h}}$ for all long returning flow line segments, and thus we will have bounded Z_{p} above by a multiple of t_{h}. Since we are only considering long returning flow line segments, we know $er\sqrt{\sin 2\theta} \leq \frac{2}{\lambda^{-2}+\lambda^2}$. Thus

$$\begin{aligned}t_{\mathrm{h}} &= \frac{1}{2\ln\lambda}\cdot\ln\left(\frac{1+\sqrt{1-e^4r^4\sin^2 2\theta}}{e^2r^2\sin 2\theta}\right)\\ &\geq \frac{1}{2\ln\lambda}\cdot\ln\left(\frac{1}{e^2r^2\sin 2\theta}\right)\\ &= \frac{1}{\ln\lambda}\cdot\ln\left(\frac{1}{er\sqrt{\sin 2\theta}}\right)\\ &\geq \frac{1}{\ln\lambda}\cdot\ln\left(\frac{\lambda^{-2}+\lambda^2}{2}\right),\end{aligned}$$

so

$$t_{\mathrm{h}} > \frac{1}{\ln\lambda}\cdot\ln\left(\frac{\lambda^{-2}+\lambda^2}{2}\right) = D_3 \tag{A.2}$$

where D_3 is a constant. Therefore

$$\begin{aligned} Z_{\mathrm{p}} &\leq 1 + (\ln \lambda) \cdot t_{\mathrm{h}} \\ &\leq \frac{1}{D_3} \cdot t_{\mathrm{h}} + (\ln \lambda) \cdot t_{\mathrm{h}}. \end{aligned}$$

Hence we obtain the desired result:

$$Z_{\mathrm{p}} \leq Q \cdot t_{\mathrm{h}}, \tag{A.3}$$

where $Q = \frac{1}{D_3} + \ln \lambda$.

3. Since $Z_{\mathrm{p}} \leq Q \cdot t_{\mathrm{h}}$ by equation (A.3) above, taking the natural log of both sides gives

$$\ln(Z_{\mathrm{p}}) \leq \ln(Q) + \ln(t_{\mathrm{h}}).$$

By equation (A.2), $D_3 < t_{\mathrm{h}}$ where D_3 is a constant independent of choice of flow line; therefore $\ln(D_3) \leq \ln(t_{\mathrm{h}})$. Letting $R = \ln(D_3)$ gives

$$R \leq \ln(t_{\mathrm{h}}), \tag{A.4}$$

and so $1 \leq \frac{1}{R} \ln(t_{\mathrm{h}})$. Hence

$$\begin{aligned} \ln(Z_{\mathrm{p}}) &\leq \ln(Q) + \ln(t_{\mathrm{h}}) \\ &\leq \ln(Q) \cdot \frac{1}{R} \ln(t_{\mathrm{h}}) + \ln(t_{\mathrm{h}}) \\ &= (\frac{\ln(Q)}{R} + 1) \cdot \ln(t_{\mathrm{h}}). \end{aligned}$$

Therefore

$$\ln(Z_{\mathrm{p}}) \leq (\frac{\ln(Q)}{R} + 1) \cdot \ln(t_{\mathrm{h}}) \tag{A.5}$$

4. If γ is the geodesic segment connecting $a = F(-t_{\rm h})$ to $b = F(t_{\rm h})$, then

$$\begin{aligned} d_\gamma(a,b) &= d_\gamma((X(-t_{\rm h}),Y(-t_{\rm h}),Z(-t_{\rm h})),(X(t_{\rm h}),Y(t_{\rm h}),Z(t_{\rm h}))) \\ &\geq d_\gamma((X(-t_{\rm h}),0,0),(X(t_{\rm h}),0,0)) \\ &\geq d_\gamma((-t_{\rm h}-t_c,0,0),(t_{\rm h}-t_c,0,0)). \end{aligned}$$

By the Distance Calculation in the Cusp found in the appendix (Section B.6), this last term has length

$$\begin{aligned} d_\gamma((-t_{\rm h}-t_c,0,0),(t_{\rm h}-t_c,0,0)) &= 2\ln(\sqrt{1+(\frac{2t_{\rm h}}{2})^2}+\frac{2t_{\rm h}}{2}) \\ &= 2\ln(\sqrt{1+t_{\rm h}^2}+t_{\rm h}) \\ &\geq 2\ln(t_{\rm h}). \end{aligned}$$

Therefore,

$$d_\gamma(a,b) \geq 2\ln(t_{\rm h}). \tag{A.6}$$

Putting steps 1, 3, and 4 together gives

$$\begin{aligned} d_\ell(a,b) &\leq P\cdot\ln(Z_{\rm p}) \\ &\leq P\cdot[(\frac{\ln(Q)}{R}+1)\cdot\ln(t_{\rm h})] \\ &\leq \frac{P}{2}\cdot(\frac{\ln(Q)}{R}+1)\cdot(2\ln(t_{\rm h})) \\ &\leq \frac{P}{2}\cdot(\frac{\ln(Q)}{R}+1)\cdot d_\gamma(a,b). \end{aligned}$$

Let $K_{\rm r} = \frac{P}{2}\cdot(\frac{\ln(Q)}{R}+1)$. Then

$$\frac{1}{K_{\rm r}}\cdot d_\gamma(a,b) \leq d_\ell(a,b) \leq K_{\rm r}\cdot d_\gamma(a,b),$$

as desired. Thus returning flow lines are K_{r}-quasigeodesics, where the constant K_{r} is uniform for all choices of returning flow line. $\square$

Appendix B

Useful Properties of Hyperbolic Space

B.1 Geodesic Projection Lemma

Lemma B.1.1 (Geodesic Projection Lemma) *Let γ be a geodesic in $\mathbb{H}^3$, and let c be a segment of path which lies outside a neighborhood of radius r of γ, with endpoints a and b on the boundary of the neighborhood. Then projecting c orthogonally onto γ decreases distance by a multiplicative factor of at least $\frac{e^r}{2}$; that is,*

$$d_c(a,b) \geq \frac{e^r}{2} \cdot d_\gamma(\pi_\gamma(a), \pi_\gamma(b)).$$

Proof: [Geodesic Projection Lemma] Choose coordinates so that γ is the vertical geodesic given by $x = y = 0$ in the upper half space model of $\mathbb{H}^3$. Then c is a path in the upper half space with endpoints a and b lying on the Euclidean cone which bounds the neighborhood of radius r of γ.

We will replace c be an even shorter path c'' in two steps, then establish that the length of this shorter path reduces by a factor of $\frac{1}{2}(e^{-r} + e^{r})$ upon projection onto γ, which will complete the proof.

Produce c' from c as follows. Rotate all the points of c in their horizontal plane around the vertical line γ until the image c' lies entirely in the first quadrant of the xz-plane; let a' and b' be the rotated endpoints. Thus $\pi_\gamma(a) = \pi_\gamma(a')$ and $\pi_\gamma(b) = \pi_\gamma(b')$. This action can only decrease length, as the 'θ' contribution to the length of c is neglected after rotation.

Let c'' be the line segment in the first quadrant of the xz-plane which follows along the boundary of $N_r(\gamma)$ from a' to b'. Then c'' is even shorter than c', for projecting along circles perpendicular to γ clearly reduces distance.

Let θ be the angle that the Euclidean line containing c'' makes with the positive x-axis. The line segment c'' can be parametrized in the upper half space model of $\mathbb{H}^3$ using $y = (\tan\theta) \cdot x$ for x between $\cos\theta$ and $e^{d_\gamma(\pi_\gamma a', \pi_\gamma b')}$.

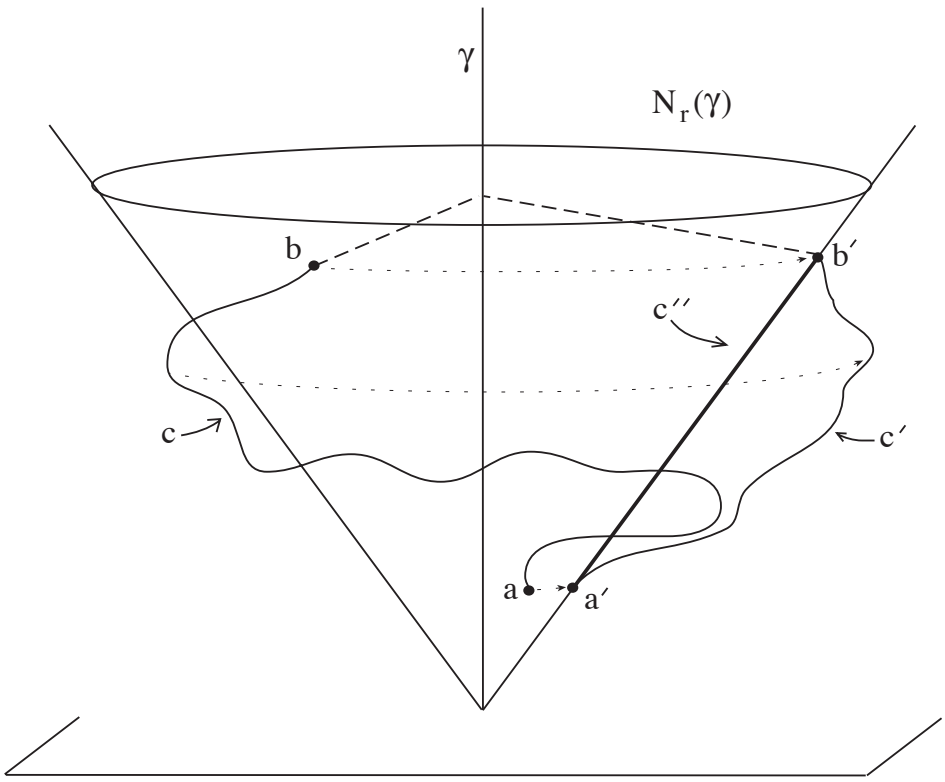

Figure B.1: Projecting a path c onto γ decreases distance.

$\cos\theta$. So the length of c'' from a' to b' is given by

$$\begin{aligned} d_{c''}(a',b') &= \int_{\cos\theta}^{e^{d_\gamma(\pi_\gamma a',\pi_\gamma b')}\cos\theta} \frac{\sqrt{1+\tan^2\theta}}{\tan\theta\cdot x}\,dx \\ &= (\sqrt{\cot^2\theta+1})\cdot\ln|\frac{e^{d_\gamma(\pi_\gamma a',\pi_\gamma b')}\cos\theta}{\cos\theta}| \\ &= \csc\theta\cdot d_\gamma(\pi_\gamma a',\pi_\gamma b') \\ &= \frac{1}{2}(e^{-r}+e^r)\cdot d_\gamma(\pi_\gamma a',\pi_\gamma b') \end{aligned}$$

by the Tube Slope Lemma (Lemma B.5.1). Thus

$$\begin{aligned} d_c(a,b) &\geq d_{c''}(a',b') \\ &= \frac{1}{2}(e^{-r}+e^r)\cdot d_\gamma(\pi_\gamma a',\pi_\gamma b') \\ &\geq \frac{e^r}{2}\cdot d_\gamma(\pi_\gamma a,\pi_\gamma b), \end{aligned}$$

as desired. □

B.2 Horosphere Projection Lemma

Lemma B.2.1 (Horosphere Projection Lemma) *Let c be a segment of path outside a neighborhood of radius r of a horosphere S in $\widetilde{M}$, the*

universal cover of M, between points a and b on the boundary of this neighborhood. Then projecting c onto S decreases distance by a factor of e^r; that is

$$d_c(a,b) \geq e^r \cdot d_{\pi_S(c)}(\pi_S(a), \pi_S(b)).$$

Proof: [Horosphere Projection Lemma] Choose coordinates so that the horosphere in question is the plane $z = 1$ in the upper half space model of hyperbolic space. Let c be a segment of path outside a neighborhood of radius r of a horosphere S between points a and b on the boundary of this neighborhood. Parametrize this subpath of c by $c(t) = (c_1(t), c_2(t), c_3(t))$, $0 \leq t \leq 1$, where $c(0) = a$ and $c(1) = b$. Since this subpath lies a distance at least r from the horosphere S, for every $t \in [0,1]$,

$$r \leq d_{\mathbb{H}^3}(c(t), S) = \int_{c_3(t)}^{1} \frac{1}{z}\, dz = \ln(\frac{1}{c_3(t)}).$$

Thus the length of c is given by

$$\begin{aligned} d_c(a,b) &= \int_0^1 \frac{\sqrt{[c_1'(t)]^2 + [c_2'(t)]^2 + [c_3'(t)]^2}}{c_3(t)}\, dt \\ &\geq \int_0^1 e^r \sqrt{[c_1'(t)]^2 + [c_2'(t)]^2 + [c_3'(t)]^2}\, dt \\ &= e^r \int_0^1 \sqrt{[c_1'(t)]^2 + [c_2'(t)]^2 + [c_3'(t)]^2}\, dt \\ &\geq e^r \int_0^1 \sqrt{[\pi_S(c_1'(t))]^2 + [\pi_S(c_2'(t))]^2 + [\pi_S(c_3'(t))]^2}\, dt, \end{aligned}$$

since after projection by π_S, there is no change in z coordinate. Therefore

$$\begin{aligned} d_c(a,b) &\geq e^r \int_0^1 \sqrt{[\pi_S(c_1'(t))]^2 + [\pi_S(c_2'(t))]^2 + [\pi_S(c_3'(t))]^2}\, dt \\ &= e^r \cdot d_{\pi_S}(\pi_S(a), \pi_S(b)), \end{aligned}$$

because the metric on any horosphere is Euclidean. □

B.3 Convexity of Tubes

Lemma B.3.1 (Convexity of Tubes) *Let γ be a geodesic and $R > 0$. If α is a geodesic connecting points a and b on the boundary of the neighborhood of radius R about γ, then the segment of α between a and b lies entirely within this neighborhood.*

Proof: Think of γ as a vertical geodesic in the upper half space model of $\mathbb{H}^3$. Then the neighborhood of radius R about γ is a cone about γ (see Figure B.2). If α is the geodesic connecting points a and b on the boundary of this neighborhood, then α is represented as a semicircle perpendicular to the x-axis. From the figure, it is visibly clear that the segment of α between a and b is contained within this cone.

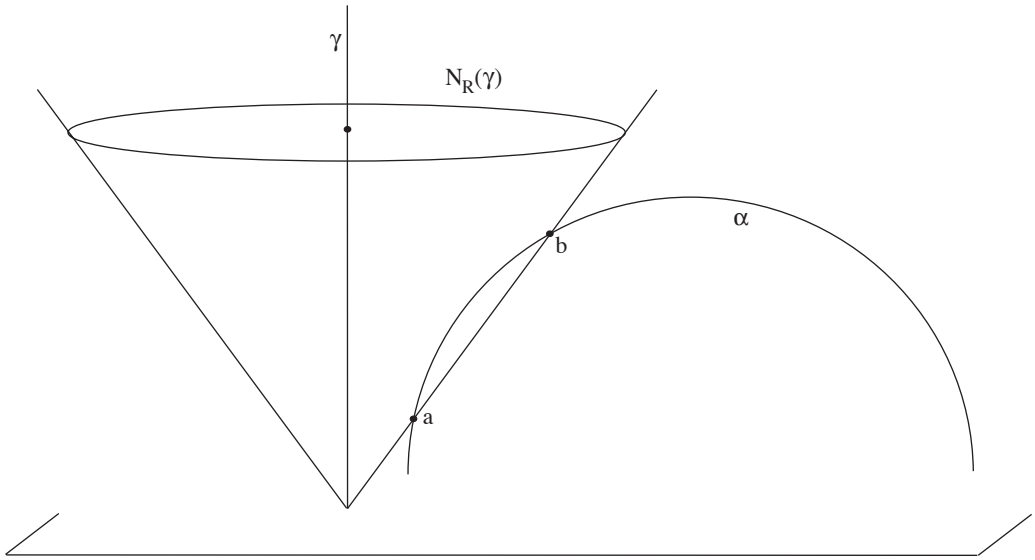

Figure B.2: An R-neighborhood of a geodesic is convex.

□

B.4 Taxicab Lemma

Lemma B.4.1 (Taxicab Lemma) *Let $c(t) = (x(t), y(t), z(t))$, $t \in [a, b]$, be a segment of path in the upper half space model of hyperbolic space which is monotonic in all three variables. Then the length of $c(t)$ is bounded above by $\frac{|\Delta x|+|\Delta y|+|\Delta z|}{z_{min}}$, where $\Delta x, \Delta y$, and Δz are taken between $t = b$ and $t = a$, and z_{min} is the minimum value that z obtains on the interval $[a, b]$.*

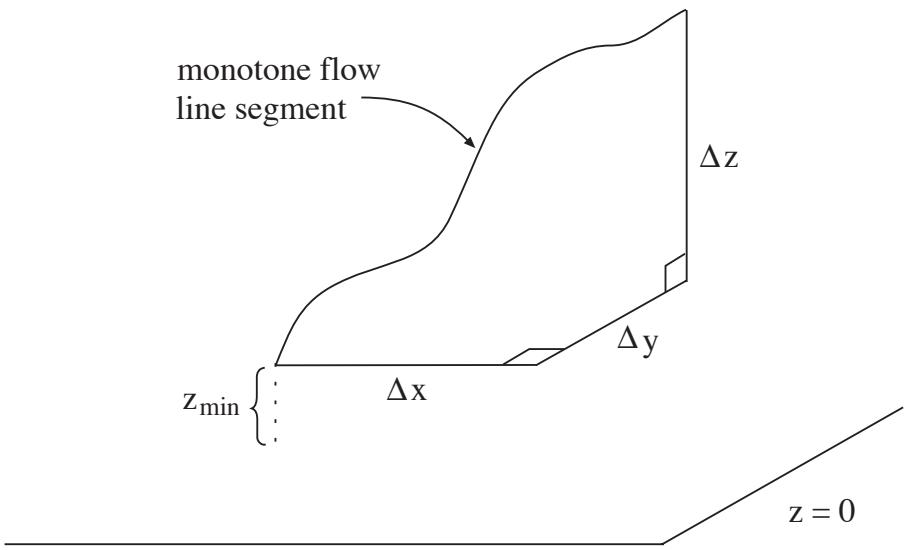

Figure B.3: The length of a leaf is bounded above by $|\Delta x| + |\Delta y| + |\Delta z|$

Proof: The length of $c(t)$ can be found by the integral

$$\begin{aligned} |c(t)| &= \int_a^b \frac{\sqrt{[x'(t)]^2 + [y'(t)]^2 + [z'(t)]^2}}{z(t)}\, dt \\ &\leq \int_a^b \frac{\sqrt{[x'(t)]^2 + [y'(t)]^2 + [z'(t)]^2}}{z_{\min}}\, dt \\ &\leq \frac{1}{z_{\min}} \int_a^b |x'(t)| + |y'(t)| + |z'(t)|\, dt \\ &= \frac{1}{z_{\min}} \cdot (|\Delta x| + |\Delta y| + |\Delta z|). \end{aligned}$$

□

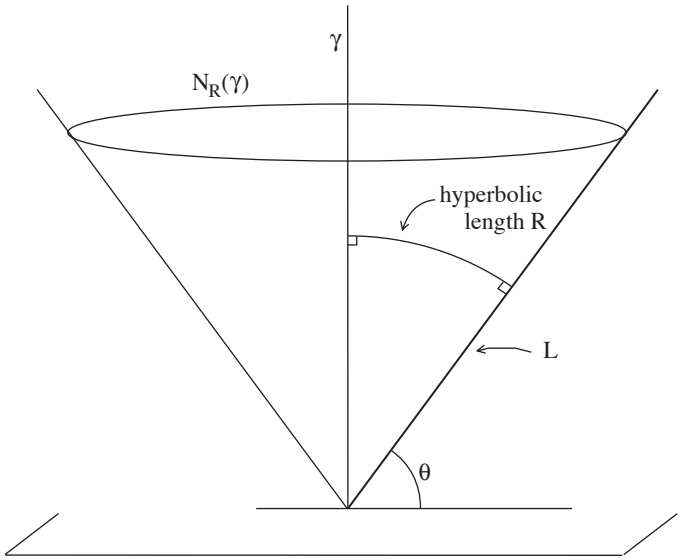

Figure B.4: Set-up for Tube Slope Lemma

B.5 Tube Slope Lemma

General Set-Up Let γ be the vertical geodesic in the upper half space model of $\mathbb{H}^3$ which passes through the origin, and choose $R > 0$. A regular neighborhood $N_R(\gamma)$ of γ then appears as a Euclidean cone about γ with vertex at the origin. Denote the Euclidean straight line given by the intersection of the first quadrant of the xz-plane with the cone by L, and let θ be the angle the cone makes with the positive x-axis.

Lemma B.5.1 (Tube Slope Lemma) *Let γ be such a vertical geodesic and let L and θ be as above. Then R and θ are related by the following equivalent expressions:*

1. $e^R = \dfrac{\sin\theta}{1-\cos\theta}$

2. $\csc\theta = \dfrac{1}{2}(e^R + e^{-R})$

Proof: [Tube Slope Lemma] The radius R of the regular neighborhood is the geodesic distance between γ and L. By parametrizing a geodesic perpendicular to both γ and L, we see

1.

$$\begin{aligned} R &= \int_\theta^{\frac{\pi}{2}} \frac{\sqrt{r^2\cos^2 t + r^2\sin^2 t}}{r\sin t}\,dt \\ &= \int_\theta^{\frac{\pi}{2}} \csc t\,dt \\ &= \ln|\csc t - \cot t|\,|_\theta^{\frac{\pi}{2}} \\ &= \ln(\frac{\sin\theta}{1-\cos\theta}); \end{aligned}$$

in other words, $e^R = \dfrac{\sin\theta}{1-\cos\theta}$.

2. Simple algebra will produce the formula $\csc\theta = \frac{1}{2}(e^R + e^{-R})$ from this point:

$$\begin{aligned} e^R = \frac{\sin\theta}{1-\cos\theta} &\Rightarrow \sin\theta e^R = 1 - \cos\theta \\ &\Rightarrow \cos^2\theta = (1 - e^{-R}\sin\theta)^2 \\ &\Rightarrow 1 - \sin^2\theta = 1 - 2e^{-R}\sin\theta + e^{-2R}\sin^2\theta \\ &\Rightarrow \sin\theta((e^{-2R}+1)\sin\theta - 2e^{-R}) = 0 \\ &\Rightarrow \sin\theta = \frac{2e^{-R}}{e^{-2R}+1} \\ &\Rightarrow \csc\theta = \frac{e^{-2R}+1}{2e^{-R}}, \end{aligned}$$

thus $\csc\theta = \frac{1}{2}(e^{-R} + e^R)$ as desired.

□

B.6 Distance Calculation in a Cusp

Lemma B.6.1 (Distance Calculation in a Cusp) *Let γ be a geodesic in $\widetilde{M}$ which passes through a cusp at points a and b, and let d be the distance along the horosphere between a and b. Then $d_{\mathbb{H}^3}(a,b) = 2\ln\{\sqrt{1+(\frac{d}{2})^2} + \frac{d}{2}\}$. Thus, any path segment entering a cusp at a point a and exiting at b must have length at least $2\ln\{\sqrt{1+(\frac{d}{2})^2} + \frac{d}{2}\}$.*

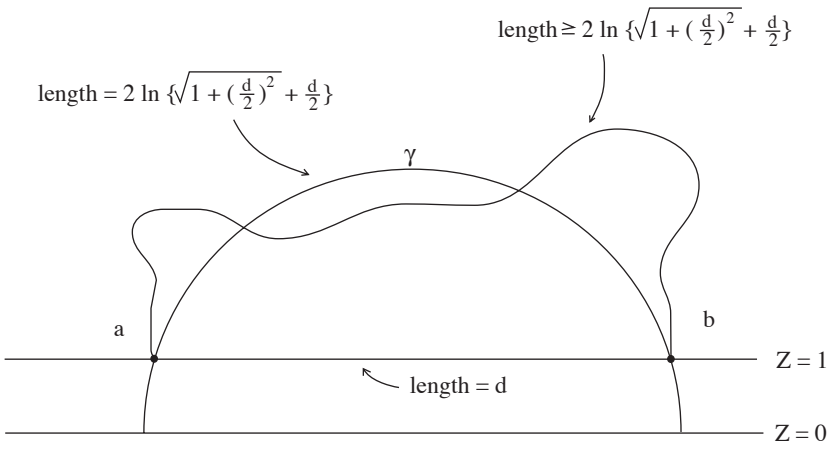

Figure B.5: Distance calculation in a cusp

Proof: [Distance Calculation in a Cusp] Choose new coordinates so that γ sits in the xz-plane in the upper half space model of $\mathbb{H}^3$ as a semicircle centered at $(0,0)$, with the cusp in question as the horoball $z \geq 1$. Then, since the distance along the horosphere between points a and b is just the euclidean distance between these points, the coordinates of the points of intersection of γ with $z = 1$ are $(\pm\frac{d}{2}, 1)$.

The geodesic γ is a Euclidean semicircle of radius $r = \sqrt{x^2 + z^2} = \sqrt{(\frac{d}{2})^2 + 1^2} = \frac{1}{2}\sqrt{4 + d^2}$. Parametrize this circle using the parametrization $x = r\cos t$, $y = 0$, $z = r\sin t$. Then the angle θ corresponding to the point $(\frac{d}{2}, 1)$ on γ has the properties: $\cos\theta = \dfrac{x}{r} = \dfrac{d}{\sqrt{4+d^2}}$, $\sin\theta = \dfrac{z}{r} = \dfrac{2}{\sqrt{4+d^2}}$. Using the Tube Slope Lemma, the geodesic distance between the two end-

points can be computed as

$$\begin{aligned} d_{\mathbb{H}^3}(a,b) &= 2\ln(\frac{\sin\theta}{1-\cos\theta}) \\ &= 2\ln(\frac{\frac{2}{\sqrt{4+d^2}}}{1-\frac{d}{\sqrt{4+d^2}}}) \\ &= 2\ln|\frac{2}{\sqrt{4+d^2}-d}| \\ &= 2\ln\{\frac{2(\sqrt{4+d^2}+d)}{4}\} \\ &= 2\ln\{\sqrt{1+(\frac{d}{2})^2}+\frac{d}{2}\} \end{aligned}$$

□

Appendix C

Glossary of Symbols

Page	Symbol	Description
1	M	a hyperbolic three-manifold which fibers over $\mathbb{S}^1$
1	F	a hyperbolic surface; the fiber of the fibration of M
4	$\widetilde{M}$	the universal cover of M
6	Φ	a flow
7	$d_c(a, b)$	the distance along the curve c between points a and b
12	F^+	the closure of the punctured surface F; F plus finitely many points
14	Ψ^+	the extension of Ψ to F^+
14	M^+	the closure of the manifold M; obtained from M by Dehn filling
14	$\mathcal{F}$	a one-dimensional foliation
15	Ψ	the pseudo-Anosov monodromy map glueing surface $F \times \{1\}$ to $F \times \{0\}$ to create the manifold M
16	v_+	the eigenvector of an Anosov map which points in the unstable direction
16	v_-	the eigenvector of an Anosov map which points in the stable direction
17	λ	stretching and shrinking factor of a pseudo-Anosov map

Page	Symbol	Description
24	N	neutered space; the space obtained by removing the horoballs from M
24	$\widehat{F}$	the intermediate cover of F; $\widetilde{F^+} \setminus \{\text{preimages of punctures}\}$
26	$\widehat{M}$	the intermediate cover of M given by $\widehat{F} \times \mathbb{R}^1$
29	$\widehat{T}$	preimage in $\widehat{M}$ of a cusp in M; homeomorphic to $(D^2 - *) \times \mathbb{R}^1$
31	R,Q	tracking constants
36	$\overline{c}$	the path c which has been pushed out to the boundary of each cusp it enters
60	f	the map whose pull-back defines the modification of the singular Solv metric in a cusp
65	K_{t}	K_{trapped}; quasigeodesic constant for a trapped flow line
72	F	a reparametrization of f
73	Z_{p}	the Z value at the peak of a returning flow line
73	Z_{m}	the Z value at half the Euclidean distance between $Z = 1$ and $Z = Z_p$
75	t_m	the (positive) t value on the reparametrization of a flow line where $Z = Z_{\mathrm{m}}$
75	t_{h}	the (positive) t value on the reparametrization of a flow line where $Z = 1$; that is, where the flow line hits the boundary of the horoball

Page	Symbol	Description
79	B	lower bound on the length of a returning flow line segment so that constants C_x and C_y bound $\lvert\frac{dZ}{dX}\rvert$ and $\lvert\frac{dZ}{dY}\rvert$ below
82	C_x,C_y	constants which bound $\lvert\frac{dZ}{dX}\rvert$ and $\lvert\frac{dZ}{dY}\rvert$ below
83	K_{r}	$K_{\mathrm{returning}}$; quasigeodesic constant for a returning flow line
85	K_{c}	K_{cusp}; quasigeodesic constant for flow line segments in a cusp
89	$\lvert c\rvert$	denotes the length of c
95	N_∞, M_∞	infinite cyclic covers of N and M, respectively
96	K_{p}	K_{pushed}; quasigeodesic constant for pushed flow lines in N
100	π_{γ_+}	the map which projects onto the string of beads γ_+
104	J	maximum length of a connector path between segments projected to a string and a bead under π_{γ_+}
111	R_{p}	R_{pushed}; an upper bound for the hyperbolic distance that pushed flow line segments can be away from the string of beads connecting its endpoints
111	R_{s}	$R_{\text{string of beads}} = R_{\mathrm{p}}+R_{\mathrm{c}}$; an upper bound for the hyperbolic distance that flow line segments may be away from the string of beads connecting its endpoints

Page	Symbol	Description
113	R_{c}	R_{cusp}; an upper bound for the hyperbolic distance that flow line segments inside a cusp may be away from the geodesic connecting its endpoints
124	B_{ce}, B_{cd}	upper bounds for lengths of paths ce and cd (see Figure 3.17)
126	L	if ℓ is a segment of flow line of length at least L which lies outside the cusps, then any path c with the same endpoints which travels through exactly one cusp will have length at least $\frac{1}{2}\lvert\ell\rvert$.
124	L_1	if ℓ is a segment of flow line with $\lvert\ell\rvert > L_1$ which projects entirely outside the cusp $\widehat{T}$ under π_x, then the horizontal distance between the furthest endpoint of ℓ from the cusp $\widehat{T}$ to $\widehat{T}$ itself is at least $.9\lvert\ell\rvert$.
129	B	upper bound for the length of a segment of geodesic inside an R-neighborhood of a horoball yet outside the horoball.
134	R_{fs}	$R_{\text{flow segments}} = R_{\mathrm{s}} + M_{\mathrm{s}} + R_{\mathrm{c}}$; an upper bound for the hyperbolic distance that a flow line segment may be away from the geodesic segment connecting its endpoints
135	M_{s}	$M_{\text{string of beads}}$; the maximum length of a flow line segment which lies entirely inside a neighborhood of radius R_{s} of a horoball, yet outside the horoball itself

Page	Symbol	Description
137	R_Φ	$R_\Phi = R_{\text{fs}} + 1$; an upper bound for the hyperbolic distance that an entire flow line may be away from the geodesic connecting its endpoints
121	B_q	an upper bound for the length of a segment of flow line which projects to inside a covering cylinder of a cusp under both the projection maps π_x and π_y
147	LN	a larger neutered space than N; obtained by shrinking the cusps in N
147	Q_{b}	if a and b are boundary endpoints of a flow line segment inside a big cusp whose length is at least Q_{b}, then $d(\pi a, \pi b) > 1$.
149	Q_Φ	a (reasonable progress) tracking constant that applies to the suspension flow Φ

Bibliography

[CL] Daryl Cooper and D. Darren Long, *Foliations of Some 3-Manifolds Which Fiber Over the Circle*, Proc. Amer. Math. Soc. 126 (1998), no. 3, 925–931.

[CT] J. Cannon and W. P. Thurston, *Group Invariant Peano Curves*, Unpublished Preprint.

[Ot] J-P. Otal, *Le Theoreme D'Hyperbolization Pour les Varietes Fibrees de Dimension 3*

[Th] W. P. Thurston, *Hyperbolic Structures on 3-Manifolds II: Surface Groups and Manifolds Which Fiber Over the Circle*, Preprint.

Index